Sorbonne Université

École doctorale 394 : Physiologie, Physiopathologie & Thérapeutique
Institut de la Vision

Effect of high lipid exposure on retinal glial cell activation

Présentée par

Aude COUTURIER

Thèse de Doctorat

Présentée et soutenue publiquement le mercredi 12 décembre 2018

Jury

Pr Bahram BODAGHI	Président
Dr Patrice FORT	Rapporteur
Pr David GAUCHER	Rapporteur
Pr Catherine CREUZOT-GARCHER	Examinatrice
Dr Xavier GUILLONNEAU	Directeur de thèse

À mon grand-père, Georges Duréault

Remerciements

À mes Maîtres et juges,

Monsieur le Professeur Bodaghi,
Je vous remercie très sincèrement de me faire l'honneur de présider ce jury de thèse. Je vous remercie également de m'avoir accordé votre soutien et votre confiance pour les fonctions universitaires que j'ai la chance d'exercer.

Monsieur le Docteur Patrice Fort,
Je te remercie très sincèrement d'avoir accepté de juger mon travail et du temps que tu y as accordé. C'est un honneur et une grande chance pour moi d'avoir ton avis d'expert sur ce travail. J'espère sincèrement que les collaborations entre notre service et le tien pourront se poursuivre et se renforcer à l'avenir.

Monsieur le Professeur David Gaucher,
Je te remercie vivement d'avoir accepté d'être rapporteur de cette thèse et du temps précieux que tu as pu y consacré. Je n'ai pas eu la chance de travailler directement à tes côtés mais j'espère sincèrement que les relations d'amitiés et les travaux communs de recherche se poursuivront longtemps entre nos deux services.

Madame le Professeur Catherine Creuzot-Garcher,
Je te remercie de tout cœur d'avoir accepté de juger ce travail. Je te remercie également sincèrement pour ton soutien et ta bienveillance à mon égard depuis plusieurs années. J'espère en être digne et avoir la chance de poursuivre une carrière telle que la tienne.

À mon directeur de thèse,

Monsieur le Docteur Xavier Guillonneau,
Je te remercie énormément d'avoir dirigé ce travail pendant ces trois années. Je suis extrêmement chanceuse d'avoir pu apprendre à tes côtés. Merci d'avoir pris tant de temps et eu la patience de m'enseigner de nombreuses techniques au labo, à la paillasse. Merci d'avoir su guider ce travail sur la bonne voie avec tant de gentillesse. J'espère sincèrement avoir la chance de continuer à travailler à tes côtés à l'avenir, pour poursuivre ce travail et d'autres nombreux projets.

À mon Maître et chef de service,

Monsieur le Professeur Ramin Tadayoni,
Je ne pourrai jamais assez te remercier de m'avoir accordé ta confiance et ton soutien depuis toutes ces années. C'est évidemment grâce à toi que j'ai eu la chance immense de pouvoir faire ces trois années de thèse et poursuivre la recherche qui me passionne. Merci sincèrement pour tout ce que tu fais pour moi et pour le service, avec toujours tant de simplicité, d'humilité et de gentillesse. Tu es évidemment un modèle à suivre pour moi et j'espère sincèrement être digne de ta confiance à l'avenir.

À mes Maîtres et aînés,

Monsieur le Professeur José-Alain Sahel,
Je vous remercie très sincèrement de m'avoir accueillie à l'Institut de La vision pour mes trois années de thèse. C'est un grand honneur et une vraie chance pour moi d'avoir pu travailler et tant apprendre au sein d'équipes aussi brillantes. Ma passion pour la recherche n'en a fait que grandir et j'espère vraiment pouvoir poursuivre à l'avenir de nombreux travaux en collaboration avec vous et vos équipes. Recevez l'expression de ma sincère reconnaissance et de ma profonde admiration.

Monsieur le Professeur Gaudric,
C'est un immense privilège pour moi d'avoir tant appris et de continuer chaque jour à apprendre à vos côtés. Votre expertise et vos connaissances immenses m'impressionnent toujours et sont pour moi un exemple à suivre. Je vous remercie infiniment pour tout ce que vous m'avez enseigné et pour votre aide si précieuse encore aujourd'hui dans tous mes travaux de recherche.

Madame le Professeur Pascale Massin,
J'ai eu la chance que vous m'accordiez votre confiance pour être chef de clinique puis poursuivre mon chemin dans le service de Lariboisière que j'affectionne tant. Votre expertise et tout ce que vous accompli dans le domaine de la rétinopathie diabétique ont toujours fait mon admiration. J'espère avoir la chance de continuer à travailler avec vous et accomplir à l'avenir d'aussi beaux projets que ceux que vous avez menés.

Aux chefs de l'équipe S14,
Florian Sennlaub, Michel Paques, Xavier Guillonneau, Cécile Delarasse,
J'ai eu l'honneur et la chance de travailler dans votre équipe et je vous remercie énormément pour tout ce que vous m'avez appris. Ça a été un bonheur et un vrai privilège pour moi de travailler avec des personnes brillantes comme vous. Merci pour vos enseignements, votre confiance et votre gentillesse.

À Sacha Reichman
Je te remercie sincèrement d'avoir mis en place avec Xavier la collaboration entre nos deux équipes qui a permis de faire aboutir cette thèse et pour ce beau projet. Un très grand merci pour ta confiance, ta gentillesse et ta disponibilité. J'espère vraiment avoir l'occasion de travailler avec toi sur de nouveaux projets à l'avenir.

À mes collègues et amis,

Mes collègues de l'équipe S14,
Guillaume, Lucile et Wassila, cette thèse n'aurait pu se faire sans votre aide. Je vous remercie sincèrement pour tout ce que vous avez fait pour moi ces derniers mois, toutes les manips, les conseils, les petites attentions. J'ai beaucoup de chance d'avoir pu être avec vous pendant cette thèse !
Sébastien, Christophe, Sara, JB, Hugo et Fanny, une équipe de choc ! Merci beaucoup pour votre aide et aussi pour votre bonne humeur (les chansons et rires du bureau me manqueront et resteront graver dans ma mémoire). Je garderai un excellent souvenir de ces années de thèse grâce à vous tous !

Mes collègues de Lariboisière,
Élise, tu es pour moi plus qu'un collègue bien sûr, une amie précieuse que j'adore. Merci pour ton aide, ton soutien, tes conseils à chaque instant, même dans les moments difficiles. Tu es une femme extraordinaire, ne change rien !
Valérie MT et Carlo, merci infiniment pour votre aide dans ce travail. J'ai beaucoup de chance de pouvoir travailler avec vous ! Un grand merci pour votre travail, votre gentillesse, votre bonne humeur et optimisme à toute épreuve !
Ali, Valérie K, Bénédicte, Sophie, Dan et Sara, merci d'être des collègues aussi géniaux. L'équipe de Lariboisière est grâce à vous une vraie famille pour moi et travailler avec vous est un bonheur et une chance immense. J'espère de tout cœur que notre équipe restera soudée encore longtemps.
Les orthoptistes, infirmières, aides-soignantes et secrétaires, qui par leur compétence, gentillesse et bonne humeur, font de chaque journée dans le service un vrai bonheur pour moi.

Mes collègues de Cochin,
Elodie, tu es également une vraie amie pour moi. Nous partageons beaucoup de choses dont une passion pour la recherche et j'espère que notre amitié durera très longtemps.
Pierre-Raphaël, Raphaël, Wilfried et tous mes collègues de l'ophtalmopôle, merci pour les bons moments partagés au bloc. Je suis ravie que nos équipes soient réunies.

Mes collègues des autres services,
Audrey Giocanti, je suis très heureuse d'avoir pu te connaître mieux ces dernières années. Toujours positive et de bonne humeur, c'est un bonheur de travailler avec toi et j'espère que nous continuerons à travailler ensemble de nombreuses années.
Sarah Mrejen, je n'oublierai jamais que c'est grâce à toi que j'ai choisi de faire de la rétine et c'est bien sûr un choix que je n'ai jamais regretté. Mon admiration pour toi est toujours immense et j'espère avoir la chance de continuer à travailler avec toi à l'avenir.

À mes amis,

Merci à mes amis fidèles,
Ma Celou, Marraine Bree, tellement de chance de t'avoir! Merci d'être toujours à mes côtés et de ton amitié si forte et si fidèle. Je sais que je pourrais toujours compter sur toi même si nous ne nous voyons pas tous les jours. Ton amitié est si précieuse à mes yeux.
Ma petite Clem, merci pour tes bons mots et conseils à chaque instant. J'admire ta sérénité et te force tranquille. J'ai beaucoup de chance de t'avoir comme amie!
Daëna, Delphine, Raquel, Béné, notre amitié s'étend au-delà des frontières! Je vous adore, vous me manquez (et le BRT aussi)
Zak, Stéphane, Thomas, Jean, je vous adore, vous êtes géniaux, ne changez rien !

À Joris. Je sais que tu aurais été présent à mes côtés en ce jour important. Ton amitié, tes conseils, ton humour me manquent chaque jour.

À mes amis Bérengère, Émilie, Vanessa, Christophe, que je prends toujours autant de plaisir à voir même après toutes ces années !

À ma famille,

À mon grand-père, bien sûr. Tu avais absolument tenu à venir de Cannes pour assister à la soutenance de ma thèse de médecine et je sais que tu aurais été là aussi aujourd'hui. Je suis fière d'être ta petite-fille, tu me manques beaucoup.

À mes mamies, mes oncles, tantes, cousins et cousines, que j'aime tant. J'espère que notre famille sera toujours unie et pleine d'amour.
À Mon Florian et à Christian, vos sourires sont toujours gravés dans ma mémoire et m'accompagnent chaque jour.

À mon papa que j'aime, merci d'être toujours là pour nous.

À ma maman adorée. Je n'aurais jamais pu écrire cette thèse sans toi ! Comment te remercier pour les innombrables heures passées avec mes enfants et tous ces allers-retours Aulnay-Paris pour venir m'aider, mais surtout pour tout l'amour que tu nous donne. J'espère être une maman aussi extraordinaire pour mes enfants que tu l'es pour moi. Je t'aime si fort.

À mes trois incroyables sœurs que j'adore,
Nathalie, ma phénoménat, dont j'admire le talent et la bonne humeur,
Carine, ma Cawaine, dont j'admire la douceur et la gentillesse,
Estelle, mon étoile, que j'admire tellement. Ta force, ton courage, ton sourire, ta positivité et ta générosité m'inspirent chaque jour et font de moi le médecin que je suis aujourd'hui. Merci du rayon de soleil que tu mets sur ma vie.

À mes enfants, Chloé, Timothée, Raphaël,…
Vous êtes ma première passion, ma raison de vivre. Je suis tellement fière de vous. Mon amour pour vous est infini.

À Chady, l'amour de ma vie. Je t'aime tellement. Aucun mot n'est assez fort. Merci de tout le bonheur que tu m'apporte chaque jour. Jtm forever & everywhere

TABLE OF CONTENT

Abbreviation list

α2M: α2Macroglobulin
AA: arachidonic acid
ACCORD: Action to Control Cardiovascular Risk in Diabetes
AHDF: adult human dermal fibroblast
AGE: advanced glycation end
ALEs: advanced lipoxidation end products
ANGPTL4:
AMD: age-related macular degeneration
AMPK: AMP-activated protein kinase
AO-SLO: adaptive optics scanning laser ophthalmoscopy
AQP: aquaporine
ATF: activating transcription factor
ATP: adenosine triphosphate
BCVA: Best-corrected visual acuity
BDNF: Brain-derived neurotrophic factor
BRB: blood retinal barrier
BSA : bovine serum albumin
CCL2: chemokine ligand-2
COX: cyclooxygenase
CRALBP: cellular retinaldehyde-binding protein
CXCL: chemokine (C-X-C motif) ligand
CYP450: cytochrome P450
DAPI: 4',6-diamidino-2-phenyl-indole
DCCT: Diabetes Control and Complication Trial
DCP: deep capillary plexus
DHA: docosa-hexaenoic acid
DME : diabetic macular edema
DMEM: Dulbecco's Modified Eagle Medium
DR: diabetic retinopathy
DRCR.net: Diabetic Retinopathy Clinical Research Network
EAAT: excitatory amino acid transporter
EC: endothelial cell
ER: endoplasmic reticulum
EDP: epoxydocosapentaenoic acid
ETDRS: Early Treatment Diabetic Retinopathy Study
ETT: epoxyeicosatrienoic acid
EVAS : extravascular signal
FAZ: foveal avascular zone
FIELD: Fenofibrate Intervention and Event Lowering in Diabetes
GABA: gamma- aminobutyrique acid
GAPDH: glycéraldéhyde-3-phosphate déshydrogénase
GCL: ganglion cell layer
GDH : glutamate dehydrogenase
GDNF: glial cell line-derived neurotrophic factor
GFAP: glial fibrillary acid protein
GF: Growth Factor
GLAST: glutamate-aspartate transporter
GluR: glutamate receptor

GLUT: glucose transporter
GS: glutamine synthetase
HbA_{1c}: glycated hemoglobin
HFL: Henle fiber layer
HG: hyperglycemic
HHG: hyper high glucose
hiPSC: human induced pluripotent stem cell
HIF-1α: hypoxia-inducible factor 1α
Iba-1: ionized calcium-binding adaptor molecule 1
ICAM: intercellular adhesion molecule
IGF-1: insulin like growth factor-1
IL: interleukin
ILM: inner limiting membrane
INL: inner nuclear layer
INFγ: interferon gamma
IPL: inner plexiform layer
iPSC: induced-pluripotent stem cell
Kir 4.1: Inwardly rectifying potassium 4.1
LDL: low-density lipoprotein
LOX: lipoxygenase
LPS : lipopolysaccharide
LRP1: lipoprotein-related protein 1
Mφs: macrophages
MAGE: mean amplitude of glucose excursions
MAPK: mitogen-activated protein kinase
MCP monocyte chemoattractant protein
MCT: monocarboxylate transporter
MGC: Müller Glial Cells
MMP: matrix metalloproteinase
Mos: monocytes
NFL: nerve fiber layer
NG: normoglycemic
NGF: nerve growth factor
NHIR: Neonatal Hyperglycemia-induced Retinopathy
NPDR: Non-proliferative diabetic retinopathy
OCT: Optical coherence tomography
OCTA: Optical Coherence Tomography Angiography
OIR: oxygen-induced retinopathy
OLM: outer limiting membrane
ONL = outer nuclear layer
OPL: outer plexiforme layer
PA: palmitic acid
PAG: phosphate-activated glutaminase
PAR: projection artifact removal
PBMC: Peripheral blood mononuclear cell
PDGF: platelet-derived growth factor
PDR: Proliferative diabetic retinopathy
PEDF: pigment epithelium-derived factor
PEDF-R: pigment epithelium-derived factor receptor
PKC: protein kinase C
PRP : pan-retinal photocoagulation
RPE: retinal pigment epithelial

ROS: reactive oxygen species
SD: Spectral domain
SNAT: sodium-coupled neutral amino acid transporters
SSADA: Split-spectrum amplitude-decorrelation angiography
SSPiM: suspended particles in motion
STZ: streptozotocin
SVP: superficial vascular plexus
TLR4: Toll-like receptor 4
TNFα: tumour necrosis factor alpha
Trk: Tropomyosin receptor kinase
VEGF: vascular endothelial growth factor
VEGFR: vascular endothelial growth factor receptor

I. INTRODUCTION

I. Diabetic Retinopathy Physiopathology

Diabetic retinopathy (DR) remains a major cause of vision loss in diabetic patients which affects up to 25% of diabetic patients, i.e. around 1 million people in France. Undiagnosed, it may lead to severe vision loss and blindness. Progression of DR is slow, and DR remains asymptomatic for a long time until visual loss occurs due to DR complications. To prevent DR complications, annual screening has been recommended for all diabetic patients.

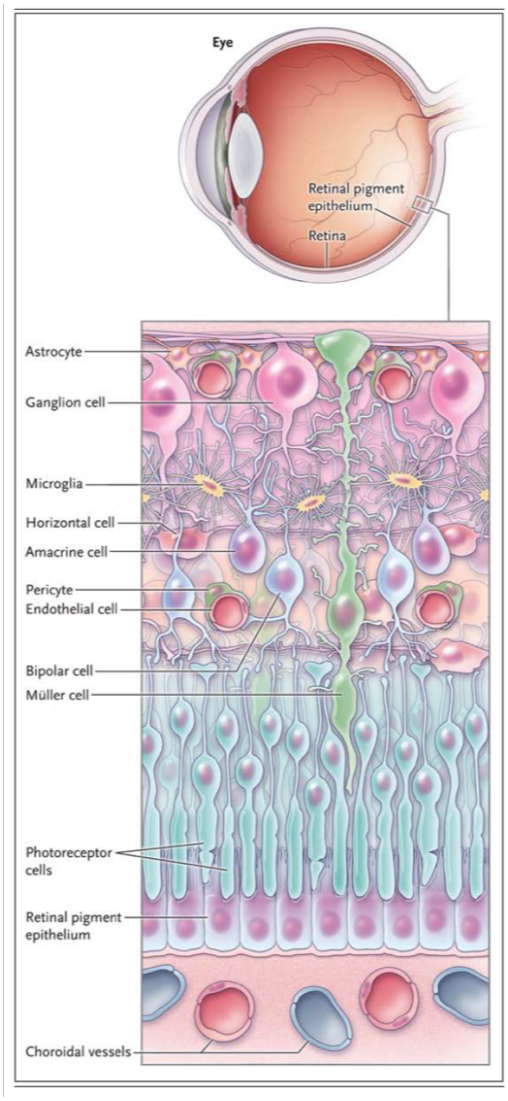

Figure 1: Relationship and interconnection between the neurons (Ganglion cells, bipolar cells and photoreceptors), the glia (astrocytes, Müller cells and microglial cells) and the retinal vessels (endothelial cells and pericytes) forming a neurovascular unit in a healthy retina. This close interconnection maintains retinal homestasis, blood-retinal barrier and synaptic transmission to allow vision. Adapted from Antonetti DA et al., NEJM 2012.

DR pathogenesis is complex and multifactorial. For years, the treatment of DR was limited and relied only on metabolic control. Recently, in the last decade, research advances have highlighted the relationship between the neural retina and the retinal vasculature forming a neurovascular unit (**Figure 1**) (Antonetti DA et al., 2012) and have identified the central role of vascular endothelial growth factor (VEGF) and of multiple pro-inflammatory cytokines in the vascular lesions observed in DR.

1. Microvascular lesions pathogenesis

a) Capillary occlusion

Numerous investigators have suggested that the pathogenesis of DR includes glucose-mediated microvascular damage. Pathways related to hyperglycemia involved in DR pathogenesis include oxidative stress, activation of protein kinase C (PKC), and advanced glycation end products and their receptor (Lu M et al., 1998; Stitt AW, 2003; Aiello LP, 2002; Caldwell RB et al., 2005). Mechanisms of vascular injury include both vascular permeability due to tight junction disassembly (Antonetti DA et al., 1999) and capillary occlusion due to endothelial cell-mediated leukostasis (Miyamoto K et al., 1999). First histological changes in diabetic retinal vessels have been reported to be basal membrane thickening, loss of pericytes and of endothelial cells. Adhesion molecules, such as ICAM-1, expressed on endothelial cells support leukocyte rolling and adhesion leading to capillary occlusion.

The features of DR were first described in the 19th century using ophthalmoscopy. The first visible retinal change is the appearance of microaneurysms. Microaneurysms are thought to be an early sign response to retinal ischemia and correspond to proliferation of endothelial cells that usually develop at the edge of non-perfusion areas (**Figure 2**) (Tolentino MJ et al., 2002).

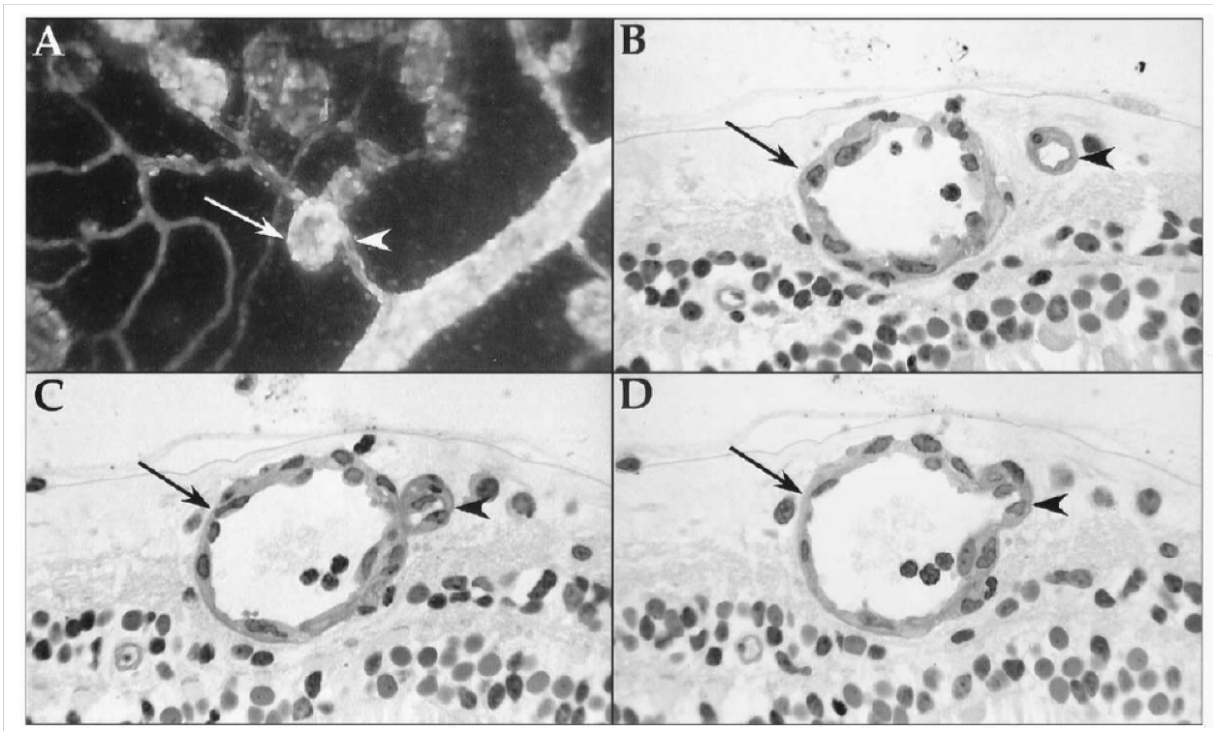

Figure 2: Microaneurysms in the superficial retinal vascular in VEGF-induced retinopathy in non-human primate: dark-field view with original magnification x 110 (**A**) and semi serial sections (**B, C, D**) showing a single microaneurysm and its communication to adjacent capillary (arrowheads). The saccular structure consists of hyperplasic endothelial cells and basement membrane material. Adapted from Tolentino et al., AJO 2002.

These microaneurysms may lead to intra-retinal leakage of plasma and of lipoproteins inducing macular edema and hard exudates deposits (**Figure 3**).

A turn-over of microaneurysms has been observed in the retina, with disappearance of some microaneurysms due to spontaneous occlusion and appearance of new microaneurysm. A rapid turn-over has been reported to be a risk factor for macular edema occurrence (Nunes S et al. 2013).

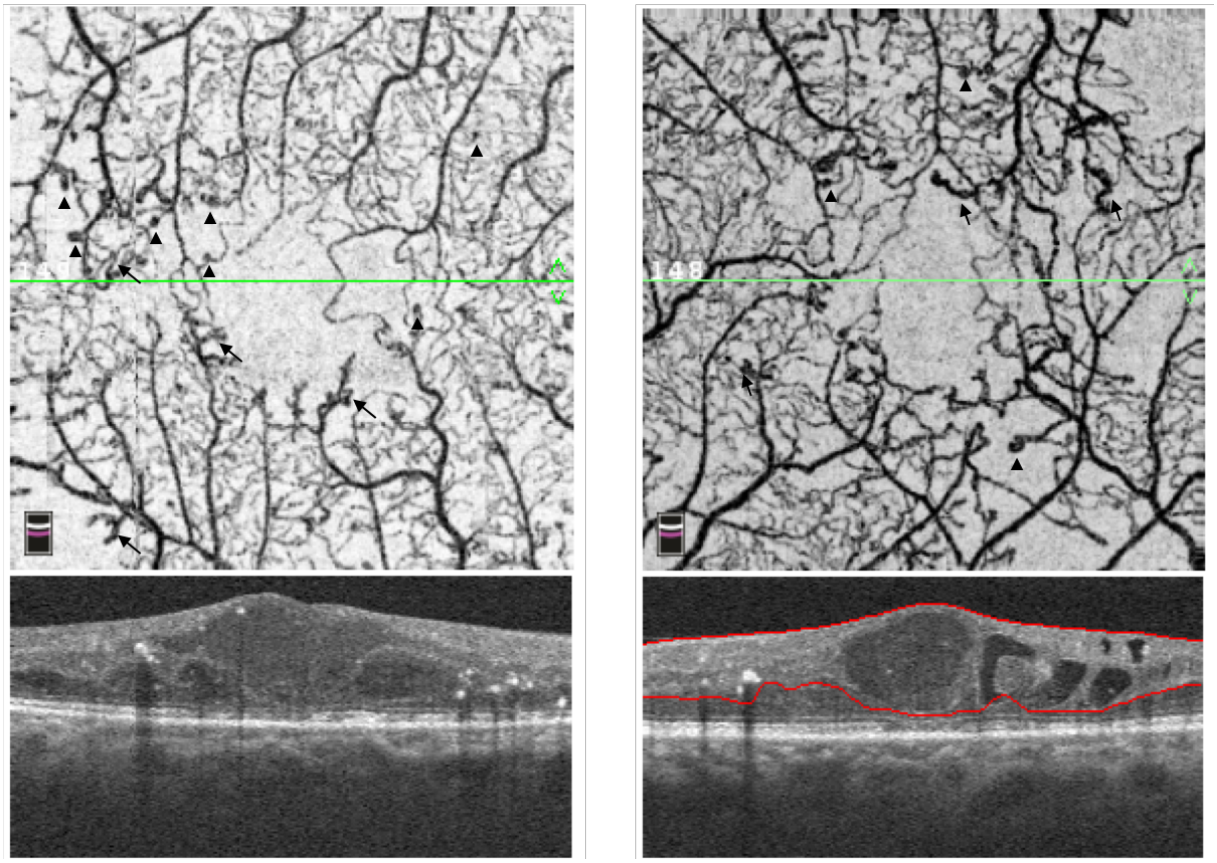

Figure 3: Optical coherence tomography angiography imaging of both eyes of a type-2 diabetic patient with severe non-proliferative DR and macula edema. Loss of capillary is visible in both eyes on angiograms (upper row). Microaneurysms (arrowheads) and intra-retinal microvascular abnormalities (arrows) are visible in the non-perfusion areas. B-scan OCT shows macular thickening and intra-retinal cystoid spaces in both eyes (lower row). Image from the department of Ophthalmology, Lariboisiere.

The progression of retinal ischemia induces the appearance of others retinal lesions: cotton-wool spots secondary to infarcts of the nerve-fiber layer, venous beading and intra-retinal microvascular abnormalities (**Figure 3 and 4**).

Figure 4: Fluorescein angiography and optical coherence tomography angiography imaging of both eyes of a type-2 diabetic patient with proliferative DR. Multiple intra-retinal microvascular abnormalities are visible in the non-perfusion areas. Pre-papillary newvessels induce leakage on fluorescein angiography. Image from the department of Ophthalmology, Lariboisiere.

Without treatment, capillary occlusion progress and lead to proliferative changes: abnormal vessels developed from veins on the optic disc and at the surface of the retina (**Figure 5**). Proliferation of fibroblasts supporting these abnormal vessels form a fibrovascular proliferation that may induce traction on retinal surface and lead to tractional retinal detachment.

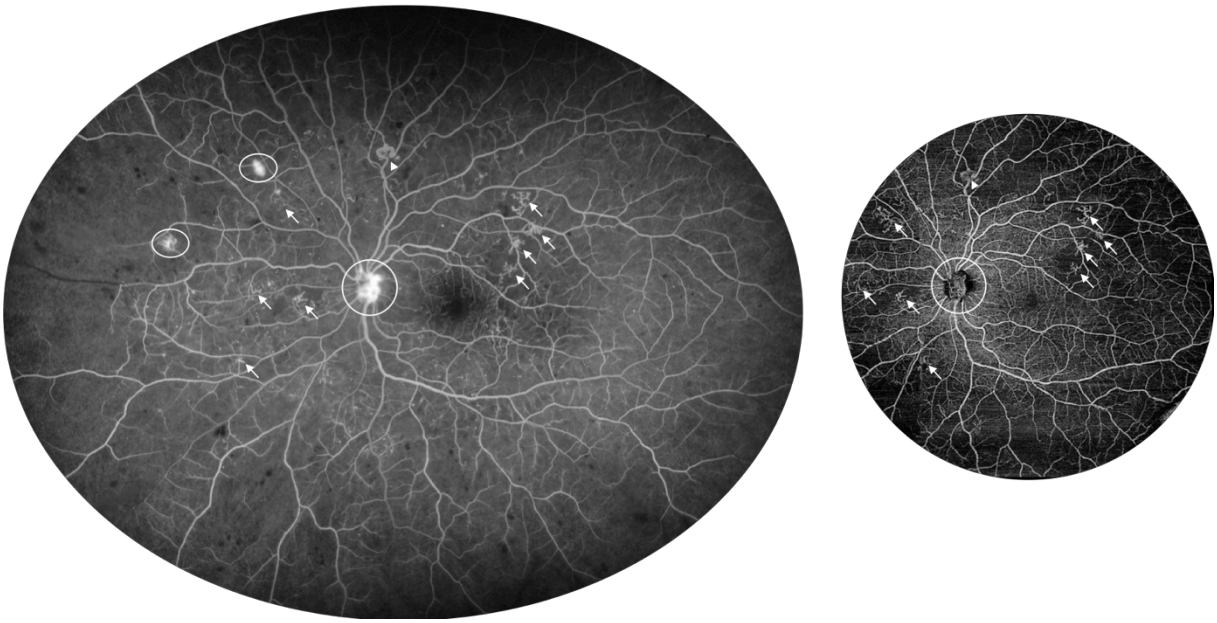

Figure 5: Ultra-wide-field fluorescein angiography and wide-field swept-source optical coherence tomography angiography imaging of the left eye of a type-2 diabetic patient with proliferative DR. Multiple intra-retinal microvascular abnormalities are visible in the non-perfusion areas (arrows) as well as venous binding (arrowhead) on both imaging modalites. Pre-papillary and pre-retinal newvessels (circle) induce leakage on fluorescein angiography. The pre-papillary newvessel (circle) is also easily detected using optical coherence tomography angiography. Image from the department of Ophthalmology, Lariboisiere.

The molecular events associated with microvascular lesions in DR are multiple and include (Antonetti DA et al., 2012):

- Microvascular permeability: altered tight-junction and adherence-junction expression and post-transcriptional modifications
- Focal hypoxic events
- Production of growth factors (GF), including VEGF, platelet-derived GF, basic fibroblast GF, connective-tissue GF, erythropoietin, and angiotensin II
- Loss of pigment-epithelium-derived factor
- Protease changes: matrix metalloproteinases, serine proteases (urokinase), kallikrein, and bradykinin
- Pericyte and endothelial cell apoptosis
- Receptor-signaling defects.

b) Macular edema

Macular edema is a well-known complication of various ocular disease including DR. Present in 25% of diabetic patients, macular edema remains the main cause of visual impairment in DR. Optical coherence tomography (OCT) is now the gold-standard for macula edema diagnosis, showing both intra-retinal cystoid spaces and thickening of the central fovea. Fluorescein angiography shows pooling and leakage in the cystoid spaces (**Figure 6**).

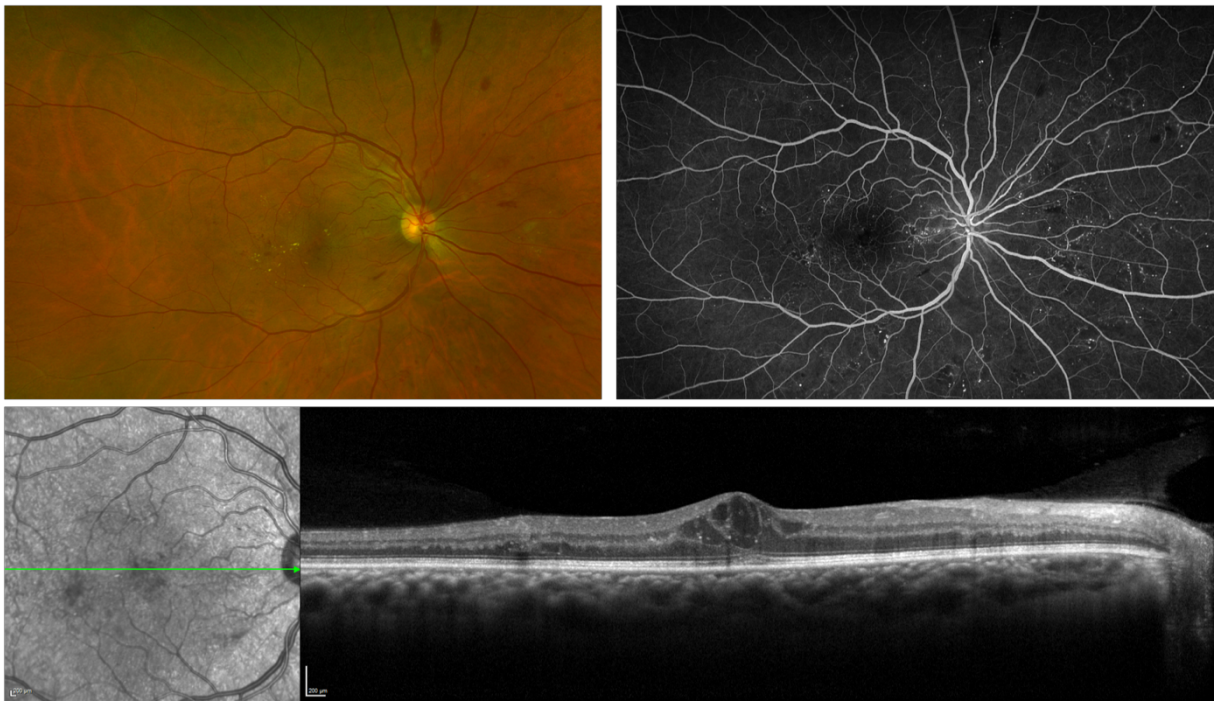

Figure 6: Multimodal imaging of the right eye of a type 2-diabetic patient with severe non-proliferative DR and central macular edema. Visual acuity was 20/50 in this eye. Color fundus photography shows microaneurysms and hard exudates in the posterior pole. Fluorescein Angiography shows a pooling in cystoid spaces as well as leakage from microaneurysms in the macula. B-scan Optical coherence tomography shows thickening of the macular center with cystoid spaces and hyperreflective dots. Image from the department of Ophthalmology, Lariboisiere.

In DR, the mechanisms of blood retinal barrier homeostasis are impaired. These mechanisms are complex, including both intercellular junction complex, transcellular transport, and active efflux of smaller molecules in the vascular endothelial cells, which are supported by perivascular components including the basement membrane, pericytes, and glial cells.

The efficacy of anti-VEGF agents (such as aflibercept, bevacizumab and ranibizumab) as a treatment for diabetic macular edema confirms that VEGF is a key factor contributing to the blood retinal barrier disruption in this disease.

Hard exudates are intra-retinal yellowish deposits associate with macular edema and visible in the fundus in DR. They appear as confluent hyperreflective foci with various sizes, shapes and reflectivity levels on SD-OCT (Bolz M et al., 2009). According to histological reports, hard exudates are the precipitates of extravasated components and contain hyaline, and lipid-laden macrophages (**Figure 7**) (Toussaint D et al., 1962; Wolter JR, 1957; Cusik M et al., 2003).

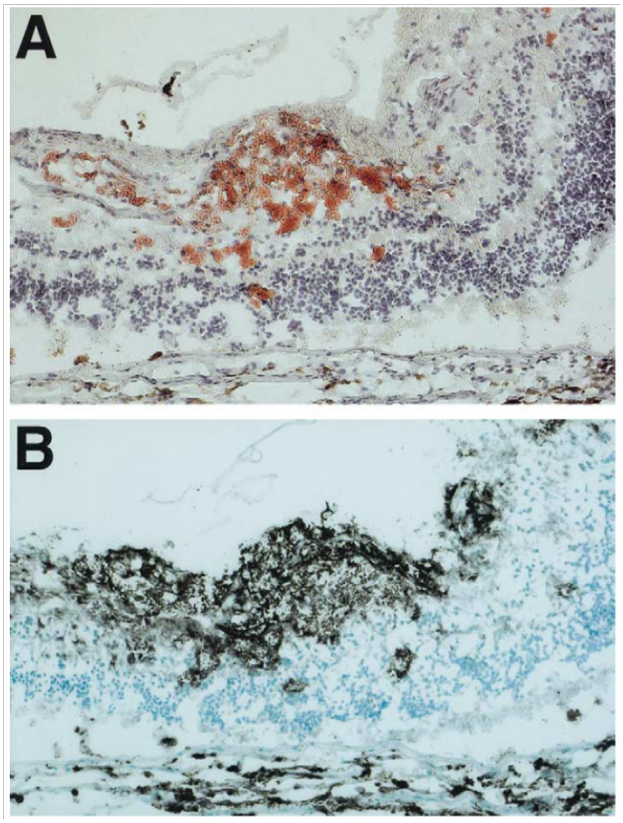

Figure 7: Histologic analysis of diabetic retina.
A) Presence of abundant lipid-rich deposits and lipid-laden macrophages in the inner retina (stain, oil red O; original magnification x 200)
B) Heavy infiltration of macrophages (stain, avidin-biotin-peroxidase and ant-CD68; original magnification x 200). Adapted from Cusik M et al., Ophthalmology 2003.

Recently, adaptive optics scanning laser ophthalmoscopy (AO-SLO) have revealed irregular lesions within hard exudates and an individual turnover rates (Yamaguchi M et al., 2016).

Yamagushi et al. showed using AO-SLO that some hard exudates consisted of an accumulation of spherical particles with hyperreflective dots, and these AO-SLO images resembled the histological images in published literature (Wolter JR and al., 1957). Although the spherical particles were slightly larger (27 µm) than a macrophage (20 µm), they might represent enlarged macrophages that have phagocytosed lipid (**Figure 8**).

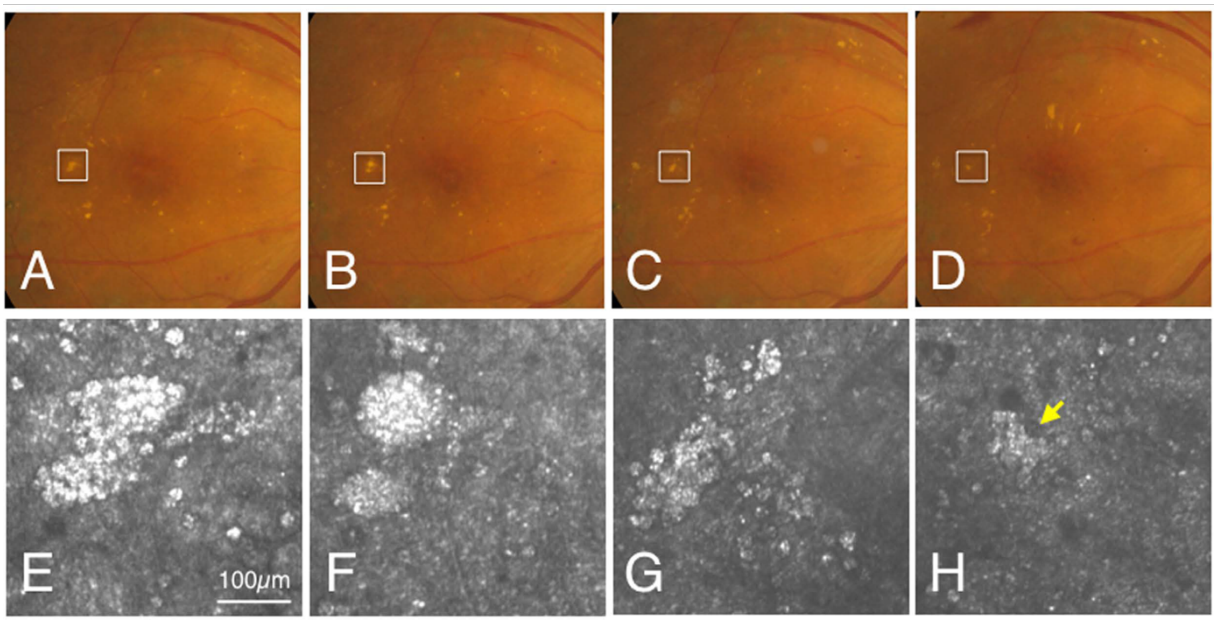

Figure 8: Changes in hard exudates imaged using color fundus photographs (A-D) and AO-SLO (E-H) in a diabetic patient, at baseline (A,E), one month (B,F), two months (C,G) and four months (D,H). AO-SLO allows to visualize the transformation of hard exudates from round to irregular type (yellow arrow). Adapted from Yamaguchi M et al., Scientific Report 2016.

The presence of hyperreflective foci in SD-OCT with no apparent clinical changes detected by the color fundus photograph have also been reported (**Figure 9**) (Bolz M et al., 2009).

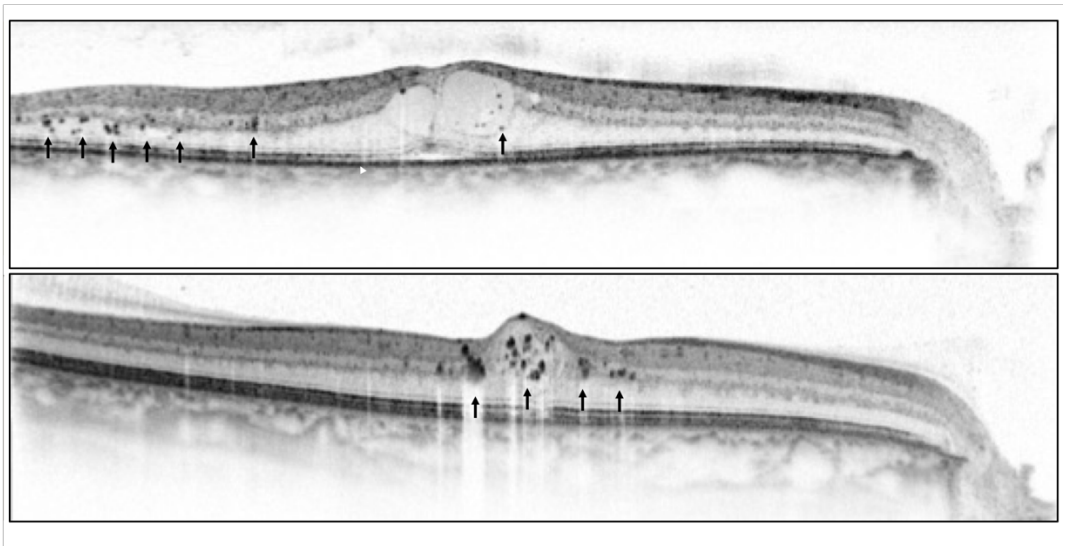

Figure 9: B-scans optical coherence tomography of two cases of central diabetic macula edema. Hyperreflective dots are detected in the inner nuclear layer and in the cystoid spaces (arrows). Images from the department of Ophthalmology, Lariboisiere.

These hyperreflective foci are heterogenous in shapes, positions and optical properties (Gelman SK et al., 2014). Three-dimensional OCT imaging demonstrated that hyperreflective foci were randomly deposited in the INL, whereas most lesions in the HFL appeared to be radiating toward the foveal center (Murakami T et al., 2018).

Several publications suggest the clinical relevance of hyperreflective foci in DR, but there is still a lack of consensus regarding the origin and significance of all hyperreflective material in the retina. Vujosevic et al evaluated characteristics of these hyperreflective spots and compared them with features on en face images (Vujosevic S et al., 2017). The authors suggested that when these spots are larger than 30 µm, they may represent hard exudate in the outer retina. For patients with DME, Bolz et al suggest that hyperreflective material may represent subclinical extravasation of lipoproteins and/or proteins, secondary to breakdown of the blood retinal barrier (Bolz et al, 2009).

Reflectance-decorrelated foci were described as a novel OCT-Angiography finding by Murakami T et al. (Murakami T et al., 2018). The authors proposed that these foci could be either a sign of neuroglial dysfunction or of lipoprotein deposits in DR.

According to Yamagushi et al., the spherical particles in AO-SLO might correlate with the hyper-reflective foci in SD-OCT (Yamaguchi M et al., 2016). These hyper-reflective dots are thus most likely to be phagocytosed lipids in macrophages suggesting that their contribution to the pathogenesis but also to the activity of DR.

2. Neural retinal lesions

Recent work strongly suggests that DR involves more than hyperglycemia and microvascular lesions, and evidence for alterations of the neural retina and insulin action has been reported (Lieth E et al., 2000; Antonetti DA et al., 2006).

The retina is a vascularized neural tissue and this neurovascular unit should be considered in DR pathogenesis. This neurovascular unit refers to physical and biochemical relationship and interdependence between neurons, glia and vessels (Antonetti DA et al., 2012) (**Figure 10**). DR could thus be considered not only as a microvascular manifestation of diabetes but also as a neuro-glial disease (Rübsam A et al., 2018). Indeed, multiple evidence of cellular, histologic and functional neural alterations has been reported.

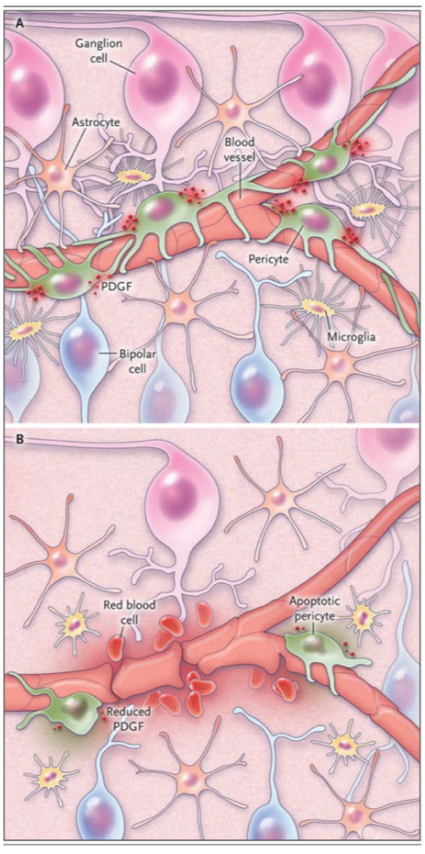

Figure 10: Disruption of the neurovascular unit of the retina in healthy eye (A) and diabetic (B).
A. In healthy retina, pericytes and glial cells participate to the blood-retinal barrier and maintain a proper electrolytic environment for neural function.
B. Diabetes leads to glial cell activation and increased pro-inflammatory cytokines level, contributing to the breakdown of the blood-retinal barrier and neuronal apoptosis.
Adapted from Antonetti DA et al., NEMJ 2012.

At the cellular level, an early apoptosis of ganglions cells has been reported both in post-mortem human diabetic retina (Abu El-Asrar AM et al., 2004), and in animal models (Barber AJ et al, 1998; Park SH et al., 2003).
In animal models of DR, neuronal apoptosis in ganglion cells has been also shown to be an early event in DR and to occur before any vascular changes as early as two weeks to 1 month (Barber AJ et al., 1998, Ning X et al., 2004). Oscillatory changes on electroretinogram are an early change in streptozocin-induced diabetic rats and as has been reported as early as 2 weeks (Sakai H et al., 1995; Li and al., 2002).
Retinal cell death has also been observed in the photoreceptor layer and the inner nuclear layer in a later phase of the disease (Ning et al., 2004; Park et al., 2003).
Results in mice DR models are more controversy: in mice with streptozocin-induced diabetes, Asnaghi et al. reported no increase in the number of apoptotic cells after 10 and 24 weeks of diabetes, whereas Martin et al. reported such retinal apoptosis at 2, 6 and 12 weeks (Asnaghi et al., 2003; Martin et al., 2004). In mice with alloxan-induced diabetes, no cell death was detected in any cell layer after three months of diabetes. Early ERG changes are not a consequence of retinal cell death (Gaucher D et al., 2007; Asnaghi et al., 2003).

In humans, histopathologic studies have shown the loss of neurons in DR (Wolter JR, 1961; Bloodworth JMB, 1962). Since then, numerous studies have demonstrated the loss of neuroretinal function using electrophysiology, dark adaptation, contrast sensitivity, and color vision tests. These tests showed that compromised neural function in the retina is an early phenomenon in DR occurring even before the onset of vascular lesions (Parisi V and Uccioli L, 2001; Greenstein VC and al., 1992; Bearse MA et al., 2004). In addition, loss of oscillatory potentials on electroretinograms have been shown to predict the onset of neovascular proliferation better than the vascular lesions visible on fundus photographs or on fluorescein angiography (Bresnik GH and Palta M, 1987).

Similarly, visual field defects may be present before the onset of vascular lesions and may predict DR severity better than visual acuity (Han Y et al, 2004; Bengtsson B et al, 2005). Recently, the 5-year results of DRCR.net protocol S showed a progression of visual field loss in both PRP and Ranibizumab groups (Gross JG et al., 2018). This decline may be due to the progression of neuro-retinal lesions that are not prevent by laser or anti-VEGF treatment. This hypothesis needs to be confirmed in futures clinical studies.

Today, it is not known whether vascular or neural cell defects occur first; most likely they are interdependent. In a primary vascular lesion, neuronal and glial damage could be du the entry of circulating macrophages or fatty acids into the retina. In a primary neural and glial lesion, capillary occlusion and hyper-permeability could be secondary to glial dysfunction and proinflammatory cytokines (Antonetti DA et al., 2006).

3. Role of inflammation and glial activation

Systemic inflammation is an intrinsic response to obesity and diabetes. In the past decade, a variety of physiologic and molecular changes consistent with a role of inflammation have been found in the retinas or vitreous humor of diabetic animals and patients. Indeed, an increase secretion of many inflammatory mediators such as interleukin (IL)-1β, IL6, IL8, chemokine ligand 2, tumor necrosis factor (TNF)-α, and monocyte chemoattractant protein 1 (MCP-1), together with an activation of glial cells have been detected in early DR (**Figure 11**) (Rübsam et al., 2018). The increase in these cytokines produced by activated microglia, endothelial cells, macroglia, and later even neurons, also highlights the progression of the inflammatory response throughout all cell types of the retina. Increase inflammatory cytokines and VEGF from activated glial cells and the loss of platelet-derived growth factor (PDGF) signaling in pericytes contribute to the breakdown of the blood-retinal barrier and to angiogenesis in DR. Impairment of blood retinal barrier lead to macrophage migration into the retina, as well as accumulation of inflammatory and angiogenic factors in the vitreous cavity (Antonetti et al., 2012). The accumulation of these inflammatory mediators has also been proposed to contribute to early neuronal cell death in DR.

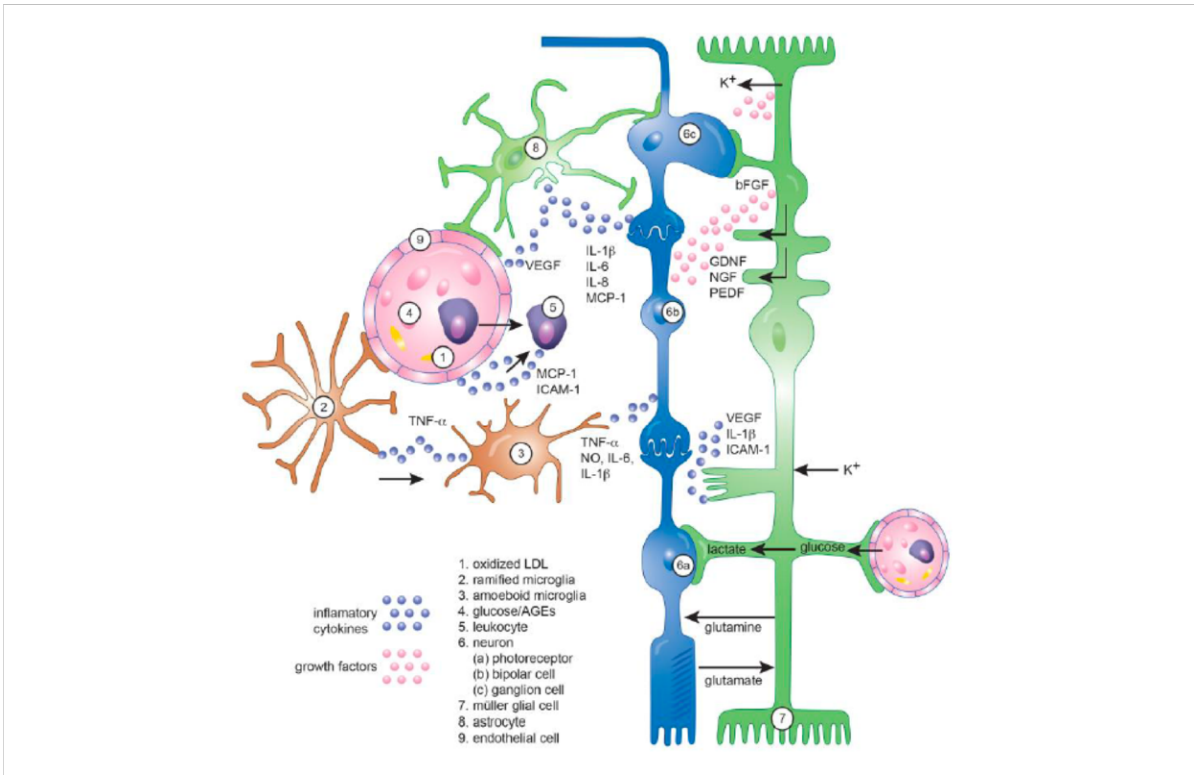

Figure 11: Role of inflammation in diabetic retinopathy: Schematic of a mammalian retina depicting the interactions between glia, neurons and endothelial cells with special regard to the inflammatory chemokines involved. Blood vessels and endothelial cells in pink (9), leukocytes in purple (5), macroglial cells in green (7,8), microglia in brown (2,3) and neurons in blue (6a–c). Scheme showing kalium homeostasis, glutamate metabolism and the secretion of trophic factors, chemokines and interleukins. AGEs, advanced glycation end products. Adapted from Rübsam A et al., International Journal of Molecular sciences 2018.

a) Müller cell activation

The neurovascular unit includes astrocytes and Müller cells, implicated in the regulation of retinal vascular blood flow (Pournaras CJ and al., 2008).
Müller glial cells are immunocompetent cells implicated in retinal inflammatory reaction to injury, together with microglia and astrocytes.

In vitro studies have shown that the receptor of the advanced glycation end product (AGE) was overexpressed in Müller cells exposed to high glucose and triggered pro-inflammatory cytokines synthesis (Zong H et al., 2010).

Hyperglycemia was reported to induce several changes in Müller cells: upregulation of GFAP, which is indicative of Müller cell activation, alteration of the aquaporin expression and reduction of the interaction between insulin receptor and insulin receptor substrate 1 (Fukuda M et al., 2010).

Multiple studies have reported that this glial cell reaction to hyperglycemia in an early event occurring in animal models of DR. In rats with streptozocin-induced diabetes, the glial reaction characterized by hyperplasia of Müller cells and GFAP overexpression, which is the key feature of gliosis, appeared after 6 to 15 weeks of diabetes (**Figure 12**) (Li Q et al., 2002; Lieth E et al., 1998; Rungger-Brandle E et al., 2000). GFAP expression was detected in the endfeet of the Müller cells after 6 to 7 weeks of diabetes (Li Q et al., 2002).
The loss of Müller cell functionalities has been shown to be correlated with a decrease in tight junctions between endothelial cells, increasing vascular permeability (Shen W et al., 2010).
The role of Müller cell reaction in DR pathogenesis is detailed below in the introduction section part II.

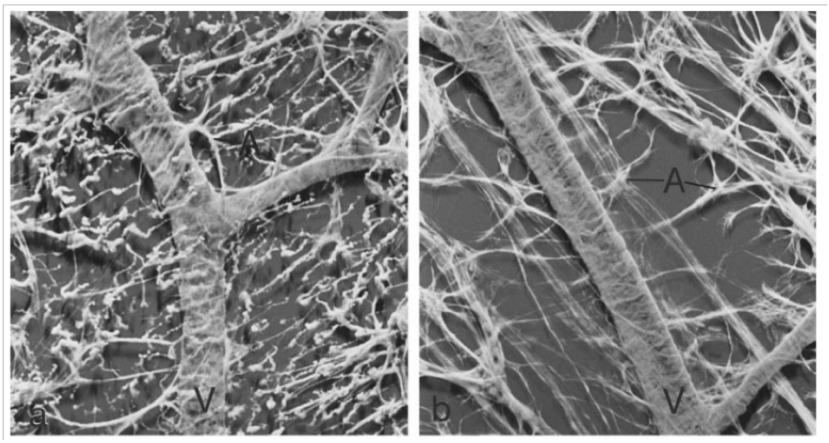

Figure 12: Expression of GFAP in retinal flatmounts of a 12-week diabetic rat (a) and an age-matched control (b). Double immunofluorescence to visualize GFAP (glia revealed by fluorescein isothiocyanate FITC) and a smooth muscle actin (medial layer of blood vessels V, revealed by Texas red). Analysis by confocal microscopy and simulated fluorescent image treatment reveal the abundance of filament bundles in Müller cells in the diabetic retina (b), as well as the scarcity of astrocytic filaments (A).
Adapted from Rungger-Brandle et al., IOVS 2000.

b) Microglial cell activation

Besides Müller cell reaction, microglial cells are also activated early in diabetic animal models (Rungger-Brandle E et al., 2000; Zeng XX et al., 2000). The activation of microglial cells is characterized by morphological changes including hypertrophy in cell bodies, thicker processes and shorter dendrites.

Zeng et al. also reported Müller cell and microglial reaction in streptozotocin-induced diabetic rats (Zeng XX et al., 2000). In this study, GFAP immunoreactivity was largely confined to astrocytes in the nerve fiber layer (NFL) and ganglion cell layer (GCL) in control rats whereas in diabetic rats GFAP immunostaining could be traced along the entire length of Müller cell processes, extending from the inner to the outer limiting membrane.
In diabetic rats, neuronal cells were reduced in both GCL and more importantly in the inner nuclear layer (INL). In control rats, microglial cells were distributed mainly in the NFL and GCL, whereas in diabetic rats, microglial number in different layers of the retina was significantly increased. Microglial cells activation is demonstrated by the hypertrophy of microglial cells after 1 month of diabetes, the number of cells increased after 4 months and their migration into the outer nuclear layer after 14 to 16 months (Zeng XX et al., 2000; Omri S et al. 2011). Authors concluded that microglial reaction in induced diabetes was elicited by neuronal cell loss in both GCL and INL as well as by some pathologic changes affecting the photoreceptors.

Rungger-Brandle et al. also detected glial cell reaction as early as 1 month after diabetes induction in streptozotocin-induced diabetic rats. They showed that the individual glial cell types react differentially to diabetes: Müller cells undergo hyperplasia preceding GFAP expression, microglial cells are activated, whereas astrocytes regress (Rungger-Brandle E et al., 2000). In this study, the leakage of the blood retinal barrier was observed at 2 weeks of hyperglycemia, the earliest time point investigated. The authors concluded that the leakage of the blood retinal barrier before glial reactivity suggests that glia are early targets of vascular hyperpermeability.

Gaucher et al. investigated blood retinal barrier permeability and retinal cell activity in vivo in another DR animal model. In mice with alloxan-induced diabetes, they found that changes in microglial cells morphology are the first detectable changes occurring in the retina, preceding

neuronal apoptosis and increase in blood retinal barrier permeability. The authors hypothesized that the sequence of retinal modifications early in DR may be first an early microglial activation, associated with electrophysiologic changes, followed by ganglion cell apoptosis and subsequent macroglial reaction (Gaucher et al., 2007).

Chen et al. the investigated early sequential changes of microglia in the retinas of 4-week, 8-week, and 12-week streptozotocin-induced diabetic rats. In this study, the proportion of activated microglia as well as the retinal Iba-1 mRNA expression increased significantly in diabetic rats at each time point, confirming that retinal microglia changes parallel with the progression of the disease in early-stage diabetic rats (Chen X et al., 2015).

Ganglion cells degeneration was attributed to glial reaction of Müller cells in many DR animal model studies (Asnaghi V et al., 2003, Li Q et al., 2002; Lieth E et al., 1998; Rungger-Brandle E et al., 2000; Zeng XX et al, 2000).
The spatial arrangement of glial cells closely to ganglion cell bodies and axons could favor an initial glial activation by compromised neurons, with release of free fatty acids, being a likely inducer. During long-standing diabetes, however, microglial cells are frequently found in outer retinal layers and in association with blood vessels (Thanos S et al., 1993). This behavior may be triggered by an increasingly damaged blood retinal barrier.

Anti-VEGF drugs may exert significant unsuspected effects on retinal microglia that play important and complex roles in the pathogenesis of retinal diseases. In another previous work, we investigated intravitreal anti-VEGF influence on retinal microglia and macrophage activation. To dissociate the effect of anti-VEGF on microglia and macrophages subsequent to its antiangiogenic effect, we chose a model of acute intraocular inflammation (Couturier A et al., 2014). We found microglia and macrophages expressed VEGF receptors, and that intra-vitreal anti-VEGF influenced the microglia and macrophage activation state (**Figure 13**). Considering that anti-VEGF drugs are repeatedly injected in the vitreous of patients with retinal diseases, part of their effects could result from unsuspected modulation of the microglia activation state.

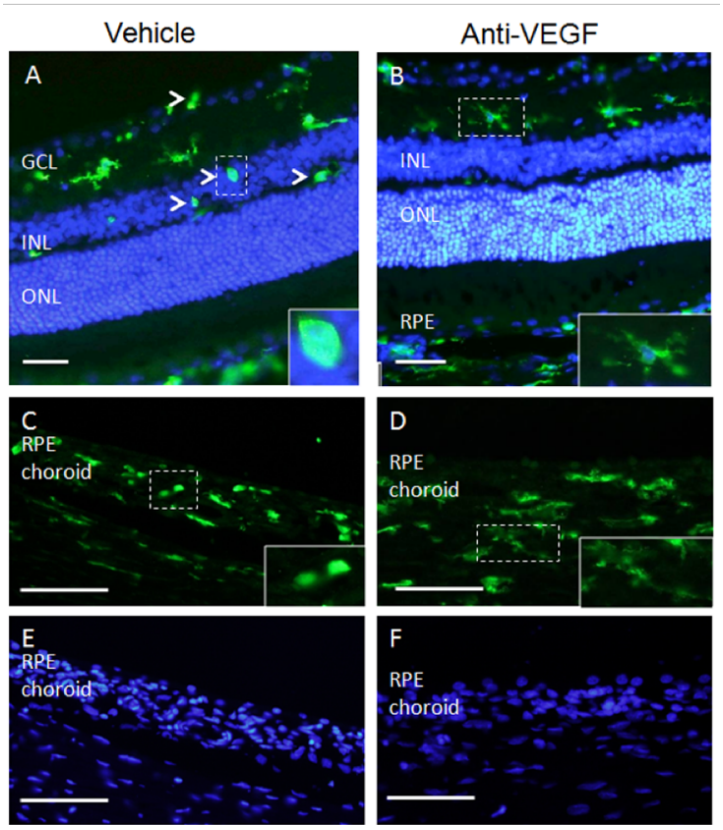

Figure 13: Ionized calcium-binding adaptor molecule 1 immunostaining of microglia and macrophages in endotoxin-induced uveitis at 24 h after lipopolysaccharide injection. **A**. Retina section after vehicle intravitreal injection; in green ionized calcium-binding adaptor molecule 1 (IBA1) staining and in blue nuclei are stained with 4',6-diamidino-2-phenyl-indole (DAPI). Arrowheads indicates round IBA1-positive cells, magnified in the inset. Bar = 50 µm, GCL = ganglion cell layer, INL = inner nuclear layer, ONL = outer nuclear layer. **B**. Retina section after anti-vascular endothelial growth factor (VEGF) intravitreal injection. IBA1-positive cells (in green) are ramified and elongated in the inner retina as magnified in the inset. Nuclei are stained in blue with DAPI. Bar = 50 µm, GCL = ganglion cell layer, INL = inner nuclear layer, ONL = outer nuclear layer. **D**–**F**. Choroid section after vehicle intravitreal injection stained with IBA1 (**D**) and DAPI (**F**), showing round amoeboid cells (magnified in the inset). Bar = 50 µm, RPE = retinal pigment epithelial cells. **E**–**G**. Choroid section after anti-VEGF intravitreal injection stained with IBA1 (**E**) and DAPI (**G**), showing round elongated ramified cells (magnified in the inset). Bar = 50 µm, RPE = retinal pigment epithelial cells. Adapted from Couturier A et al., Mol Vis 2014.

No animal model recapitulates all features of human diseases, but the fact that in a specific model of acute inflammation, anti-VEGF exerts direct effects on the activation of microglia and macrophages in the retina and the choroid suggests that similar effects could intervene in more complex retinal diseases where sub-clinical inflammation and microglial activation are suspected to be pathogenic, such as in DR. Microglia deactivation by anti-VEGF could be a mechanism that mediates this beneficial effect.

II. Role of dyslipidemia in diabetic retinopathy

1. Dyslipidemia-induced inflammation

Diabetes is a multifactorial pathology and dyslipidemia was shown to be one of the risk factors in the development of type 2 diabetes.

Epidemiologic studies have shown the effects of hyperglycemia, hypertension, and dyslipidemia on the incidence and progression of DR and macular edema. The Diabetes Control and Complication Trial (DCCT; NCT00360815) showed that intensive metabolic control reduces the incidence and progression of DR. Although the glycated-hemoglobin level is the strongest risk factor for predicting the progression of DR, glycated hemoglobin accounted for only 11% of the risk of DR in DCCT (Hirsch IB and al., 2010). Similarly, the values of glycated hemoglobin, blood pressure, and total serum cholesterol together account for only 10% of the risk of DR in the Wisconsin Epidemiologic Study of DR (Klein R, 2008).

In addition to hyperglycemia, type 2 diabetes is also commonly associated with lipid disorders such as hypertriglyceridemia and increased free fatty acids (Chehade JM et al., 2013).

Diabetic patients were demonstrated to have elevated serum level of saturated fatty acids, which was associated with an increased risk of DR (Sasaki M et al., 2015).

This is in accordance with the results of the Fenofibrate Intervention and Event Lowering in Diabetes (FIELD) and the Action to Control Cardiovascular Risk in Diabetes (ACCORD) studies, showing that fenofibrate, a lipid lowering drug PPAR-α agonist, reduces the risk of progression by up to 40% among patients with non-proliferative retinopathy, (Keech AC et al., 2007; The ACCORD Study Group and ACCORD Eye Study Group. 2010). Whether the mechanism of action underlying this preventive effect of fenofibrate is related to its lipid-

lowering action remains unclear. The AMP-activated protein kinase (AMPK) activation could be one of the mechanism given that fenofibrate is an AMPK activator.

Indeed, an imbalance in lipid metabolism is correlated with chronic inflammation in most tissues including the retina. In human and animal models, diabetes increases fatty acid concentrations in systemic circulation and tissues, leading to inflammation, insulin resistance, and disease progression. Previous studies have demonstrated that fatty acids are diabetes-relevant stimulus in retinal endothelial cells and in extra-ocular tissues (Boden G, 2006; Decsi et al., 2007).
Free fatty acid is known to upregulate proinflammatory cytokine expression (Ralston JC et al., 2016) and as previously described inflammation is now known to have a pivotal role in the pathogenesis of DR (Rübsam A et al., 2018).

2. Effect on retinal endothelial and glial cells

Dyslipidemia-induced inflammation is associated with endothelial dysfunction and apoptosis in diabetes (Van den Oever et al., 2010).

Free fatty acids, in addition to hyperglycemia, have been demonstrated to induce apoptosis in retinal pericytes, the first cells lost in the diabetic retina (Cacicedo JM et al., 2005). Palmitate, the most abundant saturated fatty acid in human, was mainly studied as a DR-relevant stimulus (Xu L et al., 2007; Tikhonenko M et al., 2010; Korani M et al., 2012).
Cacicedo et al., reported that incubation with the saturated fatty acid palmitate, but not the monounsaturated fatty acid oleate, elicited cytotoxicity in a manner dependent on oxidative stress, NF-κB activation, and ceramide accumulation (Cacicedo JM et al., 2005). More recently, the same authors showed that AMPK downregulated these pathways and, in doing so, protected pericytes from apoptosis (Cacicedo JM et al., 2011).

Palmitate was also demonstrated to induce apoptosis in microvascular endothelial cells, which is another early key event inducing vascular lesions in DR (Yamagishi S et al., 2002, Lu Z et al., 2018).

Fatty acid were then shown to interact not only with endothelial cells but also with retinal glial cells. Indeed, incubation with free fatty acids, in particular linoleic acid, have been shown to increase IL-6, IL-8 and TNF-α secretion by Müller cells (Capozzi ME et al., 2016; Yong PH et

al., 2010). The signaling pathways responsible for these effects have not been yet fully elucidated.

Recently, Capozzi et al., have shown the effectiveness of palmitic acid (PA) as a stimulator of primary human Müller cells, alone and in combination with high glucose (Capozzi ME et al., 2018). In this study, RNA sequencing identified multiple signaling pathway, including NFκB signaling and inflammation, angiogenesis and MAPK signaling, that were stimulated by PA, while high glucose alone did not significantly alter these DR-relevant signaling pathways (**Figure 14**).

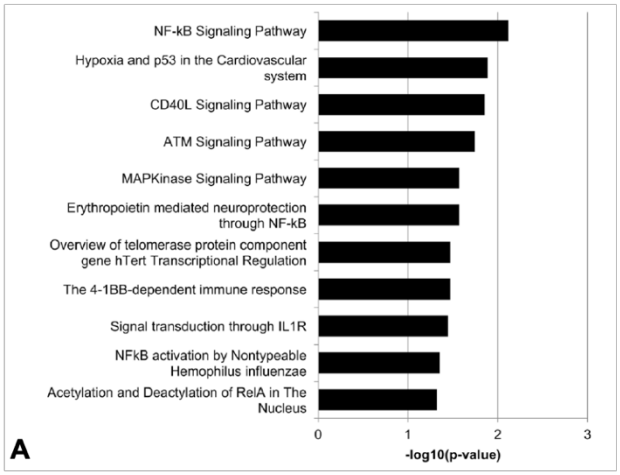

B

Ensembl Gene ID	Gene Target	Log2fold change	Adj p value
ENSG00000081041	CXCL2	5.131169228	3.48E-121
ENSG00000180535	BHLHA15	4.970842312	2.06E-107
ENSG00000167861	HID1	4.556667723	4.04E-110
ENSG00000078081	LAMP3	4.125085146	3.52E-55
ENSG00000173110	HSPA6	4.097445282	6.88E-64
ENSG00000167772	ANGPTL4	3.943015061	0
ENSG00000004799	PDK4	3.804721573	1.73E-73
ENSG00000163734	CXCL3	3.763486125	9.79E-57
ENSG00000130487	KLHDC7B	3.660859835	4.54E-51
ENSG00000162772	ATF3	3.640394145	0
ENSG00000169429	CXCL8	3.546291509	4.45E-97
ENSG00000147872	PLIN2	3.366381211	7.28E-273
ENSG00000137491	SLCO2B1	3.359650884	1.19E-23
ENSG00000099958	DERL3	2.985336774	9.33E-42
ENSG00000133134	BEX2	2.952925525	4.57E-46

Figure 14: Pathways and genes upregulated in primary human Müller cells cultured with palmitic acid (PA) and low glucose for 24 hours. **A.** Biocarta pathways enriched by PA-treatment alone. Pathway enrichment was determined using DAVID v6.7 with a $p < 0.05$. Eleven pathways were significantly upregulated in response to PA treatment compared to BSA control. **B.** List of the top 15 upregulated genes in PA-treated Müller cells compared with BSA controls. Log2 fold change is the average from all statistic tests. Adjusted p-value is reported from EdgeR analysis. Adapted from Capozzi ME et al., Scientific Reports 2018

Besides fatty acids, lipopolysaccharide (LPS) is another potent inflammatory mediator in DR (Lu Z et al., 2018). LPS was shown to stimulate proinflammatory cytokine expression in human retinal microvascular endothelial cells (Zhang HY et al., 2014), pericytes and microglia (Ding X et al., 2017). LPS has been implicated in DR as several clinical studies showed that polymorphism of Toll-like receptor 4 (TLR4), a specific receptor for LPS, is associated with DR (Buraczynska M et al., 2009; Singh K et al., 2014; Xu Y et al., 2015).

Recently, Lu Z et al. demonstrated that palmitate alone exerted a robust and sustained stimulation on proinflammatory cytokine expression in human retinal endothelial cells. In addition, Palmitate interacts with LPS to further increase cytokine expression via free fatty acid receptor-mediated inflammatory signaling and ceramide production in human retinal endothelial cells (Lu Z et al., 2018).

3. Effect on retinal pigment epithelium cells

Lipid metabolism was also pointed out to be responsible for the increased oxidant species in senescent cells. Key enzymes in the fatty acid synthesis pathway are known to be regulated by glucose; and high glucose could increase lipid droplets in many cell types (Chen Q et al., 2018). Recent report from Donato et al. demonstrated that several genes and non-coding regulatory RNA involved in regulation of lipid metabolism in oxidative stressed retinal pigment epithelium (RPE) cells exhibit expression alterations (Donato L et al., 2018).

Another recent study, Chen Q et al., reported that high glucose induces lipid accumulation in RPE cells and RPE dysfunction. They found that high glucose led to senescence of RPE cells but not apoptosis by the accumulation of ROS (**Figure 15**) (Chen Q et al., 2018).

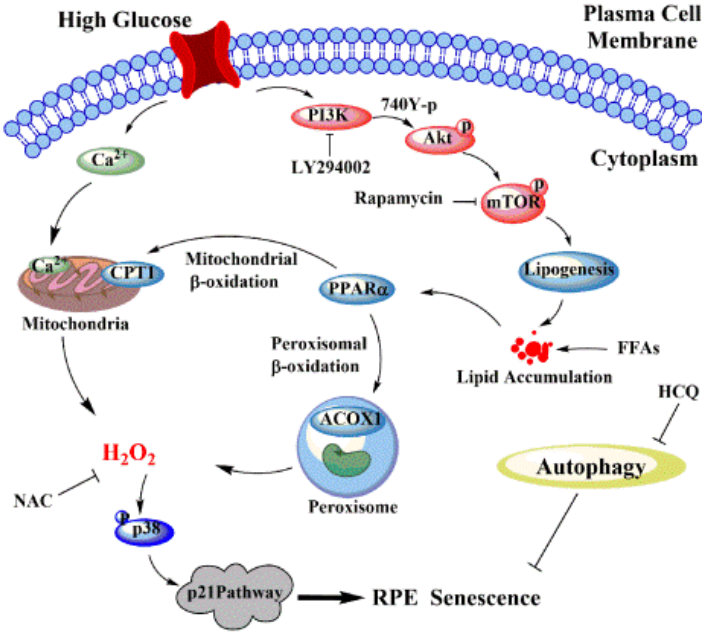

Figure 15: High glucose induces lipid accumulation in retinal pigment epithelium (RPE) cells and RPE cell senescence. ARPE-19 treated with high glucose present accumulated lipid droplets, and subsequent lipid oxidation advanced by up-regulating the key enzymes of fatty acids oxidation made this ROS accumulation more serious. Accumulated lipid droplets are regulated by PI3K/AKT/mTOR pathway via increasing the expression of fatty acid synthase. Meanwhile, high glucose induced autophagy in ARPE-19 with the treatment of glucose for 48 h. An autophagy inhibitor (HCQ) further aggravates the senescence with an increase of oxidant species, which indicates that autophagy played a cytoprotective role by resisting oxidative stress caused by high glucose.

4. Protective role of epoxygenated fatty acids

Diabetes is known to alter multiple pathways involved in endogenous fatty acid metabolism. Tissues can metabolize fatty acids to biologically active lipid mediators through the cyclooxygenase (COX), lipoxygenase (LOX) or cytochrome P450 epoxygenase (CYP) pathways. The implication of these enzymes in DR has been largely studied. CYP enzymes are endoplasmic reticulum membrane-bound monooxygenases that oxidize various substrates, including polyunsaturated fatty acids. Two of these, arachidonic acid (AA) and docosahexaenoic acid (DHA), are found in high abundance in the retinal vasculature and may be of importance to retinal vasculature homeostasis (Lecomte M et al., 1996). A subset of CYP enzymes epoxygenate AA and DHA produce epoxyeicosatrienoic acids (ETT) and epoxydocosapentaenoic acids (EDP) respectively. The ETT products are known to exert anti-inflammatory activities in vascular beds, including reduced VCAM1 and ICAM1 expression (Falk JR et al., 2003). More recently, EET and EDP were shown to inhibit TNF-α-induced leukocyte adherence *in vitro* and leukostasis *in vivo* (Capozzi ME et al., 2016). Reduced levels of EET are observed in the vitreous of diabetic patients (Schwartzman ML et al., 2010).

III. Müller Glial Cells

1. Müller cells in healthy retina

Müller cells are radial glial cells that reside in the adult central nervous system. They have been discovered by Heinrich Müller, who described them in 1851 as glial fibers that supported the tissue structure. Since then, the knowledge about the functions of these cells in the retina has increased exponentially and Müller cells are now known to be essential for vision.

They have the basic bipolar morphology of radial glial cells with the complete set of glial processes/contact. Müller cells are situated transversally to all nuclear and plexiform layers. Their stroma is generally located in the inner nuclear layer (INL) (**Figure 16**) (MacDonald RB et al., 2017). Two stem processes extend into opposite directions. The outer stem process reaches to the subretinal space, into which it sends microvilli. The inner stem process contacts the vitreal surface where it forms an endfoot forming the inner limiting membrane (ILM). Both processes and stroma extend side branches which contact or ensheat all neuronal elements of the retina as well as the blood vessels.

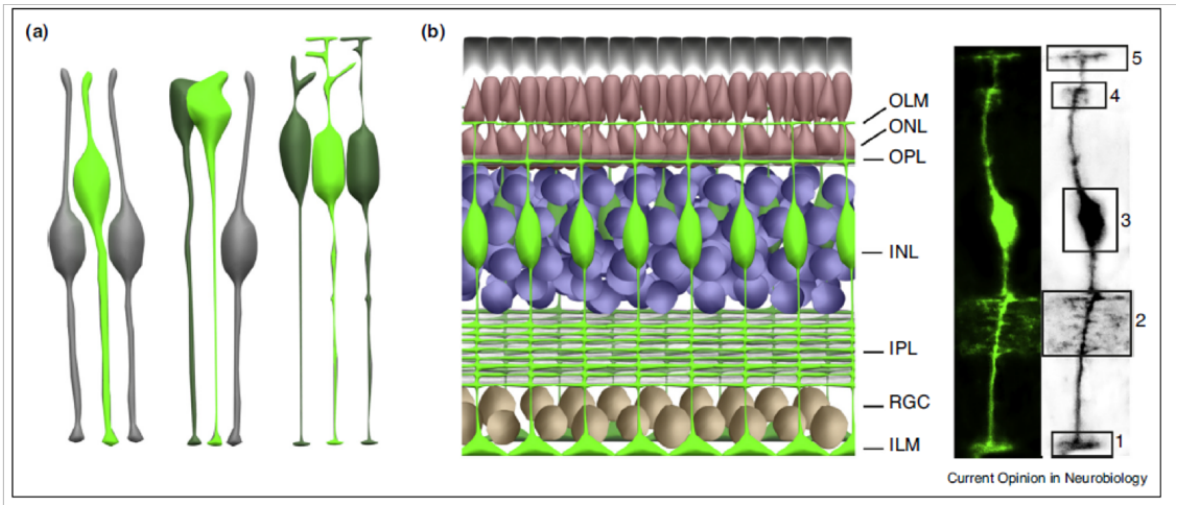

Figure 16: The pattern and morphology of the Müller glial cells in the retina. **(a)** Development of Müller cells (green) from retinal progenitor cells. **(b)** Schematic showing the general organization of the vertebrate retina. Müller cells span the entirety of the three neural layers from the apical outer limiting membrane (OLM) to the basal inner limiting membrane (ILM). The morphology of a single Müller cell (example from zebrafish) can be separated into five distinct domains: (1) The basal endfoot forming the ILM of the retinal ganglion cell (RGC) layer; (2) the fine processes contacting synapses in the inner plexiform layer (IPL); (3) the cell

body amongst neurons in the inner nuclear layer (INL); (4) the fine processes contacting synapses in the outer plexiform layer (OPL); (5) an apical process around photoreceptors. Adapted from MacDonald RB et al., Current Opinion in Neurobiology 2017.

Reichenbach et al. described Müller cells as the center of a columnar subunit, the smallest anatomical and functional structure needed for the transduction of the visual signals (Reichenbach A et al., 1995). The interaction among the cells of this columnar subunit guarantee the maintenance of homeostasis and the initiation of a protective response in case of injury.
Indeed, Müller cells have a variety of retinal specific functions, including developmental, physiological, structural and even optical. Müller cells have also been implicated in many retinal diseases and have the ability to regenerate the retina in some vertebrate species (Wan J et al., 2016; Hamon A et al., 2016).

a) Role in neuronal metabolism and protection

The position of Müller cells within the retina enables them to constitute an anatomical and functional link between retinal neurons and the retinal blood vessels for exchanging molecules (Vecino E et al., 2016). Neuronal and Müller cells interplay is considered a mutual benefit relationship. This is based on the fact that certain processes are regulated by some enzymes present in Müller cells and others in neurons; and some feedback signals are required by both cells. Müller and others glial cells also secrete several trophic factors implicated in survival and activity of nerve cells (Harada T et al., 2002; Toft-Kehler AK et al., 2018).

Müller cells are crucial for neuronal metabolism. They provide energy metabolites to neurons as they synthetize glycogen by glycogenesis, store it and then release glucose on demand (**figure 17B**). Photoreceptors transform glucose into lactate, which is the main source of carbons for gluconeogenesis in Müller cells that have a low expression of pyruvate kinase in the outer retina (Hurley JB et al., 2015; Lindsay KJ et al., 2014).

In the retina, most of the excitatory transduction signals are mediated by glutamate. Müller cells participate in the uptake of this amino acid from the synaptic cleft, avoiding excitotoxicity. Moreover, glutamate is recycled to glutamine in Müller cells and returned to neurons for neurotransmitter synthesis (**Figure 17C**) (Toft-Kehler AK et al., 2018).

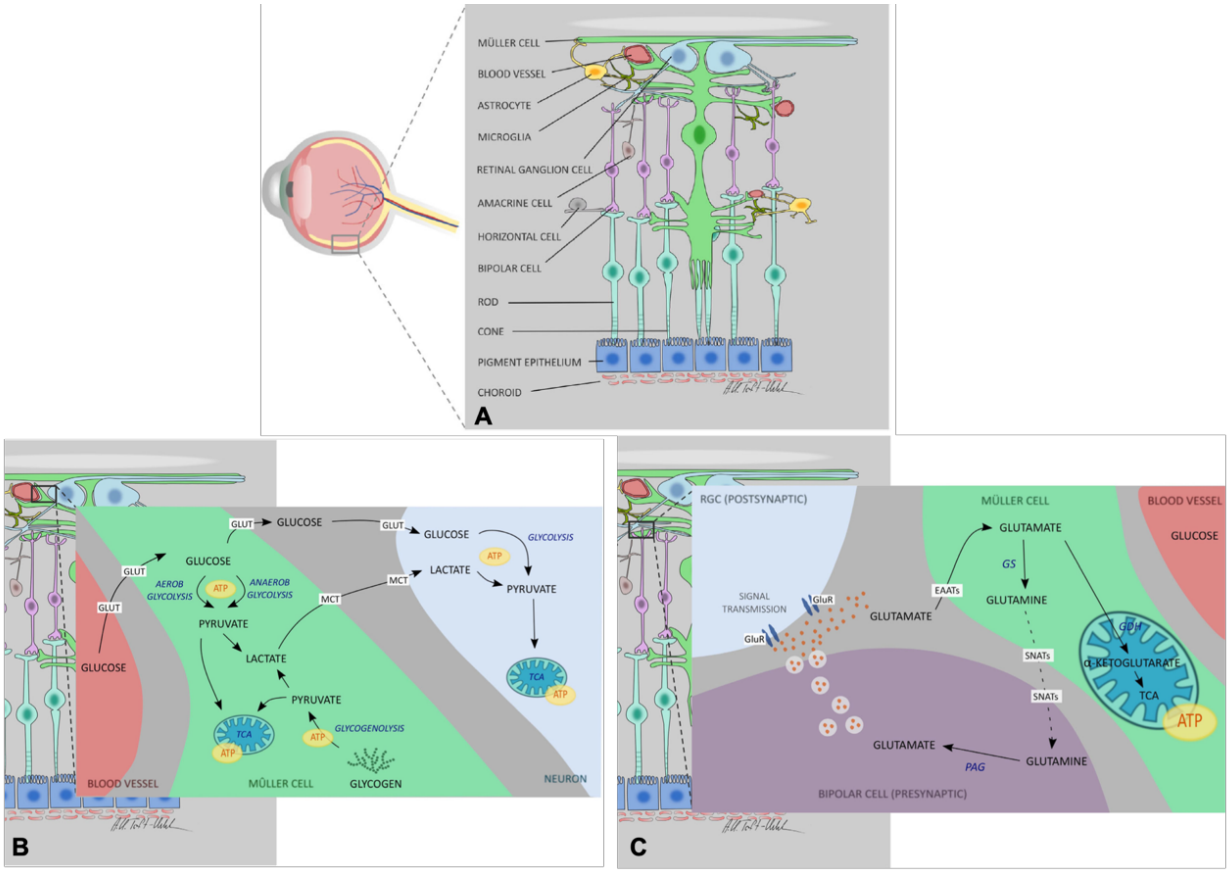

Figure 17: Müller cell-Neuron metabolic partnership in the inner retina.

A. The anatomy of Müller cells and their interrelation their close relationship with retinal ganglion cells (RGCs) in the inner limiting membrane, as well as with photoreceptors in the outer limiting membrane.

B. Illustration of Müller cell-neuron metabolic interaction in the retina. Glucose from the circulation is taken up by glucose transporters (GLUTs) represented in capillary endothelial cells and Müller cells. Glucose is converted to pyruvate, which is further metabolized into lactate by glycolysis (referred to as the Warburg effect). Lactate is transported to the neurons by monocarboxylate transporters (MCTs) and is included as an energy substrate in the neuronal metabolism by its conversion to pyruvate followed by entrance in the TCA cycle and the oxidative phosphorylation process. Such transportation of lactate between Müller cells and neurons is known as the lactate shuttle. An additional energy source is the endogenous glycogen reservoir in Müller cells. Glycogenolysis rapidly degrades glycogen to glucose-6-phosphate, and the subsequent glycolysis produces pyruvate, which again may be metabolized in the TCA cycle or reduced to lactate followed by a lactate shuttling to surrounding neurons by MCTs.

C. Illustration of the Glutamine-glutamate cycling. Neurotransmitter glutamate is released from the presynaptic neurons and stimulates glutamate receptors (GluRs) on the postsynaptic neuron,

and the glutamatergic signaling is terminated by glutamate uptake into Müller cells. The glutamate is taken up by excitatory amino acid transporters (EAATs) and proceeds into distinct metabolic pathways. Glutamate can be amidated to glutamine by the Müller cell-specific enzyme glutamine synthetase (GS) and released to the extracellular space through the sodium-coupled neutral amino acid transporters (SNATs). Following being shuttled back to neurons, glutamine is reconverted to glutamate by phosphate-activated glutaminase (PAG) and used to replenish the neuronal neurotransmitter pool. Subsequently, vesicular glutamate molecules can be released from the presynaptic neuron in order to stimulate the postsynaptic neuron inducing a novel neuronal signal transmission. Alternatively, glutamate may be converted to the TCA cycle intermediate α-ketoglutarate through glutamate dehydrogenase (GDH) or an aminotransferase. Through such entry in the TCA cycle, glutamate may function as an alternative energy substrate during insufficient glucose availability.
Adapted from Toft-Kehler AK et al., Mol Neurobiol 2018.

GABA, an inhibitory neurotransmitter is also degraded by Müller cells via the citric acid cycle (Reicheinbach A and Bringmann A, 2016).
In addition, Müller cells synthetize glutathione, a molecule involved in the reduction of reactive oxygen species (ROS). Recently, it was described that glutathione also activates calcium-mediated signaling (Freitas HR et al., 2016).

Müller cells are also crucial for photoreceptor activity, as they actively participate in the recycling of photopigments from photoreceptors, catalyzing the conversion of all-trans-retinal in 11-cis-retinol by retinaldehyde-binding protein. The 11-cis-retinol is then returned to photoreceptors to restart the visual cycle (Xue Y et al., 2015). Given their transversal morphology, it is also believed that Müller cells are responsible for guiding the beam of light, as an optic fiber, directly to cones and rods (Agte S et al., 2011).

The **figure 18** summarizes the main functional relationships between retinal glial cells and neurons (Vecino E et al., 2016).

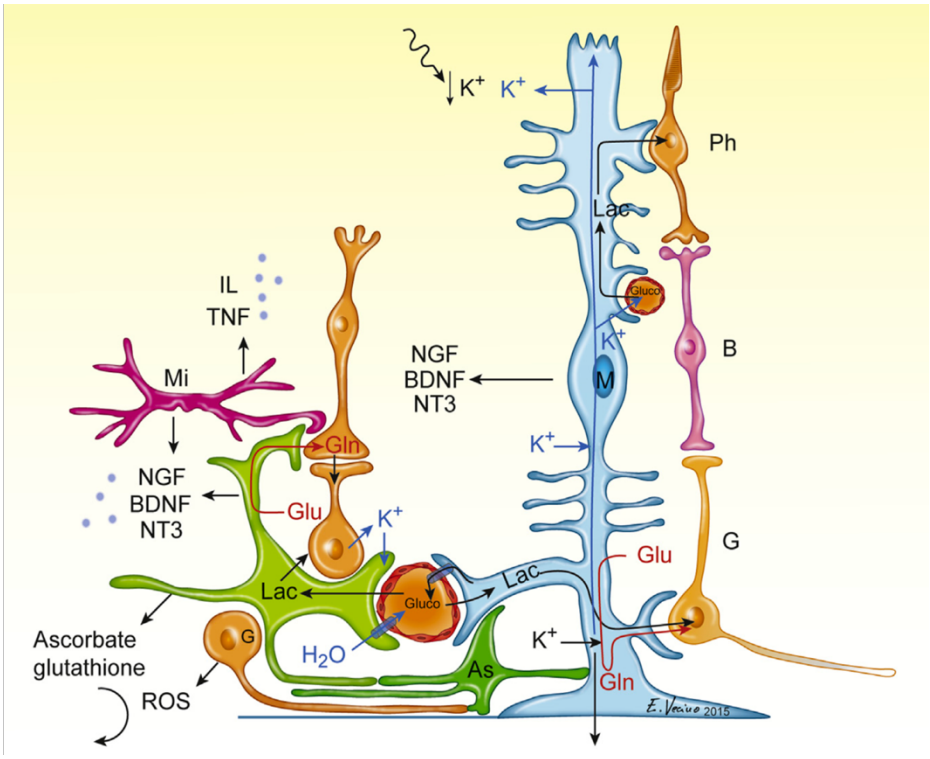

Figure 18: Illustration summarizing the main interactions of glial cells with neurons. Scheme showing glucose metabolism, K. homeostasis, H2O, glutamate (Glu) to glutamine (Gln) metabolism, the secretion of trophic factors and interleukins: A (astrocytes, in green), B (bipolar cells), G (ganglion cells), M (Müller cells, in blue), Mi (microglia, in red), Ph (photoreceptors). From Vecino E et al., Progress in Retinal and Eye Research 2016.

b) Role in hydro electrolytic homeostasis

Müller cells is part of the inner blood retinal barrier and achieve hydro electrolytic balance of retinal tissue through the regulation of the extracellular ion concentration and pH. Indeed, Müller cells display ion channels, aquaporins and purinergic transporters, which allow water uptake and ion transport (Vogler S et al., 2016). The Müller cell plasmatic membrane contains ions channels and transmembrane water transporters which regulate the influx and efflux of water, potassium and sodium to maintain extracellular space homeostasis and prevent neuronal swelling. A major functional role of Müller cell in the retina is to buffer the activity-dependent variations in the extracellular potassium level via permission of transcellular potassium currents (Newman EA et al., 1984).

c) Role in vasculature and angiogenesis

The radial disposition of Müller cells enables the interaction with the vasculature in all plexus, where Müller cell protrusions wrap up vessels.

During development, Müller cells are implicated in the regression of the hyaloid vasculature and in retinal angiogenesis, by secreting metalloproteinases and trophic factors (Jacobo SM and Kazlauskas A, 2015; Lorenc VE et al., 2015).
Müller cells also secrete thrombospondin-1 to stop endothelial proliferation at the end of the angiogenic process (Yafai Y et al., 2014).

The endothelial-glial cell interaction may be the most important regulator of vessel tone in the retinal, which vessels lacks autonomic innervation. After a light stimulus, neurotransmitters stimulate glial cells that release vasoactive factors and enable an increase of the blood flow. Indeed, glial cells are able to release ATP that constrict arterioles, while calcium signaling dilate vessels (Biesecker KR et al., 2016, Kur J and Newman EA, 2014).

Together with endothelial cells and pericytes, Müller cells constitute the blood retinal barrier and prevent pathogens contacting with the retinal cells.

d) Role in retinal regeneration

Heterogeneity in the Müller cells population has been identified in zebrafish retinas: 3 types of Müller cells were detected with different expression of the transcriptional factors (STAT3, Asc11a) and RNA-binding proteins (Lin28a). These proteins enable Müller cells to re-enter the cell cycle, dedifferentiate to progenitor cells and originate new neurons.

In contrast, Müller cells mammalian retinas have a quiescent phenotype and fail to renew neurons. Stimulation of Müller cell reprogramming could be a future promising therapy for restoring neurons in the retina (Beach KM et al., 2017; Reyes-Aguirre LI and Lamas M, 2016).

2. Müller cells implication in diabetic retinopathy pathophysiology

Hyperglycemia was reported to induce several changes in Müller cells: upregulation of GFAP, which is indicative of Müller cell activation, alteration of the aquaporin expression and reduction of the interaction between insulin receptor and insulin receptor substrate 1 (Fukuda M et al., 2010; Ola MS, 2014).
The loss of Müller cell functionalities has been shown to be correlated with a decrease in tight junctions between endothelial cells, increasing vascular permeability (Shen W et al., 2010).

Besides hyperglycemia, hypoxia also induces an increase of GFAP and a reduction in glutamine synthetase in Müller cells, inducing a neuronal degeneration in the OIR mouse model (Ridano ME et al., 2017).

a) Inflammatory response

Müller glial cells are immunocompetent cells implicated in retinal inflammatory reaction to injury, together with microglia and astrocytes.
In vitro studies have shown that the receptor of the advanced glycation end product (AGE) was overexpressed in Müller cells exposed to high glucose and triggered a mitogen-activated protein kinase (MAPK) signaling pathway for pro-inflammatory cytokines synthesis (Zong H et al., 2010).
Müller glial cells are a significant source of numerous factors including inflammatory factors, that might play an early role in the onset of the inflammatory process in DR (Rübsam A et al., 2018). It has been reported elevated levels of the adhesion molecules ICAM-1 and the neutrophil chemotactic MCP-2, molecules also produced by Müller cells and involved in leukostasis.

IL-1β is believed to be a key regulator in the retinal inflammatory response. In vitro studies have revealed that high glucose conditions induce IL-1β secretion by endothelial cells, which induce an autocrine and paracrine upregulation of IL-1β expression in Müller cells and astrocytes (Liu Y et al., 2012).

IL-1β is also the only cytokine with the ability to stimulate IL-8 production in Müller cells through the activation of the p38 MAPK pathway (Liu X et al., 2014). IL-8 is responsible for the amplification of the inflammatory response, recruiting leucocytes to the injured tissue.
IL-1β has also been recently shown to downregulate glutamate uptake by decreasing Kir4.1 and GLAST transporter expression in Müller cells (Chen C et al., 2014).

In addition, in vivo studies on streptozocin-induced diabetic rats have shown that more than 70 genes implicated in the pro-inflammatory pathway were upregulated in Müller cells (Gerhardinger C et al. 2005).

Müller cells expressed IL-17A receptor, which stimulation induces VEGF secretion. IL-17A secreted by lymphocytes T helper 17 was found in plasma and vitreous sample of diabetic patients (Hang H et al., 2014; Takeuchi M et al., 2015). The intravitreal injection of IL-17A in Ins2Atika diabetic mice increased GFAP expression, decreased glutamine synthetase enzyme and aggravated blood retinal barrier breakdown (Qiu AW et al., 2016).

Zhong et al. explored the role of endoplasmic reticulum (ER) stress and the signaling pathway of ER stress-induced activating transcription factor 4 (ATF4) in the regulation of Müller cell-derived inflammatory mediators in diabetic retinopathy (Zhong H et al., 2010). In this study, in diabetic animals, elevated ER stress markers, ATF4, and VEGF expression were partially localized to Müller cells in the retina. In cultured Müller cells, high glucose induced a time-dependent increase of ER stress, ATF4 expression, and inflammatory factor production.
Inducing ER stress or overexpressing ATF4 resulted in elevated intracellular adhesion molecule 1 and VEGF proteins in Müller cells. In contrast, alleviation of ER stress or blockade of ATF4 activity attenuated inflammatory gene expression induced by high glucose or hypoxia. The authors concluded that ER stress and ATF4 play a critical role in retinal inflammatory signaling and Müller cell-derived inflammatory cytokine production in diabetes.

b) Gliosis

Reactive gliosis of Müller cells is their first answer to a harmful stimulus. This process is a protective response and takes place in early stages of DR. However, when the injured stimulus persists, the chronic changes and secretion of various factors may participate to damage of the retina.

Reactive gliosis is defined as the morphological and biochemical changes in glial cells after injury. The key feature of gliosis in Müller cells is the upregulation of glial fibrillary acidic protein (GFAP), nestin and vimentin (Coorey NJ et al., 2012). GFAP was increased in vivo, in retinas of streptozocin-induced diabetic rats, as well as in vitro in Müller cells exposed to high glucose (Layton CJ et al., 2006). The polyol pathway, with an increase of aldose reductase converting glucose to sorbitol, has been demonstrated to be mediating the rise in GFAP in diabetic rats (Asnaghi V et al., 2003).
GFAP was also shown to be increased in Müller cells after retinal explants exposure to AGEs (Lecleire-Collet A et al., 2015).

Vimentin expression is also increased in the retina of streptozocin-induced diabetic rats, as well as in cultured Müller cells under high glucose condition (Zhou T et al., 2017).

α_2Macroglobulin (α_2M) which is considered to be a biomarker of DR progression can be synthesized by Müller cells (Barcelona PF et al., 2016; Liu X et al., 2014). α_2M induces GFAP overexpression by activating the membrane receptor low-density lipoprotein-related protein 1 (LRP1) (Barcelona PF et al., 2011). α_2M/LRP1 system may activate reactive gliosis as an early response to retinal injury. α_2M was detected in vitreous of PDR patients, showing that α_2M plays a key role in the neovascular phase (Sanchez MC et al., 2007).

Hypertrophy is also a gliotic manifestation leading to edematous retina. In diabetic retina, the downregulation of Kir 4.1 channels in perivascular processes of Müller cells, which mediate potassium efflux to blood, seems to be the main reason for hydroelectrolytic imbalance.
In addition, changes in the localization of Kir 4.1, aquaporins 1 and 4 alter synaptic activity and induce neuronal apoptosis in DR (Bringmann A et al., 2002; Fukuda M et al., 2010).

Chronic hyperglycemia induces loss of glial-neuron interactions, leading to massive gliotic response. This massive gliotic response is characterized by migration and proliferation of Müller cells that acquire a fibroblast and contractile phenotype. This results in the formation of epiretinal membranes. Different stimuli of this migration and proliferation have been identified, including α_2M, IGF-1 and lipids (Sphingosine-1-Phosphate) (Barcelona PF et al., 2011; Lorenc VE et al., 2015; Simon MV et al;, 2015). IGF-1 is now known to be an important contributor in DR pathogenesis, as it enhances VEGF synthesis (Treins C et al., 2005) and extracellular

matrix remodeling via MMP-2 activity (Lorenc VE et al., 2017). Indeed, IGF-1 regulate MMP-2 activity in Müller cell filopodia to facilitate the migration of microglial cells.

c) Trophic factors

The secretion of trophic factors by Müller cells was shown to be affected in the context of DR. First, VEGF is the main factor implicated in DR pathogenesis and is synthetized by several cells in the retina: endothelial cells but also Müller cells, astrocytes, retinal pigmented epithelium and ganglion cells (Wang J et al., 2010). High level of glucose but also fatty acids (oleic and linoleic acid, palmitic acid) induce increased VEGF secretion by Müller cells (Capozzi ME et al., 2016; Capozzi ME et al., 2018). ROS levels have been also shown to be implicated in the increase of VEGF synthesis by Müller cells (Fu D et al., 2016). While anti-VEGF treatment has been shown to reduce neovascularization in the OIR model, it has no effect on Müller cell activation and neuronal damage (Ridano ME et al., 2017).
The VEGF secreted by Müller cells is believed to specifically mediate pathological changes in DR: it induces the expression of pro-inflammatory cytokines such as TNF-α and intercellular adhesion molecule (ICAM)-1 (Wang J et al., 2010). This was confirmed by reduced occurrence of newvessels and conserved retinal function in mice VEGF KO only in Müller cells that followed the OIR model (Bai Y et al., 2009).

Insulin-like growth factor 1 (IGF-1) is also an important trophic factor contributing to DR pathogenesis. In a transgenic mouse model overexpressing intraocular IGF-1, a progressive degeneration of nerve cells was observed (Villacampa P et al., 2013), as well as a loss of pericytes and the occurrence of pre-retinal neovascularization (Ruberte J et al., 2004). IGF-1 participate in newvessel formation by enhancing VEGF synthesis (Treins C et al., 2005) and MMP2-activity in Müller cells (Lorenc VE et al., 2017).

Increased evidences showed that the precursor of nerve growth factor (NGF), pro-NGF, plays an important role in the development of vascular, neuronal and inflammatory alterations of DR (Subirada PV et al., 2018). Indeed, it has been demonstrated that oxidative stress reduces MMP-7 activity, a protease secreted by Müller cells and cleaving the pro-nerve growth factor (NGF) (Ali TK et al., 2011). The misbalance between pro-NGF and NGF leads to neurodegeneration and blood-retinal barrier breakdown in streptozocin-induced diabetic rats. They also reported high level of pro-NGF in the aqueous humor of patients with proliferative

DR (Ali TK et al., 2011). In this study, treatment of diabetic animals with atorvastatin restored activity of MMP-7 and hence the balance between proNGF and NGF, allowing preservation of blood-retinal barrier integrity and preventing neuronal cell death.
A study in non-diabetic mice showed that pro-NGF induced TNF-α release from glial cells and subsequent retinal ganglion cell death (Lebrun-Julien F et al., 2010).

Zhu et al. explored the effect of high glucose concentration on the expression of glial cell line-derived neurotrophic factor (GDNF) and its family ligand receptors (GFRs) GFRα1 and GFRα2 in Müller cells (Zhu X et al., 2012). They found that the expression levels of GDNF and GFRα1 mRNA and protein increased gradually over time under high, whereas the upregulation in GFRα2 expression was observed only in the early stage of high glucose conditions. The authors concluded that Müller cells can synthesize GDNF and GFRs under high glucose conditions, and GDNF may play important role in protecting Müller cells during the early stage of diabetic retinopathy.

Recent investigations have focused on the pigment epithelium-derived factor (PEDF), a neuroprotective and anti-angiogenic trophic factor synthetized by the retinal pigmented epithelium cells but also by Müller cells. The secretion of PEDF by Müller cells was shown to activate the NF-κB signaling pathway, avoiding ganglion cell apoptosis in hypoxic conditions (Unterlauft JD et al., 2014). PEDF is also able to prevent the formation of newvessels and the breakdown of blood-retinal barrier by upregulating tight-junction proteins (Ibrahim AS et al., 2015). These beneficial functions are impaired in DR due to a reduced secretion of PEDF (Yoshida Y et al., 2009).

The role of main secreted trophic factors in retinal diseases has been recently highlight in a review by Araujo et al., including the role of factors secreting by Müller cells in DR (**figure 19**) (Araujo RS et al., 2018).

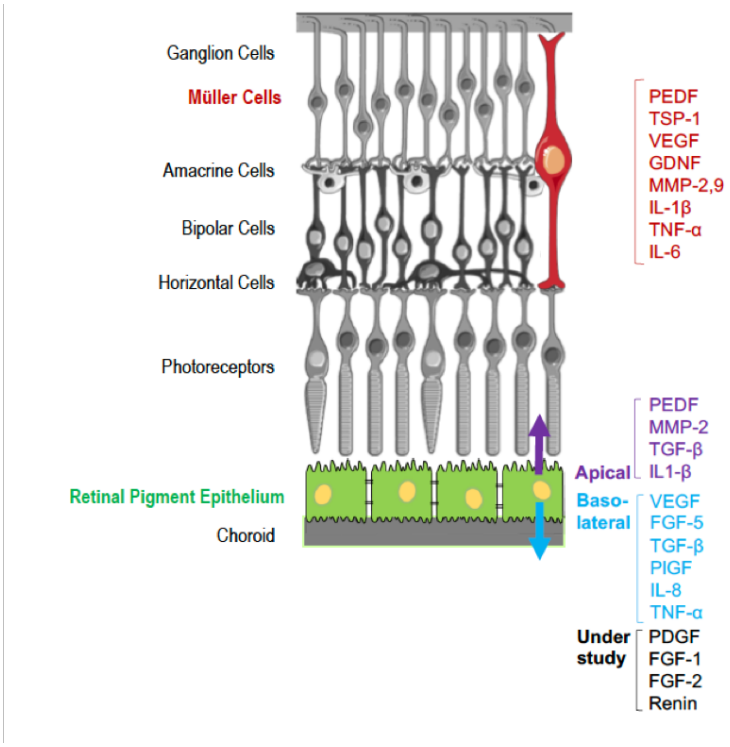

Figure 19. Main trophic factors involved in neovascular retinal pathologies, secreted by Müller cells (red) and by the retinal pigmented epithelium cells to either the apical (purple) or basolateral (blue) side, targeting photoreceptors and neurons, and the choroid, respectively. For some factors (black) the secretion side is still to be determined. Adapted from Araujo RS et al., Biochimie 2018.

d) Antioxidant pathways

Antioxidant pathways are a frequent response to oxidative stress in metabolic diseases such as diabetes. Müller cells have revealed a high resistance to oxidative stress, due to an increased expression of peroxodins-1, -4 and -6, enzymes that participate to oxygen peroxide removal (Grosche et al., 2016).

e) Summary of Müller cell activation in diabetic retinopathy

Müller cells have shown a strong involvement in the maintenance of retinal homeostasis during DR, by stimulating the migration of phagocytes for further protection and releasing trophic factors to preserve neuronal function. However, their chronic activation leads to harmful effects

with chronic inflammation, neurodegeneration and neovascularization (**Figure 20**) (Subirada PV et al., 2018).

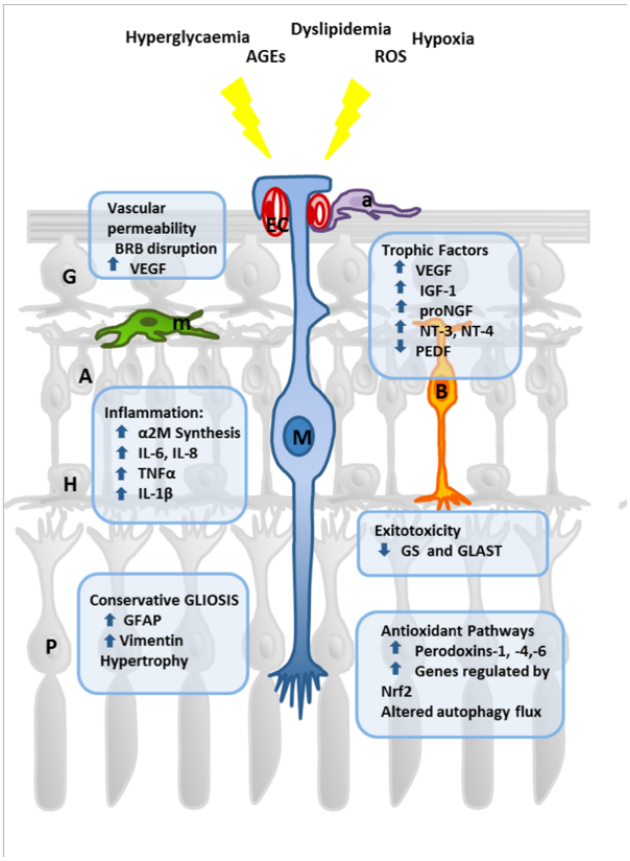

Figure 20: Illustration of main Müller cell response to diabetes stimuli. The main insults in diabetic retinopathy are hyperglycemia, dyslipidemia, hypoxia, AGEs and ROS. Müller glial cells detect changes in the retinal environment from the early stages in the onset of the disease and set up a gliotic response. Müller cells also synthesize and secrete trophic factors to avoid neuronal damage and activate antioxidant pathways. Together with microglial cells, they modulate inflammation, known as a key factor in chronic metabolic diseases.

Abbreviations: M: Müller glial cells; m: microglial cells; a: astrocytes; P: photoreceptors; H: horizontal cells; B: bipolar cells; A: amacrine cells; G: retinal ganglion cells; ECs: endothelial cells. Adapted from Subirada PV et al., EJN 2018.

II. RATIONAL AND OBJECTIVES

Historically, diabetic retinopathy (DR) was considered to be mainly a glucose-mediated microvascular disease because microaneurysms and the proliferation of new vessels are observed. Now, chronic inflammation is also known to be an important feature of the disease, as inflammatory cell infiltration, pro-inflammatory cytokines, vascular permeability and edema have a central role in its pathogenesis (Rübsam A et al., 2018). Indeed, impaired vision in patient with diabetes is most frequently associated with diabetic macular edema (DME) but the exact mechanisms by which DME decreases visual acuity remain poorly understood.

The rupture of the blood retina barrier inducing leakage from retinal capillaries is generally thought to be the main mechanism that initiate DME. Several hypotheses are reported to explain the decrease of visual acuity secondary to the presence of cysts (Antonetti DA et al., 2006). First, fluid accumulation within the retina could induce photoreceptor degeneration and neuron cell death by either direct compression or alteration of neurotransmission. The later could be secondary to change in extracellular ionic concentrations, or to compromise interchange of glutamate and glutamine between glial cells and neurons. (Lardenoye CW et al., 2000). Vascular leakage and capillary occlusions could thus impair neuronal function; however another hypothesis is that diabetes could directly damage glial cell and neural metabolism. Neurons could have increased susceptibility to excitotoxic amino acids, antibodies or inflammatory cells that reach the retina via leaking vessels (Antonetti DA et al., 2006).

Second, the macular cysts may scatter light within the retina such that it is not focused on photoreceptors (Antonetti DA et al., 2006). The reflectivity and content of the cysts in DME are highly variable between patients and could alter more or less severely the visual acuity, independently of central macular thickness. This could explain in part the weak correlation between anatomic and functional parameters in DME. The advances in OCT techniques have allowed imaging small structures with much higher resolution and detecting new entities such as hyperreflective foci within the retina. Spectral-domain OCT has also allowed detecting different levels of OCT reflectivity in the cystoid spaces in DME. These differences in reflectivity could suggest the diversity of the contents of the cystoid spaces with different amount of proteins and lipids. This is in line with pathohistological studies of retinal vascular diseases, showing that hyaline deposits are often present in the cystoid spaces (Tso MO, 1982, Wolter JR, 1961). Hyperreflective foci are associated with heterogeneity of reflectivity in the cystoid spaces on the OCT images. The origin of the hyperreflective foci remains controversial: some authors hypothesized that condensed proteins or lipids in the cystoid spaces might deposit as hyperreflective foci, resulting in emergence of hard exudates. Others stated that

hyperreflective foci are lipid-laden macrophages that migrate into the cystoid spaces through a severe break in the vascular walls and take up the concentrated proteins or lipids.

The causes and consequences of lipids deposits inside the retina and lipid content of cystoid spaces have not been fully elucidate.
The Early Treatment Diabetic Retinopathy Study (ETDRS) showed that the foveal hard exudates predict poor visual prognosis, however the comprehension of mechanisms underlying hyper-reflective deposits in the foveal cystoid spaces need to be increased.

Furthermore, multiple studies have suggested that the excess of glucose may not explain all aspects of DR. (Harrower AD et al., 1976; Barnes AJ et al.,1985; Chan JY et al.,1985). Several studies have reported that patients with impaired glucose tolerance (pre-diabetes) but without overt hyperglycemia had retinal microaneurysms and developed DR (Antonetti DA et al., 2006). Thus, hyperglycemia could not be the only determinant factor that induce the range of cellular and functional changes in DR. Impaired insulin action may directly impact the retina, but many others factors besides glucose, such as lipids, hypertension, hormones or inflammation due to insulin resistance, may also alter the retinal homeostasis.

In this project, we aimed to study the effect of short-time high glucose exposure as well as high lipid exposure on the retinal glial cells that are recognized to play a key role in retinal homeostasis and in inflammatory pathways implicated in DR pathogenesis. We also aimed to further evaluate clinically the cystoid spaces with hyperreflective fluid, that were hypothesized to have a lipid content, in eyes with DME.

III. RESULTS

I. High glucose is not sufficient to induce retinal glial cell activation

1. Aim and context of the study

a) Inflammation and diabetic retinopathy

Growing evidences indicate microglial and glial reaction contribute to the early development of DR and is associated with electroretinographic alterations before any signs of microangiopathy are clinically detectable, within the first month (Joussen AM et al., 2004). Several recent studies have suggested that neurodegenerative and inflammatory events may precede the vascular changes (Rungger-Brändle E et al., 2000; Gaucher D et al., 2007). The particular spatial arrangement of retinal macroglial cells (astrocytes and Müller cells) that are intercalated between vasculature and neurons points to their important role in the uptake of glucose from the circulation, its metabolism, and transfer of energy to neurons. However, the exact molecular events that trigger glial activation remain imperfectly understood and there seem to be discrepancies in the sequence of cellular events in the various diabetic animal models described.

Diabetic patients and diabetic animal models also demonstrate early retinal mononuclear phagocyte activation and intraocular elevated levels of inflammatory cytokines such as vascular endothelial growth factor (VEGF), interleukin- 6 and -8 (IL-6 and IL-8) and chemokine ligand-2 (CCL2) (McAuley AK et al., 2014).

Similarly, previous works from our team have shown in new born animals that short exposure to high glucose resulted in a substained retinal inflammation (Kermorvant-Duchemin E et al., 2013). In this study, a new model of Neonatal Hyperglycemia-induced Retinopathy (NHIR) was proposed with an induction of hyperglycemia in newborn rat pups by injection of streptozocin at post-natal day one (P1). In this model, the retinal vascular area was significantly reduced but also hyperglycemia was associated with CCL2 chemokine induction and a significant increase in total number of macrophages/microglia cells in the inner nuclear layer in P6 hyperglycemic animals compared to control animals (Kermorvant-Duchemin E et al., 2013). These results demonstrated the early glial reaction to short term high glucose exposure in newborn rat. We aimed to further investigated this glial activation after short high glucose exposure in adult diabetic retinopathy animal model and on glial Müller cells.

b) Müller cell response to hyperglycemia

Under hyperglycemic conditions, Müller cells were shown to release:

- Growth factors, such as vascular endothelial growth factor (VEGF) and pigment epithelium-derived factor (PEDF), and
- A variety of cytokines and chemokines including interleukin-1ß (IL-1ß), interleukin-6 (IL-6), tumor necrosis factor-α (TNF-α), and chemokine ligand-2 (CCL2) (Yego ECK et al., 2009; Zhou T et al., 2017).

The production and release of pro-inflammatory cytokines by Müller cells contributes to the chronic inflammatory environment detected in the diabetic retina that over time promotes drop-out of retinal cells. Indeed, Müller cells are a major source of retinal IL-1ß production, and hyperglycemia strongly induces the activation of this caspase-1/IL-1ß signaling pathway (Yego ECK et al., 2009). Increased caspase-1 activation and elevated IL-1ß levels have also been identified in the retinas of diabetic mice and retinal tissue and vitreous fluid of diabetic patients (Yego ECK et al., 2009; Gerhardinger C et al., 2005). Endothelial cells are extremely susceptible to IL-1ß and rapidly progress to cell death in response to this proinflammatory cytokine (Yego ECK et al., 2009).

The increase of IL-1ß is not an isolated pathobiological process. Besides IL-1ß, Müller cells produce other pro-inflammatory cytokines such as TNF-α, IL-6 and iL-8. (Yego ECK et al., 2009; Vincent JA et al., 2017). Detrimental effects of IL-6 have been associated with vascular dysfunction and promotion of angiogenesis which is why IL-6 recently has become a new therapeutical target of interest to prevent diabetes-induced vascular damage (Barnes TC et al., 2011). The concentration of IL-6 correlates well with that of IL-8 (Yuuki T et al., 2001), and their upregulation is related to the complex sequence of events implicated in the inflammation cascade, such as leucocyte migration, the upregulation adhesion molecules and growth factors. IL8 has been recognized as a potent chemoattractant activator of neutrophils and T lymphocytes but also a pro-angiogenic factor. Since IL-8 is expressed in retinal vascular endothelial cells and glial cells in response to hypoxia (Yoshida A et al., 1998; Karakurum M et al., 1994), it is believed to be involved in inflammation-mediated angiogenesis and a fundamental factor in the inflammatory basis of DR.

Several studies have also shown an increased level of IL8 in the vitreous of patients with PDR

compared with age-matched non-diabetic control subjects (Petrovic MG et al., 2007; Murugeswari P et al., 2008).

Published data on the short-term effect of high glucose exposure on microglial and Müller cells are limited and main studies focused on the glial changes occurring at least after 1 month of diabetes.

c) Role of glycemic variability

The Diabetes Control and Complications Trial (DCCT) demonstrated that the lifetime exposure to hyperglycemia, represented by the mean HbA_{1c}, was the main determinant of the risk of complications (Lachin JM et al., 2017; Brownlee M et al., 2006).

The mean amplitude of glucose excursions (MAGE), obtained from continuous blood glucose monitoring, was shown to be associated with free radical production which are markers of oxidative stress while the mean level of glucose was not (Monnier L et al., 2008). the degree of variability in blood glucose, An additional feature of hyperglycemia not represented by the HbA_{1c} may determine an additional risk of complications (Brownlee M et al., 2006).

However, the effect of glycemic variability remains debated. Other publications, including the DCCT data, showed that the within-day variability in blood glucose, expressed as the SD of the 7-point blood glucose profile, was not significantly associated with the progression of retinopathy or nephropathy when added to the effect of the mean glucose level. However, the incompleteness of the glucose profiles calls into question the robustness of the observations and conclusions (Kilpatrick ES, 2009).

To our knowledge, the direct effect of glycemic variability on glial cell activation in the retina has not been studied. *In vivo* glycemic variability may correspond to short high glucose spikes *in vitro*. We aimed to investigate the effect of a short or intermittent high glucose exposure on retinal glial and microglial reaction.

2. Effect of short-term high glucose exposure on retinal glial cells

To study the effect of short-term high glucose exposure on retinal glial cells, we used both *in vivo* and *in vitro* experiments. The *in vitro* experiments were conducted first on human induced pluripotent stem cells (hiPSCs)-derived Müller cells and on total retinal explants from C57/Bl6 mice. The *in vivo* experiments were conducted in streptozotocin-induced DR animal model.

a) Müller glial cell culture

Culture of human retinal Müller cells were performed to analyze their reaction to short high glucose exposure. In this study, we used human induced pluripotent stem cells (hiPSCs) derived Müller cells.

(1) Characterization of hiPSCs-derived Müller cells

For this *in vitro* study, we used human induced pluripotent stem cells (hiPSCs) derived from adult dermal fibroblasts. The production of hiPSCs-derived Müller cells by reprogramming adult human dermal fibroblast (AHDFs) was performed by Dr Sacha Reichman and is presented below in the section results part II.

We characterized the hiPSCs-derived Müller cells by measuring the expression of glutamine synthetase (GS) and xCT and eaat1 membrane transporters using RT-PCR. We compared their expression in hiPSCs-derived Müller cells obtained from adult human dermal fibroblasts (A2) with the expression in either Human Post-morten Müller cells obtained from one donor (Müller Post-Mortem) or hiPSCs-derived Müller cells generated from 2 other sources: post-natal foreskin (F3) or adult retina (5F).

In physiological conditions, Müller glial cells mediate glutamate uptake after synaptic release through excitatory amino acid transporters (EAATs) to avoid excitotoxic concentrations. Extracellular glutamate is mostly transported into the Müller cell through EAAT1 transporter, also called GLAST, to be converted into glutamine. Conversely, glutamate can be released form glial cells by a cystine/glutamate transporter, the xc- system (xCT).

We evaluated the expression of GS as well as xCT transporter, which are almost exclusively expressed by Müller glial cells, as well as the expression of VEGF by hiPSCs-derived Müller cells.

No difference in GS, xCT and VEGF expression was found in A2 hiPSCs-derived Müller cells compared with the expression in Human Post-mortem Müller cells and F3 or 5F hiPSCs-derived Müller cells (**Figure 21**).

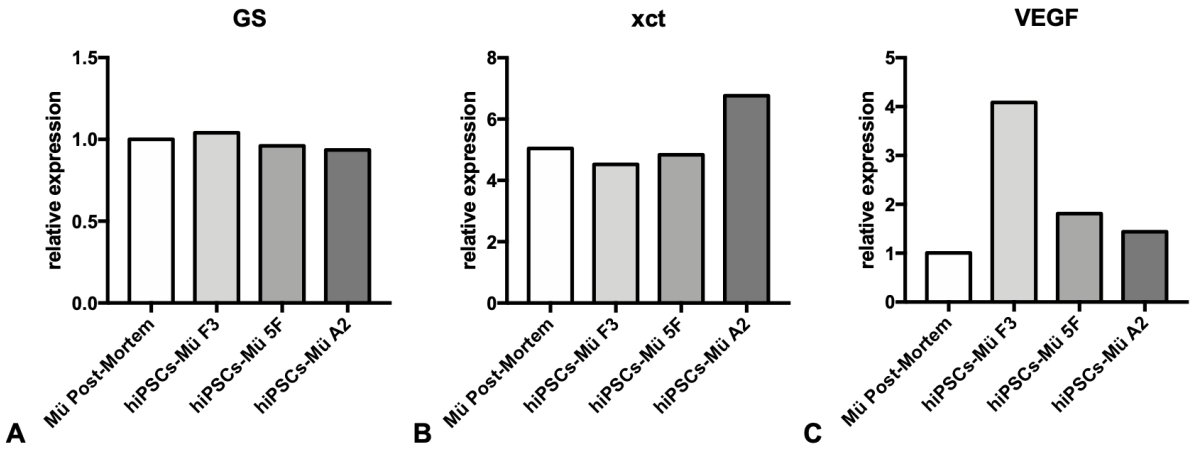

Figure 21 : The expression of glutamine synthetase (GS), xCT membrane transporter, and VEGF in hiPSCs-derived Müller cells obtained from adult human dermal fibroblasts (A2, passage 2) was determined by RT-PCR and compared with the expression in either human post-mortem Müller cells obtained from one donor (Müller Post-Mortem) or hiPSCs-derived Müller cells derived from post-natal dermal foreskin (F3, passage 2) or from adult retina (5F, passage 3). The expression of GS, xCT and VEGF did not show any difference in A2 hiPSCs-derived Müller cells compared with human post-mortem Müller cells and F3 or 5F hiPSCs-derived Müller cells. Results were normalized with expression of S26.

(2) Effect of high glucose exposure

For studying the effect of short high glucose exposure, hiPSCs-derived Müller cells were replenished with DMEM medium containing either low (5.5 mmol/l glucose), high (25 mmol/l) or hyper high glucose (35 mmol/l) at 37°C for 18 or 24 hours.

We evaluated by quantitative RT-PCR the expression of glial fibrillary acidic protein (GFAP), a common marker of reactive gliosis, which is not expressed by Müller cells in healthy conditions.

The expression of angiogenesis factors (VEGF and ANGPTL4) as well as the expression of inflammatory factors (IL-1ß, CCL2, IL6, FATP1, TGFβ2 and TNF-α) by cultured hiPSCs-derived Müller cells were also determined by quantitative RT-PCR. The analysis of VEGF production in hiPSCs-derived Müller cells in culture was also performed: media was collected from normo- and hyperglycemic cells and subjected to VEGF ELISA (Qiagen). VEGF concentration was normalized to total cellular protein content.

A non-significant increase in GFAP expression in the cultured hiPSCs-derived Müller cells was found under hyperglycemic conditions at 18h (**Figure 22A**). The VEGF expression in hiPSCs-derived Müller cells was significantly increased under high glucose exposure at 18h (**Figure 22B)** and the VEGF production by iPS-Müller cells in culture, measured using ELISA, was also significantly increased under high glucose exposure at 18h (**Figure 22C**). However, the increase in VEGF expression under hyperglycemic condition was not maintained at 24h.

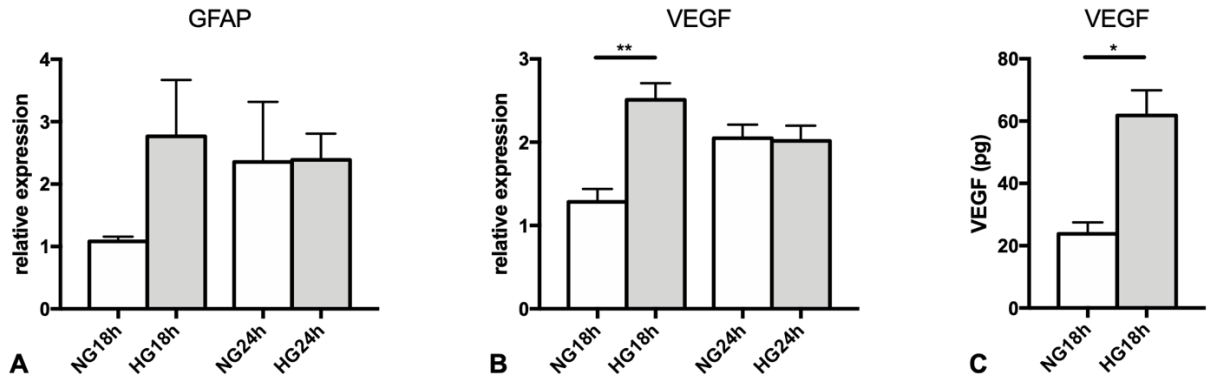

Figure 22: A) Glial fibrillary acidic protein (GFAP) expression in hiPSCs-derived Müller cells cultured in either normoglycemic (NG) medium with a glucose concentration of 5 mmol/l or hyperglycemic (HG) medium with a glucose concentration of 25 mmol/l for 18h or 24h. A non-significant increase of GFAP was found at 18h. The mean value of GFAP was of 1.082 ± 0.007762 and 3.372 ± 1.16 respectively (n=3 in each group, p = 0.0783).
B) VEGF expression in hiPSCs-derived Müller cells cultured in HG condition for 18h was significantly increased compared with cells in NG condition however this difference was not observed at 24h. Mean value of VEGF was 1.283 ± 0.1571 in NG condition compared with 2.510 ± 0.1985 in HG condition at 18h (n=3 in each group, p = 0.0084).
Results were normalized with expression of S26 and expressed as mean ± SEM (n = 3 in each group)

C) A significant increase of VEGF production by hiPSCs-derived Müller cells in HG condition was detected using ELISA (Qiagen). VEGF concentration was normalized to total cellular protein content. Mean value was 23.84 ± 5,172344683 and 61.81353333 ± 14.02784951 respectively (n = 3 in each group).

We then evaluated the expression of angiogenesis factors (VEGF and ANGPTL4) as well as the expression of inflammatory factors (IL-1ß, CCL2, IL6, FATP1, TGFβ2 and TNF-α) in hiPSCs-derived Müller cells cultured in hyper high glucose (HHG) condition (DMEM medium with a glucose concentration of 35 mmol/l) at two different time-points (18h or 24h). No difference in the expression of these angiogenesis and inflammatory factors was found in hiPSCs-derived Müller cells under HHG condition compared with NG condition (**figure 23**)

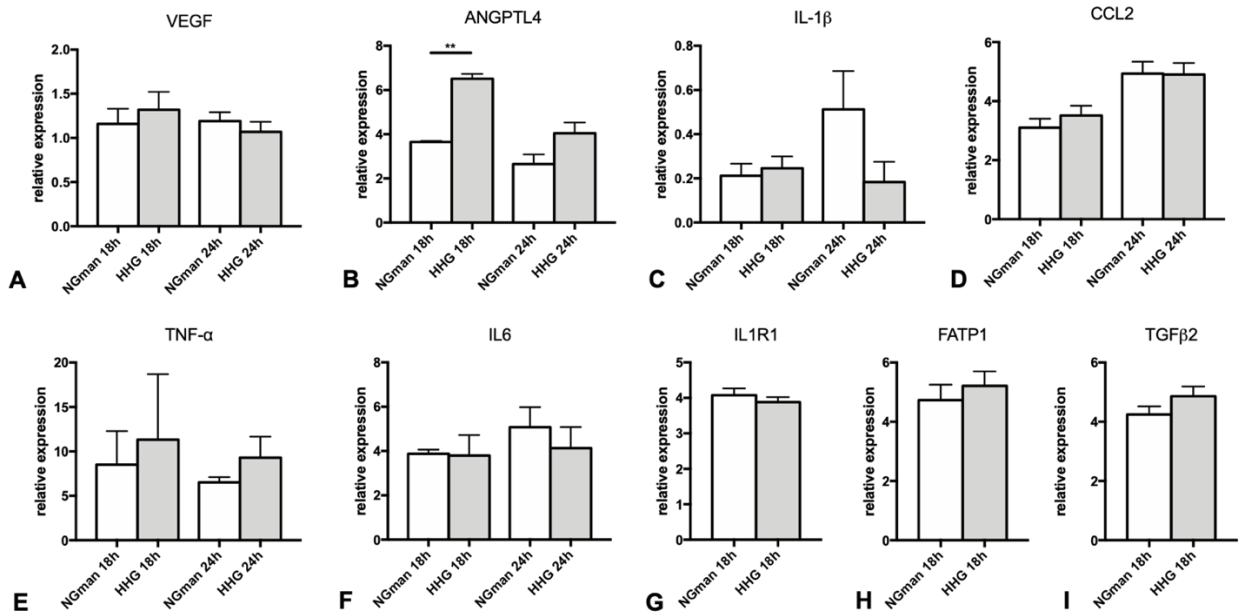

Figure 23: Expression of angiogenesis factors, VEGF and ANGPTL4, and inflammatory factors, IL-1ß, CCL2, IL6, FATP1, TGFβ2 and TNF-α in hiPSCs-derived Müller cells cultured in either hyper high glucose (HHG) condition (DMEM medium with a glucose concentration of 35 mmol/l) or normoglycemic (NG) condition during 18h or 24h.

A) The mean value of VEGF was of 1.159 ± 0.173 and 1.19 ± 0.1002 in NG condition at 18h and 24h respectively; and was of 1.32 ± 0.2028 and 1.07 ± 0.1122, in HHG condition at 18h and 24h respectively (p = 0.5785 and 0.4694 respectively).

B) The mean value of ANGPTL4 was of 3.653 ± 0.04501 in NG condition compared with 6.511

± 0.2179 in HHG condition at 18h (p = 0.0044), and of 2.648 ± 0.4408 in NG condition compared with 4.043 ± 0.4864 in HHG condition at 24h (p = 0.1015).

C) The mean value of IL-1ß was of 0.2114 ± 0.05519 in NG condition vs 0.2456 ± 0.05351 in HHG condition at 18h (p = 0.6993), and of 0.5124 ± 0.1734 in NG condition vs 0.1832 ± 0.09207 in HHG condition at 24h (p = 0.1689).

D) The mean value of CCL2 was of 3.104 ± 0.2974 in NG condition vs 3.511 ± 0.3312 in HHG condition at 18h (p = 0.4122), and of 4.935 ± 0.4026 in NG condition vs 4.905 ± 0.3888 in HHG condition at 24h (p = 0.9601).

E) The mean value of TNF-α was of 8.506 ± 3.781 in NG condition vs 11.32 ± 7.372 in HHG condition at 18h (p = 0.7513), and of 6.529 ± 0.5813 in NG condition vs 9.316 ± 2.341 at 24h (p = 0.3123).

F) The mean value of IL6 was of 3.875 ± 0.1866 in NG condition vs 3.799 ± 0.926 in HHG condition at 18h (p = 0.9392), and of 5.077 ± 0.905 in NG condition vs 4.13 ± 0.9548 in HHG condition at 24h (p = 0.5115).

G) The mean value of IL1 receptor 1 (IL1R1) was of 4.077 ± 0.1917 in NG condition vs 2.848 ± 0.4453 in HHG condition at 18h (p = 0.0643).

H) The mean value of FATP1 was of 4.733 ± 0,5197 in NG condition vs 5.215 ± 0.49 in HHG condition at 18 h (p = 0.5369).

I) The mean value of TGFβ2 was of 4.247 ± 0.2761 in NG condition vs 4.86 ± 0.3317 in HHG condition at 18h (p = 0.2283).

All results were normalized with expression of S26 and expressed as mean ± SEM (n = 3 in each group).

(3) Effect of intermittent glucose exposure on Müller glial cells

For studying the effect of intermittent glucose exposure, hiPSCs-derived Müller cells were cultured for 24h with DMEM medium containing either:

- 5.5 mmol/l glucose
- 25 mmol/l glucose
- 5 mmol/l alternating hourly with 5 mmol/l glucose
- 5 mmol/l alternating hourly with 25 mmol/l glucose

The expression of GFAP, VEGF, and IL-1ß in cultured hiPSCs-derived Müller cells were determined by quantitative RT-PCR.

Intermittent glucose exposition did not lead to any increase in GFAP, VEGF or IL-1ß expression in hiPSCs-derived Müller cells cultured for 24h, compared with constant condition (**Figure 24)**.

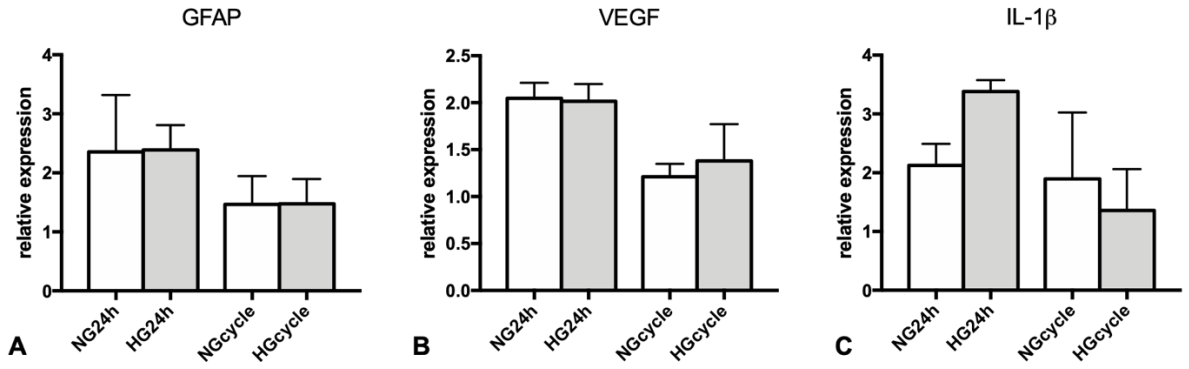

Figure 24: Glial fibrillary acidic protein (GFAP), VEGF and IL-1ß expression in hiPSCs-derived Müller cells cultured either in constant condition, normoglycemic (NG) condition (DMEM medium with a glucose concentration of 5 mmol/l) or hyperglycemic (HG) condition (DMEM medium with a glucose concentration of 25 mmol/l), or in intermittent normoglycemic condition (NG cycle : DMEM medium with a glucose concentration of 5 mmol/l change hourly with fresh medium) or intermittent hyperglycemic condition (HG cycle: DMEM medium with a glucose concentration of 25 mmol/l alternate hourly with a normoglycemic DME medium) for 24h.

A) The mean value of GFAP expression was of 2.354 ± 0.9628 in NG condition vs 1.466 ± 0.4794 in NG cycle condition (p = 0.4551), and of 2.39 ± 0.4175 in HG condition vs 1.476 ± 0.42 in HG cycle condition (p = 0.1979)

B) The mean value of VEGF expression was of 2.048 ± 0.1639 in NG condition vs 1.21 ± 0.1381 in NG cycle condition (p = 0.0175), and of 2.017 ± 0.1822 in HG condition vs 1.38 ± 0.392 in HG cycle condition (p = 0.2151).

C) The mean value ± SEM of IL-1ß was of 2.126 ± 0;3651 in NG condition vs 1.896 ± 1.129 in NG cycle condition (p = 0.8340), and of 3.382 ± 0.1937 in HG condition vs 1.359 ± 0.7022 in HG cycle condition (p = 0.0500).

All results were normalized with expression of S26 and expressed as mean ± SEM (n = 3 in each group)

In the literature, human Müller cells were shown to release multiple pro-inflammatory cytokines (IL-1ß, IL6, IL8, TNFα) and growth factors (VEGF and PEDF) (Busik JV et al 2008), however others *in vitro* studies showed no effect of high glucose exposure on inflammatory and angiogenesis responses in human retinal endothelial cells (Chen W et al., 2003). Here, we showed no significant inflammatory reaction of hiPSCs-derived Müller cells after a short-term high glucose exposure, as well as , under intermittent high glucose exposure. We then studied Müller reaction from total retinal explants to high glucose exposure.

b) Retinal explants culture

(1) Effect of high glucose exposure

For the *in vitro* experiments, we then used total retinal explants. Retinal explants were obtained by entire retina dissection from C57/Bl6 mice and were incubated in media containing two different glucose concentrations:

- 5 mmol/l for the normoglycemic condition (NG)
- 25 mmol/l for the hyperglycemic condition (HG)

The expression of GFAP in the entire retina was determined by quantitative RT-PCR at different time points (3h, 6h and 18h). A significant increase in GFAP expression in the entire retina was found under hyperglycemic condition at 6h and 18h. (**Figure 25**).
Then, we performed cell sorting in another experiment of retinal explants cultured in same conditions. The expression of IL-1ß was evaluated in microglial cell (CD11b positive cells) isolated from the others cell populations. No significant increase in IL-1ß expression in CD 11b positive cells were found, and the expression of IL-1ß was undetectable in both groups.

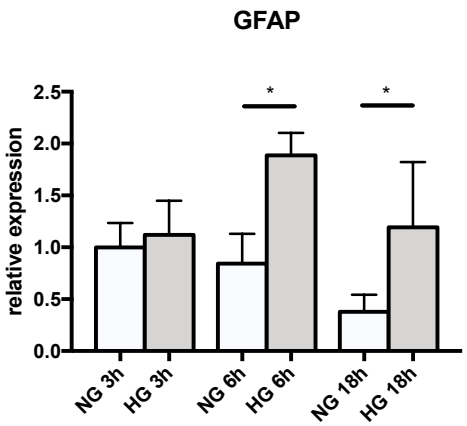

Figure 25: Glial fibrillary acidic protein (GFAP) expression in the entire retinal explants cultured in either normo- (NG: glucose concentration of 5 mmol/l) or hyper-glycemic condition (HG: glucose concentration of 25 mmol/l) during 3h, 6h or 18h. Mean value of GFAP was 0.8418 ± 0.1667 in normoglycemic condition vs 1.886 ± 0.1528 in hyperglycemic condition at 6h (n=3 in each group, p = 0.0233); and it was of 0.3776 ± 0.07367 and 1.193 ± 0.281 at 18h, (n=5 in each group, p = 0.0232). Results were normalized with expression of S26 and expressed as mean ± SEM.

(2) Effect of intermittent glucose exposure on the entire retina

To study the effect of an intermittent high glucose exposure, total retinal explants were incubated in media which were changed hourly, for 12 hours:

- 5 mmol/l glucose alternating hourly with 25 mmol/l glucose for the glycemic variability condition
- 5 mmol/l glucose alternating hourly with 5 mmol/l glucose for the controlled normoglycemic condition

The relative expression of GFAP in the entire retina, determined by quantitative RT-PCR, was not found to be significantly increased in the glycemic variability condition compared with the hourly changed normoglycemic condition. The mean value ± SEM of GFAP expression in retinal explants cultured in variable condition was of 0.8338 ± 0.1548 in normoglycemic condition compared with 0.252 ± 0.03846 in intermittent hyperglycemic condition (n=5 in each group, p = 0.0065).

To summarize explants experiments, we found an increased GFAP expression in the entire retina, indicative of a Müller cells activation in high glucose condition, however here the increase of GFAP is statistical but very mild, while Müller cell activation is usually characterized by higher increase of GFAP expression, with at least a two digit fold variation. The increase in GFAP expression under short-term high glucose exposure was here low.
In addition, microglial cells did not show any increase expression of IL-1ß; and intermittent high glucose exposure did not induce any Müller cells activation.
We then studied Müller cells reaction after a short-time high glucose exposure in an *in vivo* model of DR.

c) Sorting of retinal cell types

In the literature, glial cells were shown to be activated in diabetic animal models after 1 month of hyperglycemia. Here, we aimed to evaluate the short-term effect of hyperglycemia on these cells in an *in vivo* animal model of DR. Streptozotocin-induced diabetes were used in in vivo studies (details of the procedure are mentioned below in the method section). Müller cells (CD29 positive cells) were separated from microglial cells (CD11b positive cells) and from endothelial cells (CD31 positive cells) (Grosche A et al., 2016).

The expression of glial fibrillary acidic protein (GFAP) in Müller cells and the production of VEGF, IL-1ß, CCL2 by microglial, Müller and endothelial cells were determined by quantitative RT-PCR.

No significant increase in GFAP expression indicative of a glial reaction in Müller glial cells, as well as no increase in IL-1ß and VEGF production by microglial and endothelial cells were observed after 7 days of hyperglycemia in streptozotocin-induced mice (**Figure 26**). CCL2 expression was undetectable in diabetic as well as in healthy retinas.

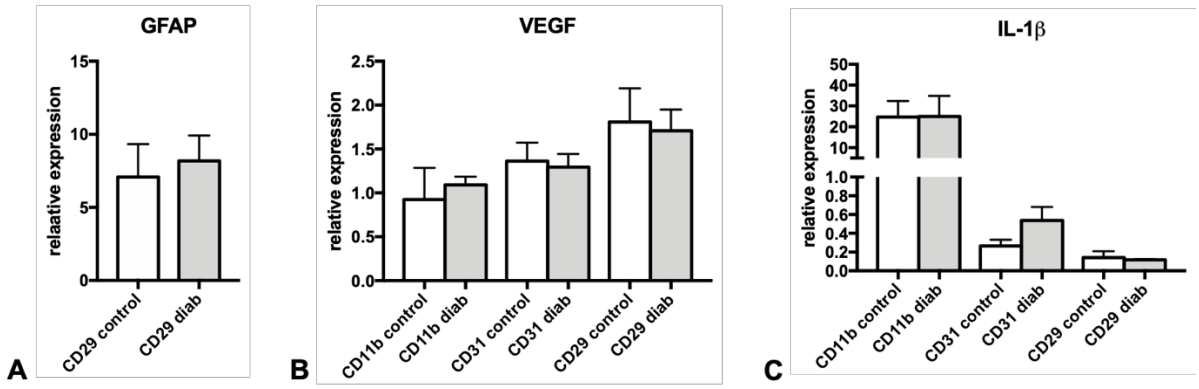

Figure 26: Glial fibrillary acidic protein (GFAP) expression (**A**) in Müller glial cells (CD29 positive cells), VEGF (**B**) and IL-1ß (**C**) production by microglial (CD11b positive cells) and endothelial cells (CD31 positive cells) observed after 7 days of hyperglycemia in streptozotocin-induced mice. Results were normalized with expression of GAPDH and expressed as mean ± SEM. n=5 animals/group.

While the activation of Müller cells was shown to be an early phenomenon under high glucose exposure, up to 4 weeks after the onset of hyperglycemia, we didn't see any effect of a very short spike of hyperglycemia in this streptozocin-induced diabetic model. However, this DR model did not reproduce all the aspects of the human disease, we thus investigated the effect of high lipid exposure, another DR-relevant stimulus.

d) Conclusions

The present study was undertaken to record, in a diabetic mice model and in vitro, glial alterations at an early time-point of hyperglycemia. Our in vivo experiments did not show any glial activation after one week of hyperglycemia in streptozocin-induced diabetic mice.
In vitro experiments showed a moderate increased GFAP expression in the entire retina, indicating Müller cells activation, in retinal explants culture under hyperglycemic condition.
However, the expression of angiogenesis factors (VEGF and ANGPTL4) as well as the expression of inflammatory factors (IL-1ß, CCL2, IL6, FATP1, TGFβ2 and TNF-α) in hiPSCs-derived Müller cells cultured under high and even hyper high glucose condition was not increased compared with normoclycemic condition.
Regarding glycemic variability experiments, no early reaction of Müller cells was observed after an intermittent exposure to high glucose level.

As shown in the literature (Capozzi ME et al, 2018) and in these experiments, glucose alone has no effect on glial cell reaction. Glucose is the most commonly used stimulus for DR basic research, however recent studies have highlighted the possible role of fatty acids in DR.

We then conducted a study focused on Müller glial cells to evaluate the effect of high lipid exposure in cultured Müller cells.

3. Methods

a) Mice

C57Bl6/J male mice were obtained from JANVIER Lab. The mice were aged between 8 and 15 weeks and were kept under specific pathogen-free condition in a 12 hr/12 hr light/dark (100 lux) cycle with no additional cover in the cage and with water and normal chow diet available ad libitum.

b) Diabetes induction

Streptozotocin-induced diabetes were used in in vivo studies. Diabetes was induced by a single injection of Streptozotocin (165 µg/g) into C57/Bl6 mice (Deeds et al., 2011). Blood glycemia and weight were controlled every day. An elevation of blood glycemia was detected at day 2 or day 3. Age-matched mice raised under similar conditions served as control. Mice were sacrificed after 7 days of hyperglycemia and retinal tissue was rapidly isolate from the eye cup.

c) Cell sorting

Isolated retinae were incubated with papain (0.2 mg/ml, Roche, Mannheim, Germany) in Ca2 -/Mg2 -free phosphate-buffered saline containing 11 mM glucose, pH 7.4, for 30 min at 37°C, followed by several washing steps with saline. After short incubation in saline supplemented with DNase I (200 U/ml), the tissue was triturated in extracellular solution (ECS, that contained (mM) 135 NaCl, 3 KCl, 2 CaCl2, 1 MgCl2, 1 Na2HPO4, 10 HEPES, and 11 glucose, adjusted to pH 7.4 with Tris) to obtain isolated retinal cells. After centrifugation, the supernatant was removed, and the cells were resuspended and incubated in ECS containing biotinylated hamster anti-CD29 (clone Ha2/5, BD Biosciences, Heidelberg, Germany) for 15 min at 4 °C. After washes in ECS and centrifugation, cells were taken up in ECS containing anti-biotin MicroBeads (Miltenyi Biotec, Bergisch Gladbach, Germany) and incubated for 10 min at 4 °C. After an additional washing step in ECS, cell populations were separated using MACS® cell separation large cell columns (Miltenyi Biotec) according to the manufacturer's recommendation. If microglia cells were isolated in addition to Müller cells, the retinal suspension was incubated with CD11b-microbeads (Miltenyi Biotec) for 15 min at 4 °C and

positively selected using MACS® cell separation large cell columns (Miltenyi Biotec) before Müller cells were surface-labeled for MACS sorting.

d) Retinal explants

After mice sacrifice at day 7, total retinal tissue was rapidly isolate from the eye cup. Residual vitreous was removed from the surface. Total retinal explants were placed on polycarbonate filters floating on DMEM medium, and cultured for 18 hours at 37°C.

e) Reverse transcription and real-time polymerase chain reaction (RT-PCR)

RT-PCR was used to measure mRNA expression levels. Total RNA was extracted from cell fractions isolated from mice retina, or total retinal explants, using the Nucleospin RNA (740955, Macherey-Nagel, Düren, Germany) according to the manufacturer's instructions and converted to cDNA using oligo (dT) as primer and Superscript II (Life Technologies).
Each RT assay was performed in a 20 mL reaction. Subsequent RT-PCR was performed using cDNA, Sybr Green PCR Master Mix (Life Technologies).

f) Statistics

Graph Pad Prism 7 (GraphPad Software) was used for data analysis and graphic representation. All values are reported as mean ± SEM. Statistical analysis was performed by unpaired t test (with Welch's correction for non-parametric 2-group experiments) for comparison among means. The p-values are indicated in the figure legends.

II. High lipid exposure induces activation of human Müller cells

1. Aim of the project

The role of glucose in DR pathogenesis is well recognized, however recent clinical and experimental studies suggested glucose may not be the only driver of DR.

First, DR pathology were observed in patients with relatively normal glucose tolerance (Chan JY et al., 1985; Harrawer AD et al., 1976).

Second, several clinical trials have demonstrated a strong association between hyperlipidemia and DR. Finofibrate, a lipid-lowering drug, has been shown to delayed DR progression, independently of glycemic control (Keech AC et al. 2007; The ACCORD Study Group and ACCORD Eye Study Group, 2010).

Third, experimental studies showed that diabetes increased fatty acid concentrations in systemic circulation, extra-ocular tissues and retinal endothelial cells (Boden et al., 2006; Decsi et al., 2007; Mohamed et al., 2014; Chen et al., 2003). Fatty acids were shown to induce inflammation and disease progression in extra-ocular experiments (Boden G, 2006; Decsi T et al., 2007).

We aimed to study the effect of high lipid exposure on human Müller glial cells. We used palmitic acid (PA) as it was demonstrated to be the most elevated fatty acid in serum of diabetic patients as well as in the retina of DR animal models (Tikhonenko M et al., 2010; Chorvathova V et al., 1983; Korani M et al., 2012).

2. Summary of the results

a) Effect of high lipid exposure on hiPSCs-derived Müller cells

We evaluate the expression of several genes that were previously demonstrated to play a key role in DR pathogenesis and that were shown to be upregulated in human primary Müller cells. In this study, as in the previous study regarding high and intermittent glucose exposure, hiPSCs-derived Müller cells were obtained by reprogramming adult human dermal fibroblast (AHDFs).

Regarding inflammatory pathways, we investigated the expression the C-X-C family of chemokines include CXCL1-2 and CXCL8 (or IL-8) in hiPSCs-derived Müller cells under PA exposure. A significant increase of the expression of ATF3, CXL1-2, CXCL8, which is

implicated in neutrophil migration and chemotaxis, has been noted in hiPSCs-derived Müller cells treated with PA for 24 hours.

Regarding WNT signaling, the expression of the tight-junction coding gene CLDN1 was also significantly increased in hiPSCs-derived Müller cells after PA treatment.

Regarding angiogenesis pathway, we evaluated the expression of VEGF and ANGPTL4. The key role of VEGF in angiogenesis and in blood barrier rupture in DR is well known. More recently, ANGPTL4, a well-characterized target of PPAR-β/δ signaling, has been demonstrated to play also an important role in the angiogenesis pathway in proliferative DR (Babapoor-Farrokhran et al., 2015, Jee et al., 2015).
The expression of both VEGF and ANGPTL4 was significantly increased in hiPSCs-derived Müller cells treated with PA for 24 hours compared with control condition.

The potential pro-angiogenic role of Müller cell under high lipid exposure was the investigated in aortic ring assays. These assays demonstrated a VEGF-independent pro-angiogenic activity of PA-exposed hiPSCs-derived Müller cells supernatants.

These results are in accordance with previous study of PA effect in primary human Müller cells cultures (Capozzi ME et al., 2018) and in streptozotocin-treated mice (Kandpal RP et al., 2012).

b) Effect of high lipid exposure in other types of hiPSCs-derived Müller cell

We then evaluated if the hiPSCs-derived Müller cell reaction after PA treatment differ depending on their origin. We evaluate the expression of angiogenesis and inflammatory increased gene expression in hiPSCs-derived Müller cells obtained from adult human dermal fibroblasts (A2) used in this study compared with hiPSCs-derived Müller cells generated from two different other sources: post-natal foreskin (F3) and adult retina (5F). We found that the increase of ANGPTL4 and ATF3 expression was similar in these 3 different hiPSCs-derived Müller cell types (**Figure 27**).

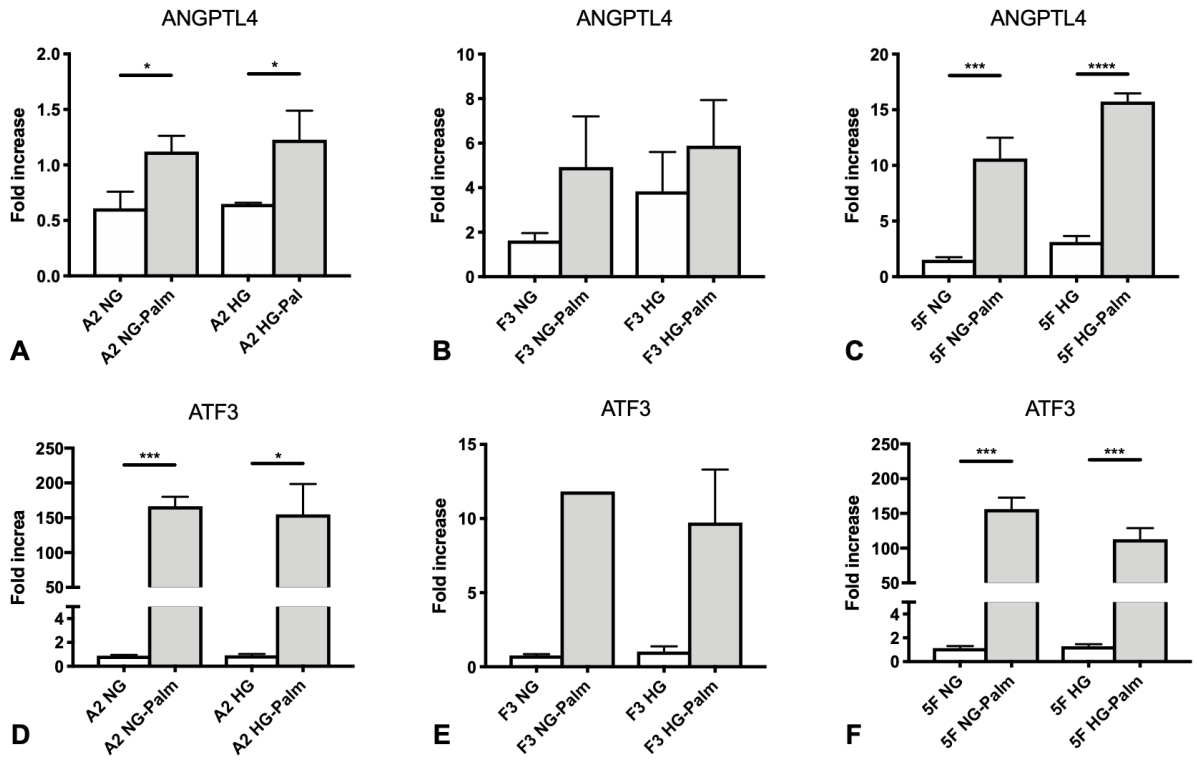

Figure 27: ANGPTL4 and ATF3 expression in hiPSCs-derived Müller cells generated from different sources: adult dermal biopsy (A2), post-natal foreskin (F3) and adult retina (5F); and cultured either in normoglycemic (NG) condition (DMEM medium with a glucose concentration of 5 mmol/l) or hyperglycemic (HG) condition (DMEM medium with a glucose concentration of 25 mmol/l), with (NG-Palm or HG-Palm) or without palmitic acid for 24h.

A) The mean value of ANGPTL4 expression in A2 hiPSCs-derived Müller cells was of 0.6087 ± 0.1499 in NG condition vs 1.121 ± 0.1422 in NG-Palm condition ($p = 0.0479$), and of 0.6488 ± 0.01017 in HG condition vs 1.228 ± 0.2613 in HG-Palm condition ($p = 0,0457$)

B) The mean value of ANGPTL4 expression in F3 hiPSCs-derived Müller cells was 1.629 ± 0.3293 in NG condition vs 4.927 ± 2.2756 in NG-Palm condition ($p = 0.2248$), and of 3.838 ± 1.768 in HG condition vs 5.889 ± 2.051 in HG-Palm condition ($p = 0.4774$).

C) The mean value of ANGPTL4 expression in 5F hiPSCs-derived Müller cells was of 1.528 ± 0.2327 in NG condition vs 10.62 ±1.87 in NG-Palm condition ($p = 0.0029$), and of 3.122 ± 0.5312 in HG condition vs 15.75 ± 0.729 in HG-Palm condition ($p < 0.0001$)

D) The mean value of ATF3 expression in A2 hiPSCs-derived Müller cells was of 0,8864 in NG condition vs 166.7 in NG-Palm condition ($p < 0.0001$), and of 0.9309 in HG condition vs 154.8 in HG-Palm condition ($p = 0.0126$).

E) The mean value of ATF3 expression in F3 hiPSCs-derived Müller cells was of 1.035 in HG condition vs 9.728 in HG-Palm condition ($p = 0.0931$).

F) The mean value of ATF3 expression in 5F hiPSCs-derived Müller cells was of 1.137 in NG condition vs 156.3 in NG-Palm condition ($p < 0.0001$), and of 1.289 in HG condition vs 112.8 in HG-Palm condition ($p = 0.0005$).

All results were normalized with expression of S26 and expressed as mean ± SEM (n = 4 in each group)

c) Effect of high lipid exposure in hiPSCs-derived Müller cell cultured at different passages

We evaluated if the hiPSCs-derived Müller cell reaction after PA treatment differ depending on their passage. We evaluate the expression of ANGPTL4 gene expression in hiPSCs-derived Müller cells obtained after 1, 2 and 3 passages. A significant increase of ANGPTL4 expression in hiPSCs-derived Müller cells was found, independently to the number of passages of the cells (**Figure 28**).

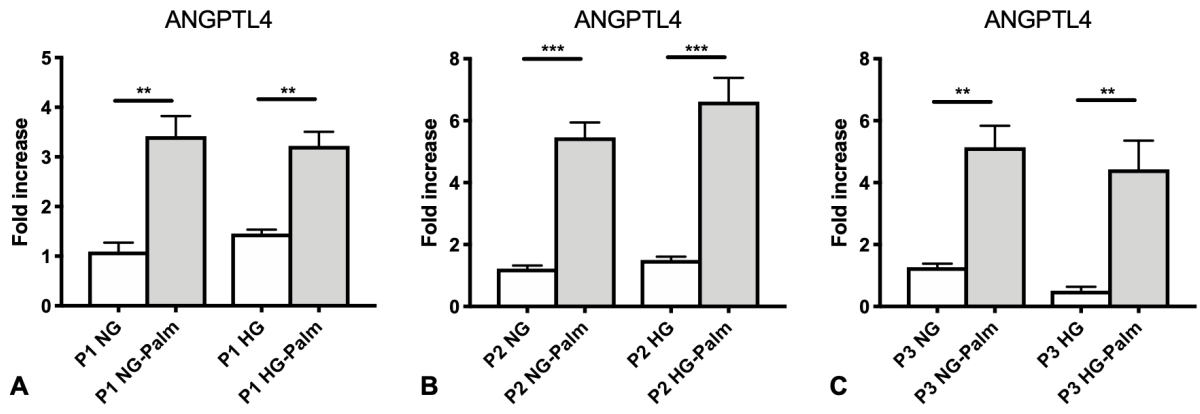

Figure 28: ANGPTL4 expression in hiPSCs-derived Müller cells cultured either in normoglycemic (NG) condition (DMEM medium with a glucose concentration of 5 mmol/l) or hyperglycemic (HG) condition (DMEM medium with a glucose concentration of 25 mmol/l), with (NG-Palm or HG-Palm) or without palmitic acid for 24h.

A) The mean value of ANGPTL4 expression in hiPSCs-derived Müller cells at passage 1 was of 1.092 in NG condition vs 3.421 in NG-Palm condition ($p = 0.0019$), and of 1.455 in HG condition vs 3.221 in HG-Palm condition ($p = 0,0010$).

B) The mean value of ANGPTL4 expression in hiPSCs-derived Müller cells at passage 2 was 1.221 in NG condition vs 5.462 in NG-Palm condition ($p = 0.0001$), and of 1.498 in HG condition vs 6.616 in HG-Palm condition ($p = 0.0006$).

C) The mean value of ANGPTL4 expression in hiPSCs-derived Müller cells at passage 3 was of 1.272 in NG condition vs 5.145 in NG-Palm condition ($p = 0.0015$), and of 0.5096 in HG condition vs 4.427 in HG-Palm condition ($p = 0.0059$)

All results were normalized with expression of S26 and expressed as mean ± SEM ($n = 4$ in each group)

3. Article 1

Human iPS-derived retinal Müller glia cells to model diabetic retinopathy

Aude Couturier[1,2], MD, Guillaume Blot[1], Lucile Vignaud[1], Céline Nanteau[1], Amélie Slembrouck-Brec[1], Valérie Fradot[1], José-Alain Sahel[1,3,4], Ramin Tadayoni[1,2], Jérôme Roger, Florian Sennlaub, Olivier Goureau[1], Xavier Guillonneau[1,*] & Sacha Reichman[1,*]

[1] Institut de la Vision, Sorbonne Université, INSERM, CNRS, Paris, France

[2] Department of Ophthalmology, Hôpital Lariboisière, AP-HP, Université Paris 7 – Sorbonne Paris Cité, Paris, France

[3] CHNO des Quinze-Vingts, DHU Sight Restore, INSERM-DHOS CIC, Paris 1423, France

[4] Department of Ophthalmology, University of Pittsburgh School of Medicine, Pittsburgh, PA 15213, USA

* Last authors contributed equally

Abbreviated Title: Human iPS-derived retinal Müller glia cells

Correspondence:

Sacha Reichman : sacha.reichman@inserm.fr

Xavier Guillonneau : xavier.guillonneau@inserm.fr

Financial support:

Conflict of interest: No conflicting relationship exists for any author regarding the content of this article

Introduction

Pluripotent stem cells, like human embryonic stem cells (hESCs) or induced pluripotent stem cells (hiPSCs), have the ability to be expanded indefinitely in culture. Recent advances in stem cell biology have allowed considering retinal cell replacement as a strategy for the treatment of degenerative retinopathies (Dalkara *et al.*, 2016; Reichman *et al.*, 2017; Zhao *et al.*, 2017). Cell replacement strategies has demonstrated their efficacy for the replacement of retinal monolayer such as RPE for the treatment of Stargard disease or geographic atrophy but reconstructing higher spatially organized multi-cellular structure such as the inner nuclear layer remains a challenge. This latest limitation prevents so far the use of replacement therapies in retinal vascular disease. Another advantage of hiPSCs is the possibility to generate appropriate non-biased cellular models from donor that can be used to explore physiology and develop screening strategies.

Diabetic retinopathy (DR) remains the first cause of visual loss in the age-working population in industrialized countries, and current treatments of the disease are not fully satisfying. Given the multiple pathways, stimuli and cells implicated in DR pathogenesis, no single animal model of the disease currently exists that faithfully reproduces all aspects of human DR and the end-stages complications of proliferative DR and macular edema. Finding new therapies are thus hampered by the lack of fully reliable and appropriate models of spontaneous diabetes in which phenotypic characteristics fully mimic the human pathogenesis (Cai X & MCGinnis JF, 2016) and new strategies for developing models of the clinical disease are needed. The use of hiPSCs should help to deciphering the particular role of different cell types in the pathology, and could be a useful model for screening potential new therapeutic drugs.

Growing evidences indicate that Müller glia cells (MGCs) reaction is involved in DR formation and may occur early, even before any vascular changes (Coughlin *et al.*, 2017). Indeed, DR is classically considered to be a microangiopathy because microaneurysms and pre-retinal neovascularization are observed. However several recent studies have suggested that neurodegenerative and inflammatory events may precede theses vascular changes (Rungger-Brandle *et al.*, 2000; Joussen *et al.*, 2004; Zeng *et al.*, 2008).

Being intercalated between vasculature and neurons, retinal Müller cells has been shown to have a crucial role in the uptake of glucose from the retinal capillaries, its metabolism, and transfer of energy to neurons (Coughlin *et al.*, 2017). Under hyperglycemic conditions, MGCs release several growth factors, such as vascular endothelial growth factor (VEGF) and pigment epithelium-derived factor (PEDF), and a variety of cytokines and chemokines including interleukin-1ß (IL-1ß), interleukin-6 (IL-6), tumor necrosis factor-α (TNF-α), and chemokine ligand-2 (CCL2). Theses pro-inflammatory cytokines produced contributes to the chronic

inflammation and the drop-out of neurons in DR. (Mizutani *et al.*, 1998; Kusner *et al.*, 2004; Gerhardinger *et al.*, 2005; Yego *et al.*, 2009; Zhou *et al.*, 2017).

Glucose may not be the only factor leading to inflammatory and vascular changes in DR, and recent studies demonstrated the role of dyslipidemia and fatty acids in this disease. Indeed, fenofibrate, a lipid-lowering drug, was shown to delay DR progression independently of glycemic control (Keech *et al.*, 2007; Wright & Dodson, 2011) and the fatty acids has been demonstrated to induce inflammatory reaction in rat and in human retinal endothelial cells (Chen *et al.*, 2003; Mohamed *et al.*, 2014; Capozzi *et al.*, 2016). More recently, Capozzi *et al.*, reported that the palmitic acid (PA), which is the most elevated fatty acid in diabetic patients (Korani *et al.*, 2012), was a strong stimulus to induce primary human MGC reaction (Capozzi *et al.*, 2018). In this study, MGC treatment with PA was effective to stimulate multiple DR-pathways such as inflammation signaling and angiogenesis; and this stimulation was potentiated by co-treatment with high glucose.

Given the central role of MGCs in the retinal homeostasis and its early implication in DR and DME pathogenesis, the use of hiPSC-derived Müller cells (hiMGCs) for DR disease modeling seems of high interest for identifying molecular pathways and new therapeutic targets. In this work, we aimed to present an innovative process to produce hiMGCs and to show that their inflammatory and angiogenic reaction to high lipid exposure is similar to that of primary human Müller cells.

Results

hiPSC-derived Müller glia cells generation

Müller glial cells are the last cell type to be generated in the retina (Donovan an Dyer, 2005, Stem cell Dev). Using a transcriptomic approach, Hoshino et al recently reported a maturation of MGCs during human retinogenesis after fetal day 136 (Hoshino et al., 2017). While methods have been developed to generate retinal neurons from IPS, generation of hiPSC-derived Müller cells has not been described so far. We previously described that MGCs were generated alongside with neurons in hiPSC-derived retinal organoids during the maturation in floating culture conditions (Reichman et al., Stem cell 2017). RLPB1 and GLAST1 MGC specific genes are expressed as early as day 56 (D56) in retinal organoids, but GS/SOX9 positive MGCs were only detected after D140 in retinal *in vitro* structure (Reichman et al., Stem cell 2017) and persist in retinal organoids until D686 (Data not shown). Taken the remarkable time correlation between human retinal retinogenesis and in vitro onset of MGC specific markers in iPS derived structures we decided to use retinal organoids between D150-200 to isolate and expand human hiMGCs. Retinal organoids between D150 and D200 were collected and the neuroretinal part was dissociated (Figure 1A-B). From D150, organoids are devoid of retinal progenitors and all neuronal cells are post-mitotic (Reichman et al., Stem cell 2017). hiMGC were selected from progenitors and neurons in vitro using previously described protocols for adult MGC isolation (Hicks and Courtois Exp Eyes Res 1990). Cells were seeded in culture flasks in a MGC culture medium (Figure 1B). To allow for mitotic active cell selection, we cultured cells in serial passages in DMEM up to passage 4. we show that from passage 2, the vast majority of cells are VIM+ and GFAP- (Figure 1C) and GS+ and SOX9+ (Figure 1D) consistent with a retinal Muller glia phenotype. hiMGCs can be cryopreserved at passage 1 (p1) and the thawed cells express the same specific marker combination as fresh hiMGCp2. To compare hiMGCp2 to human MGC, we collected post-mortem retina and expand them in culture up to passage 2 (pMGCs) (Hicks and Courtois Exp Eyes Res 1990). We show that like hiMGCp2, MGCs were VIM-, GS- and SOX9-positive (Figure 1C-H) but remarkably, pMGCs also express GFAP a retinal marker of Muller glial activation that is only found in retinal astrocytes under physiological conditions (Figure 1E and 1G). Similar results were obtained with cell from passage 5 (data not shown). The same procedures were applied to isolate MGC from two additional patients and hiMGC were similarly generated from dermal foreskin (F3) and adult retina (5F). To ensure the reproducibility in the generation of hiMGCs, RNA from passage 2 MGCs from these three independent patients and RNA from passage 2 hiMGC derived from different iPS sources were RNAseq. We show that MGCs from different origin expressed a

majority of transcripts in common (8246 transcripts) and that only a limited subset of transcripts are restricted to pMGCs (609) or hiMGCs (416) (Figure 1I). Figure 1J indicates that 18 MGC specific transcripts within different pathways (transcription factors, substrate transporter; water homeostais and cytoskeleton) are expressed to similar level in p- and Hi-MGCs. hiMGC celli line A2 was chosen as the prototypic cell line in further experiment.

Disease modeling

Recent advances in stem cell biology have allowed considering retinal cell replacement as a strategy for the treatment of retinopathies but also as a very valuable tool for disease modeling. Given the implication of MGCs in early in DR and DME pathogenesis, the use of hiPSC-derived Müller cells (hiMGCs) for DR disease modeling seems of high interest for new therapeutic targets. Primary human Müller cells react to glycemic and lipidic stresses relevant of DR and DME stress by regulating genes involved in the inflammatory and angiogenic pathway(Capozzi *et al.*, 2018). To validate the ability of hiPSCs-derived Müller cells to behave as primary human Müller cells, we study their reaction to high glucose and high lipid exposure. Protoypic hiMGC cell line A2 were treated for 24 hours as follows: NormoGlucose (NG; DMEM with 5 mM glucose); NG/PA (DMEM with 5 mM glucose plus Palmitic Acid 500 µM); HighGlucose (HG, DMEM with 25 mM glucose); HG/PA (DMEM with 25 mM glucose plus PA 500 µM). After 24h of treatment RNA were collected and we evaluated the expression of 4 genes of inflammatory/angiogenic pathways, ATF3, CXL1-2, CXCL8 (IL-8) and ANGPTL4 that were shown to be up-regulated with large log2fold changes in primary human Müller cells in DR conditions (Capozzi *et al.*, 2018). HG culture conditions only slightly increased the expression of ATF3, CXL1-2, CXCL8 and ANGPTL4 in hiMGC cell line A2 when compared to NG conditions (Figure 2A). We next quantify these genes in all patient and iPS derived MGCs in the same culture conditions, as shown in Figure 2B, HG stimulation consistently resulted into a 0.8-, 1.2- and 1.0-fold increase in the expression ATF3, CXL1-2, and ANGPTL4 respectively in patients and 1.2-, 0.9- and 1.8-fold in hiMGCs. In contrast, PA exposure resulted in a strong induction of the relative expression of these 4 genes both in NG and HG conditions (Figure 2A). Similar to hiMGC cell line A2, all patient and iPS derived MGCs respond to PA in HG conditions with a mean 28.4-, 3.7- and 5.0-fold increase in the expression of ATF3, CXL1-2 and ANGPTL4 genes in patients and 52.7-, 19.9-, 3.3-fold in hiMGCs.

Having established that all of our iPS derived MGCs respond to DR-stress as primary Muller cells we next investigate their abilities to remodel vessels. We showed that glycaemia conditions modestly regulates hiMGCS transcription, we thus next focus our study on PA-

induced regulations of hiMGCS secretome in normoglycemia. We first analyzed the expression of a large panel of angiogenic-related protein using an angiogenic blot assay (Figure 3A). We show that 24h secretome of hiMGC cell line A2 treated in NG/PA conditions contains detectable amount of 41 angiogenic-related proteins (out of the 55 blotted proteins) indicating potential vascular remodeling capacities (Figure 3B). Among these proteins, only 19 proteins appear to be regulated by palmitic acid. 17 pro-angiogenic factors were all found up-regulated. These proangiogenic factors belong to different families including growth factors (EG-VEGF, FGF1, and VEGF), Cytokine (CXCL-4, -8, -16, Il-1ß and MIP1a), proteins involved in mural cell maintenance (Ang1, Ang2) and matrix remodeling (MNP9, and PDGFAA) (Figure 3C). Two anti-angiogenic proteins were found regulated, ADAMTS1 is up-regulated while DPPIV was down-regulated (Figure 3D).

Considering the central role of VEGF in the pathogenesis of DR we next analyzed in more details the regulation of VEGF by PA in Muller cells from different origin. All derived Muller cells increase their transcription of VEGF in response to PA with a 2- and 3-fold increase for cell derived from patient and iPS respectively (Figure 4A). In contrast NG vs HG conditions resulted only in modest regulation of VEGF (data not shown). To analyze the capacities of this secretome to affect vascular growth, we used an ex-vivo test where aortic rings were allowed to form endothelial cell sprouts in the presence or not of conditioned medium (CM) of MGCs. hiMGC cell line A2 was cultured for 24H in the presence or not of PA in NG condition. As shown in figure 4B, this cell line responds to PA with a 3.5-fold increase in VEGF transcription (and the corresponding VEGF secretion, data not shown). CM were added to aortic rings after 3 days of growth in normal condition and the length of EC sprouts was evaluated at day 6 (Figure 4C). CM from hiMGC cell line A2 treated with PA significantly promotes vascular outgrowth while CM from non-treated hiMGC failed at modifying EC growth (Figure 4D).

Discussion

In this study, we described for the first time the production of Müller cells from reprogrammed iPS from different origins: adult dermal biopsy, post-natal foreskin and adult retina. These cells can be banked and passaged without losing their glial phenotype. Similar to primary MGCs, hiMGCs poorly respond to glucose but respond to high lipid exposure (a stress relevant of diabetic retinopathy) by up-regulating their inflammatory and angiogenesis reactions. Finally, we showed that PA stimulated hiMGCs secrete angiogenic factors related to DR such as VEGF, IL-8, IL-1ß and ANGPTL4 and have a pro-giangiogenic activities ex-vivo. Taken together, these hiMGCs represent an extremely valuable tool to better understand mechanisms of complex diseases and for the development of new therapeutic. In particular, hiMGCs can be generated from donors and easily expanded to be used in high-throughput drug screens.

Our data demonstrate that hiMGCs are closely related to pMGCs. Indeed IHC analysis revealed that hiMGCs express vimentin, gutamine synthetase and SOX9 as pMGCs. Using a transcriptomic approach, we further show that unstimulated hiMGCs derived from iPS of different origins express 18 key MGCs proteins at similar levels. Of note, unlike primary MGCs, hiMGCs express no to very low levels of GFAP, an actin filament expressed by retinal astrocytes and activated MGCs indicating that these cells are in a resting state relevant of a physiological situation in the retina. Easy generation and expansion of hiMGCs from different sources prone them to be use in high-throughput drug screening approaches. We showed that hiMGCs do not express significant levels of GFAP in normal culture condition. As MGCs GFAP expression is generally associated with the production of retinal deleterious mediators and loss of trophic activity, GFAP expression can thus be used as an extremely valuable additional read-out to determine the potential toxicity of drugs on non-activated MGCs and easily disqualify potential hazardous compounds. This latest read-out is not available with GFAP expressing pMGCs.

We showed that resting hiMGCs resemble pMGCs. We next assayed their response to stress relevant of diabetic retinopathies to evaluate their potential use in disease modeling approaches. Recent evidences support the role of non-glucose stimuli in DR onset and progression. The elevation of blood glucose is not the only change occurring in diabetic patients as multiple metabolic alterations, including elevated circulating lipid, may be implicated in the cellular responses observed in DR. Several *in vitro* studies showed no effect of high glucose exposure on inflammatory and angiogenesis responses in human retinal endothelial cells (Chen 2003, Madonna 2016). Similarly, several DR-relevant pathways were enriched by PA treatment in

human Müller glial cells, while no notable targets were detected with high glucose treatment alone (Capozzi *et al.*, 2018). This role of high lipid exposure in DR pathogenesis is also supported by the results of large clinical studies such as ACCORD and FIELD trials, showing that dyslipidemia treatment was effective in reducing DR progression, independently of glycemic control (Keech *et al.*, 2007; Wright & Dodson, 2011). In order to test and validate the ability of hiPSCs -derived Müller cells produced, we thus evaluate the expression of several genes that were previously demonstrated to play a key role in DR pathogenesis and that were shown to be upregulated in human primary Müller cells when culture in the presence of free fatty acids (Capozzi *et al.*, 2018). Our data demonstrate that hiMGCs cell line A2 react to PA as pMGCS for all the selected genes. We found hiMGCs response to PA very consistent from one hiMGCs cell line to the other indicating that hiMGCs can be reprogrammed from cells of different cell line without affecting their identity. All together our data demonstrate that the generation hiMGCs provide a valuable tool for future studies investigating molecular DR-pathways in human retina or testing new therapeutic drugs. We here focused our study on angiogenic and inflammatory responses to metabolic stress but similar profile of expression of MGC specific ABCC transport by hiMGCs and pMGCs predict that these cells could also be a relevant model to study substrate transport. Conversely as hiMGCs poorly express AQPs they might not be relevant to study water transport across blood retinal barriers. Deeper analysis of RNA sequence data and in particular analysis of annotated pathways will be used to pre-qualify or not these cells for the study of other functions supported by MGCs such as the production of survival factors, glutamate and water homeostasis and substrate transport.

The regulation of several DR-relevant genes implicated in angiogenesis and inflammatory pathways prompted us to interrogate the capacity of hiMGCs secretome to affect angiogenesis. We thus compared the expression of 55 angiogenesis-related factors in the conditioned media (CM) from control and PA-treated hiMGCs. We showed that the vast majority of the regulated proteins are pro-angiogenic factors. Regulated pro-angiogenic factors tested were all found up-regulated. This includes proteins associated with DR such as Angiogenin 2, endoglin, Il-1ß, Il-8, MMP9, PDGF AA and VEGF. Among anti-angiogenic factors found regulated, DPP IV protein was found down-regulated whereas ADAMTS1 and CXCL4 were found up-regulated. Given the complex blend of pro- and anti-angiogenic factors regulated by PA in hiMGCs, the angiogenic activity of their CM was unpredictable. We thus used an in vitro assay where aorta explants are embedded in a collagen matrix to allow tridimensional endothelial cell (EC) sprouting and showed that hiMGC CM treated with PA are pro-angiogenic. In contrast control hiMGC CM did not exhibit pro-angiogenic activity when compared to control media. This may reflect the subtle balance between pro- and anti-angiogenic proteins secreted by hiMGC CM

under control conditions. Indeed, apart the above mentioned pro-angiogenic proteins hiMGCs express potent anti-angiogenic proteins such as TSP-1or TIMP1 that may limit angiogenesis in control conditions. As we showed that PA mostly regulated pro-angiogenic factors, the balance may be shifted toward a pro-angiogenic effect in hyper-lipidemic conditions. Another possibility might be that PA treated hiMGC CM exert an VEGF independent pro-angiogenic activity. In the mouse aortic ring recombinant VEGF (10 ng/ml) is added for the first 4 days before to allow EC initial sprouting and favor EC survival. We showed that hiMGC CM from control and PA conditions contains VEGF, but its contribution to EC sprouting might be minimal compared to exogenous recombinant and explant-derived VEGF. In line with that we showed that control hiMGC CM did not exhibit pro-angiogenic activity when compared to control media despite detectable amount of VEGF. Future experiment using VEGF antagonists will discriminate these two possibilities.

Molecules that limit the bio-availability of intra-ocular VEGF are the leading curative treatment for retinal edema and vascular proliferation that occurs in AMD and DR. Anti VEGF are efficient in the treatment of AMD but DR patients are often resistant, or become resistant to these treatments indicating that, at least in the case of DR, angiogenesis and edema formation do not rely solely on VEGF. In line with that elevated levels of cytokine are found in the vitreous of patients with NPDR, DME and PDR (McAuley *et al.*, 2014). The observed increase in cytokine is concomitant with glial activation and macrophage infiltration and occurs generally before the onset of clinical signs. Most of these molecules have proliferative activity on EC cells or increased vascular permeability (for review (Rubsam *et al.*, 2018)). Impairing inflammation limit the progression of DR in animal model and is an effective therapeutic alternative for patient with VEGF resistance. We showed that hiMGC stimulated with PA produce and secreted a large panel of angiogenic-related molecules associated with DR such as Angiogenin 2, endoglin, Il-1ß, Il-8, MMP9, PDGF AA and VEGF and that their CM is proangiogenic. It is thus tempting to speculate that one or a combination of these factor participate to vascular remodeling that occurs in DR and that persist in VEGF-resistant patients. Among possible candidates, our study has pointed out potential cytokine involved in VEGF-independent Muller derived angiogenic factors. Regarding inflammatory pathways, we investigated by qPCR the expression of CXCL8 (or IL-8) in hiPSCs-derived Müller cells. This chemokine is implicated in neutrophil migration and chemotaxis(Ghasemi *et al.*, 2011) and participates to vascular leakage and central nervous system edema (Semple *et al.*, 2010). CXCL8 is expressed by glial cells and is up-regulated by hypoxia(Yoshida *et al.*, 1998). It has been found to be elevated in the vitreous of DR patients(Patel *et al.*, 2006; Petrovic *et al.*, 2007;

Funatsu *et al.*, 2009; Yoshimura *et al.*, 2009). As VEGF can promote CXCL8 expression, CXCL8 level might only reflect VEGF levels (Lee *et al.*, 2002). However, several studies have demonstrated that CXCL8 and VEGF level were statistically independent (Bromberg-White *et al.*, 2013). Another demonstration of VEGF and CXCL8 independent role come from the clinic where the level of CXCL8 level in patient resistant to anti-VEGF therapy is correlated to the success of anti-inflammatory therapy (Jeon, 2014). Taken together CXCL8 expression by MGC in pathological conditions may have a central role in the pathogenesis of diabetes by promoting inflammatory cell recruitment, vascular permeability and angiogenesis. Il-1ß was also found increased in the secretome of Muller cells and increase in hiMGCs placed in inflammatory conditions (data not shown) and is associated with DR (Rubsam *et al.*, 2018). Il-1ß and VEGF induce a large and common repertoire of gene in endothelial cells, making of Il-1ß a very potent angiogenic factor (Schweighofer *et al.*, 2009). Unlike VEGF, Il-1ß is not spontaneously secreted but required the activation of inflammasome (Schroder & Tschopp, 2010). The extent of Il-1ß secretion by muller cells in PA treated cells or more generally DR conditions remains to be determined.

Regarding angiogenesis pathway, beside VEGF which role has been extensively described in diabetic retinopathy, we evaluated ANGPTL4 expression by qPCR. ANGPTL4, a well-characterized target of PPAR-β/δ signaling, has been demonstrated to play also an important role in the angiogenesis pathway in proliferative DR (Babapoor-Farrokhran *et al.*, 2015; Jee *et al.*, 2017). Therapies directed against ANGPTL4 are now emerging to control EC proliferation in the context of diabetic retinopathies (Sodhi & Montaner, 2015; Yang *et al.*, 2018). Further experiment will determine the participation of hiMGC derived angiogenic and inflammatory molecules involved in VEGF-independent vascular remodeling.

The central role of Müller glial cells in DR as well as the absence of clinically-relevant animal model support the use of in vitro models. The hiPSCs-derived Müller cells may thus be used for future studies investigating molecular DR-pathways in human retina or testing new therapeutic drugs.

Materials and Methods

Human iPSC maintenance

The human iPSC-2 clone (Reichman et al., 2014) were derived from adult dermal fibroblasts using the episomal reprogrammation approach. Human iPSCs were adapted and cultured on truncated recombinant human vitronectin-coated dishes with Essential 8™ medium (ThermoFisher Scientific) as previously described (Reichman et al., 2017). Briefly, iPS colonies from hiPSC-2 clone cells were incubated 7 to 10 min in 2 ml of enzyme-free Gentle cell dissociation reagent (STEMCELL Technologies) at room temperature. After aspiration of the dissociation solution, detached cell aggregates were resuspended in 2 ml of pre-warmed chemical defined Essential 8™ medium (Thermo Fischer Scientific). Human iPSCs were transferred on truncated recombinant human vitronectin (rhVTN-N)-coated dishes with Essential 8™ medium. Cells were routinely cultured at 37°C in a standard 5% CO2 / 95% air incubator with a daily medium change. iPS cells were passaged with the enzyme-free Gentle cell dissociation reagent every week. Detached cell aggregates were collected in Essential 8™ medium and carefully pipetted up and down to obtain uniform suspension of cell aggregates and replated at ratio of 1/10 to 1/60 depending on the confluence.

Retinal differentiation

For retinal differentiation adherent iPSCs were expanded to 70-80 %, then FGF-free medium was added to the cultures for 2 days followed by a neural induction period allowing the appearance of retinal structures. Identified retinal organoids were manually isolated and cultured as floating structures for the next several weeks to follow retinal differentiation as previously described (Reichman et al., 2017 and Slembrouck-Brec et al., 2018).

Human post-mortem and hiPSCs-derived Müller glia cells isolation and amplification

Human post-mortem retinal tissue or retinal organoids were dissociated accordingly to the protocol described in Reichman et al., 2017. Briefly for iMGCs, floating retinal organoids were collected between D150 and D200. Distal pigmented RPE was discarded from the structures under a stereomicroscope and neuroretinal structures were washed 3 times in Ringer solution (NaCl 155 mM; KCl 5 mM; CaCl2 2 mM; MgCl2 1 mM; NaH2PO4 2 mM; HEPES 10 mM and Glucose 10 mM). RPE-free retinal organoids were dissociated with two units of pre-activated papain at 28.7 u/mg (Worthington) in Ringer solution during 25 min at 37°C. When cells were homogeneously resuspended with up and down pipetting, then papain was deactivated by adding 1 ml of MGC medium (DMEM High glucose, SVF 10%, 100 units/ml

Penicillin and 100 µg/ml Streptomycin). Cells were centrifuged at 110 g and resuspended in pre-warmed MGC medium. Retinal cells were plated at 50 000 cell/cm² in T-25 cm² flask previously coated with Geltrex matrix (Thermo Fischer Scientific) and incubated at 37°C in a standard 5% CO2 / 95% air incubator. Medium was changed every 2 days.

Cryopreservation of MGCs

pMGCp1 or hiMGCp1 were cryopreserved in DMSO 10%, SVF 90% solution ($4x10^5$ Cell/500µl/cryotube) and placed in isopropanol-based Mr Frosty freezing container (Thermo Fischer Scientific) at -80°C for a minimum of 4 hours. Frozen tubes were kept in a -150°C freezer for long-term storage. Frozen MGCs were thawed quickly at 37°C in a water bath and resuspended in prewarmed dedicated media for downstream investigations.

Immunostaining and imaging of MGCs

Retinal cells were fixed with 4% PAF in PBS for 5 min before immunostaining. After washes with PBS, nonspecific binding sites were blocked for 1 hour at room temperature with a PBS solution containing 0.2% gelatin and 0.25% Triton X-100 (blocking buffer) and then overnight at 4°C with the primary antibody against human VIMENTIN (VIM, 1:100, Millipore), GLIAL FIBRILLARY ACIDIC PROTEIN (GFAP, 1:200, Cell Signaling Technology), GLUTAMIN SYNTETHASE (GS, 1:500, Millipore), SRT-BOX 9 (SOX9, 1:1000; Millipore) diluted in blocking buffer. Slides were washed three times in PBS with 0.1% Tween and then incubated for 1 hour at room temperature with appropriate secondary antibodies conjugated with either AlexaFluor 488, 594 or 647 (Interchim) diluted at 1:600 in blocking buffer with 4',6-diamidino-2-phenylindole (DAPI) diluted at 1:1000 to counterstain nuclei. Fluorescent staining signals were captured with an Olympus FV1000 confocal microscope equipped with 405, 488, 543 and 633 nm lasers. Confocal images were acquired using a 1.55 or 0.46 µm step size and corresponded to the projection of 20 to 40 optical sections.

Palmitate solubilization in culture medium

To allow for the **solubilization** of palmitate (PA) in culture medium, PA is bind to bovine serum albumin FFA-free (BSA, Sigma-Aldrich). Briefly, a solution of 0.1 M of PA (Sigma-Aldrich) in 100 % ethanol (etOH) is added at 1:200 to a BSA-culture medium (0.88% w/v of BSA) to obtain a culture medium at 500 µM PA, 0.5 % v/v etOH, corresponding to a molar ratio PA/BSA of 3.85.

hiPSCs-derived Müller cells culture and treatment

hiPSCs-derived MGCs and patient-derived pMGCs were thawed and grow in Dulbecco's Modified Eagle Medium high-glucose 25 mM (DMEM HG, Gibco) with 10 % fetal bovine serum (FBS) at 37°C in a standard 5% CO2 / 95% until passage 3 (p3). 24 h before passaging, the medium was changed and p3 hiPSCs-derived Müller cells were serum-starved and cultured under Dulbecco's Modified Eagle Medium normo-glucose 5 mM , 20 mM mannitol (Man) complemented (DMEM NG with 5 mM glucose, 20 mM mannitol, no FBS). 20 mM Man was added to keep osmotic condition similar to DMEM HG). P3 Cells were then passed in geltrex-coated dishes (16 000 cells/cm^2) and allow to attach for 4h in DMEM NG. When attached hiMGCs and pMGCs were kept for 18 h or 24 h in 4 different culture conditions referred as follow NG (DMEM 5 mM glucose, 20 mM mannitol, BSA 0.88 w/v, etOH 0.5 v/v) or HG (DMEM 25 mM glucose, BSA 0.88 w/v, etOH 0.5% v/v) or NG/PA (DMEM 5 mM glucose, BSA 0.88 w/v, etOH 0,5 v/v) or HG/PA (DMEM 25 mM glucose, BSA 0.88 w/v, PA 500 µM, etOH 0.5% v/v).

RNA isolation, reverse transcription and real-time quantitative polymerase chain reaction

Treated hiMGCs were lysed and RNA purified using the RNA XS kit (740902, Macherey-Nagel, Düren, Germany) according to the manufacturer's protocol. Total RNA was isolated and converted to cDNA using QuantiTect Reverse Transcription Kit (Quiagen). Each reverse transcription assay was performed in a 20 µL reaction. Subsequent real-time qPCR (RT-qPCR) was performed using cDNA, Sybr Green PCR Master Mix (Life Technologies). RT-qPCR was performed using StepOne Plus real-time PCR system (Applied Biosystems) with the following profile: 10 min at 95°C, followed by a total of 40 two-temperature cycles (15 sec at 95°C and 1 min at 60°C). To verify the purity of the products, a melting curve was produced after each run according to the manufacturer's instructions. Results were expressed as fold induction after normalization by RPS26 gene expression. Primers for RT-qPCR were purchased from IDT technology (primer sequences at request).

Angiogenic assay

Aortic rings were prepared from the aorta of 3-weeks-old mice. After excision from the animal, the aortas were placed in a serum-free Opti-MEM medium (Gibco) plus 0,1% primocin (InvivoGen). Under dissection microscope, all extraneous fat, tissue and branching vessels were removed with forceps and microscissors, blood clot was flushed out of the lumen with a needle fixed to a syringe filled with Opti-MEM. The aortic tube was then cross-sectioned into

approximately 0.5-mm-long rings. A collagen gel mixture was prepared at 4°C by mixing of 1:2 of 2 mg/mL collagen rat tail (Roche) solution in 0,2 % v/v acetic acid with 1:2 of DMEM without glucose and pyruvate (Gibco) and few drop of 5 N NaOH to equilibrate around pH 7. Aortic rings (AR) were then embedded individually in 96 wells-plate into 60 µL collagen mixture. When all the AR were embedded, the culture plate was placed in incubator at 37°C for 20 minutes to allow the collagen gel to solidify and 150 µL of Opti-MEM medium complemented with Glutamax 1% (Gibco), FBS 1%, VEGF 10 ng/mL (R&D Research), primocin 0,1 % was added in each well. After 3 days of culture pictures of AR sprouts were taken. AR were equitably split according to their grow in 4 groups 130 µL of culture medium was replaced by the following medium: NG medium, conditioned medium from NG-treated hiMGCs (hiMGs CM), NG/PA medium or conditioned medium from NG/PA-treated MGCs (PA-hiMGCs CM). All these medium were complemented with FBS 1%, glutamax 1% and primocin 0,1%. The medium wass renewed every 2 days. After 5 days of culture of stimulation, AR were fixed by addition of 100 µL of PFA 4% per well for 30 min. Fixed AR were washed in PBS, permeabilized by addition of Triton X100 0,5% for 20 minutes and labeled overnight with Isolectine GS-IB4, Alexafluor 568 conjugate (InvitroGen) 1:100. Pictures of endothelials sprouts were taken with a CoolSNAP HQ2 (Photometrics, Tucson, AZ, USA) camera on Eclipse Ti (Nikon, Tokyo, Japan) microscope. The length aortic sprouts were then measured and quantification is processed on the mean length of the ten longer sprouts of each rings using Fiji software (Rueden et al, 2017; Schneider et al, 2012).

Profiling of angiogenesis related protein in hiMGCs secretome

The relative expression profile of 55 human angiogenesis-related proteins was performed using Proteome Profiler Human Angiogenesis Array kit (R&D Systems, NE, Minneapolis, U.S.A) following the manufacturer's instructions. Briefly, 700 µL of 24 h supernatant from NG or NG/PA-treated hiMGCs was analyzed and pictures acquired using Fusion 7 blot reader (Vilbert, Marne la vallée, France). Each duplicate spot represents detection of a specific antigen. The relative level of angiogenesis related proteins were quantified by measurement of pixel intensity, following subtraction of local background level. Reference spots served as a positive control to normalized pixel intensity for each membrane. Results were expressed in RDUs.

Legends to Figure

Figure 1: Generation and characterization of hiMGCs. (A) Schematic diagram of retinal organoids generation and maturation**.** Retinal organoids are allowed to differentiate up to 150 - 200 days in previously described conditions **(B)** Schematic diagram of the selection, amplification and banking of human iPSC-derived Muller glia cells (hiMGCs). Between D150 and 200 retinal organoids are dissociated and MGC are cultured in conditions favorizing Muller cell expansion. Between day 7 and 14 MGC cells are dissociated and serial passaged. At days 14, passage2 (P2) MGCs are cryopreserved. Cryopreserved cells can be expand in serial passages from p3 to p4. **(C-H)** Immunochemistry analysis of fresh or thawed hiMGCs at passage 2 (hiMGCp2) **(E-F)** and thawed patient MGCs (pMGC) at passage 2 (hiMGCp2) (G-H) for the Müller glia cell makers VIM and GFAP (C, E and G) or GS and SOX9 (D, F and H). Scale bar = 50 µm. (I-J) Transcriptomic profile of patient and iPS-derived MGC. pMGC from 3 different donor and from 3 different iPS clone were cultured up to passage 2. RNA were collected, extracted and submitted to RNAseq. **(I)** Schematic representation of transcript with FPKM >=10 specitific to pMGC (orange), hiMGC (light blue) or common to pMGC and hiMGC (yellow). **(J)** Log2 representation of know Muller cell specific genes in the 3 pMGC derived from 3 independent donnors and 3 hiMGCs derived from 3 different iPS cell lines.

Figure 2: Patient and iPS-derived Muller glial cells responses to hyperglycemic and free fatty acid DR-relevant stress. Protoypic hiMGC cell line A2 **(A)** and Patient and iPS-derived Muller glial cells **(B and C)** were treated for 24 hours as follows: NormoGlucose (NG; DMEM with 5 mM glucose); NG/PA (DMEM with 5 mM glucose plus Palmitic Acid (PA) 500 µM); HighGlucose (HG, DMEM with 25 mM glucose); HG/PA (DMEM with 25 mM glucose plus PA 500 µM). After 18h of treatment RNA were collected, reverse transcribed and analyzed by qPCR. **(A)** hiMGC-A2 relative expression of *ATF3, CXL1-2, CXCL8* (*IL-8*) and *ANGPTL4* transcripts normalized by RPS26 house-keeping gene expression. hiMGC-A2 kept in NG was selected as reference, white bars represent MGC cells cultured in the absence of PA, black bars with PA. Experiments were repeated twice. (n=6/conditions, Kruskal-Wallis test followed by Dunn's multiple comparison, *p<= 0.05). **(B and C)** Relative expression of *ATF3, CXL1-2, CXCL8* (*IL-8*) and *ANGPTL4* normalized by *RPS26* house-keeping gene expression in MGC cells from patients (white bars) (n=3) or derived from iPS cells lines (grey bars) (n=3). The fold increase represents the mean ± SEM ratio of HG on NG **(B)** and HG/PA on HG **(C)** for each group. transcript with a ration of 1 (Dashed red line) are not regulated in the corresponding experimental conditions. (n=4/cell line; n=3 per group).

Figure 3: The expression of potent angiogenic factors is regulated by PA in hiMGC-A2. The expression of a 55 angiogenic-related protein was analyzed in the secretome of 24h-treated hiMGC-A2 using an angiogenic blot assay. (A) Representative photograph of a blot using NG+PA hiMGC-A2 secretome as a probe. (B) Quantification of the expression of the 55 blotted proteins in NG+PA conditions. Images were acquired on a Fusion 7 blot reader and gray values were normalized using the positive controls spotted in 3 corners. Negative controls served as reference. Error bars represent the SD between two contiguous spots for each protein. (C) For each protein, the ratio of its expression in NG+PA vs NG was calculated. Up regulated protein (ration >1) are plotted in (C). Blots are presented for each protein in NG (left panel) and NG+PA (right panel) with corresponding up-regulation value.

Figure 4: The secretome of PA-stimulated hiMGC-A2 is pro-angiogenic. (A) Patient and iPS-derived Muller glial cells were treated for 24 hours in control conditions (NormoGlucose (NG); DMEM with 5 mM glucose) or treated with Palmitic Acid (PA) (NG/PA, DMEM with 5 mM glucose plus; PA 500 µM). After 24h of treatment RNA were collected, reverse transcribed and *VEGF* expression analyzed by qPCR. (**A**) Relative expression of *VEGF* transcripts normalized by *RPS26* house-keeping gene expression in MGC cells derived from patients (white bars) (n=3) or derived from iPS cell lines (grey bars) (n=3). The fold increase represents the mean ± SEM ratio of NG vs NG/PA for each group. Red dashed line is set to 1. (n=4/cell line; n=3 per group). (**B**) hiMGC-A2 relative expression of *VEGF* transcripts normalized by *RPS26* house-keeping gene expression. hiMGC-A2 kept in NG was selected as reference, white bars represent MGC cells cultured in the absence of PA, black bars with PA. Experiments were repeated twice. (n=6/conditions, Mann-Withney test, *p<= 0.05). (C and D) hiMGC cell line A2 conditioned medium (CM) were tested in the mouse aortic ring assay to evaluate angiogenic properties. hiMGC cell line A2 MGC cell line was cultured in the presence or not of PA and conditioned medium (CM) were collected after 24H. Mouse aortic rings were allowed to form endothelial cell sprouts for 3 days and then treated with CM from control (hiRMG CM) or PA-treated (hiMGC PA-CM) for an additional 3 days. **(C)** Representative microphotographs of mouse aortic rings after 6 days of culture in the presence of hiRMG CM (left panel) or hiMGC PA-CM (right panel). **(D)** Quantification of the vascular sprout length after 6 days of culture in the presence from D3 to D6 of vehicle (Vehi; BSA and EtOH, white bar), vehicle + PA (PA, X µM, light gray bar), hiRMG CM (dark gray bar) or hiMGC PA-CM (black bar). Values are represented ± SEM, n>10 per conditions. *p<= 0.05 (Kruskal-Wallis test followed by Dunn's comparison, hiRMG CM selected as control)

Bibliography

Babapoor-Farrokhran, S., Jee, K., Puchner, B., Hassan, S.J., Xin, X., Rodrigues, M., Kashiwabuchi, F., Ma, T., Hu, K., Deshpande, M., Daoud, Y., Solomon, S., Wenick, A., Lutty, G.A., Semenza, G.L., Montaner, S. & Sodhi, A. (2015) Angiopoietin-like 4 is a potent angiogenic factor and a novel therapeutic target for patients with proliferative diabetic retinopathy. *P Natl Acad Sci USA*, **112**, E3030-E3039.

Bromberg-White, J.L., Glazer, L., Downer, R., Furge, K., Boguslawski, E. & Duesbery, N.S. (2013) Identification of VEGF-independent cytokines in proliferative diabetic retinopathy vitreous. *Invest Ophthalmol Vis Sci*, **54**, 6472-6480.

Capozzi, M.E., Giblin, M.J. & Penn, J.S. (2018) Palmitic Acid Induces Muller Cell Inflammation that is Potentiated by Co-treatment with Glucose. *Sci Rep*, **8**, 5459.

Capozzi, M.E., Hammer, S.S., McCollum, G.W. & Penn, J.S. (2016) Epoxygenated Fatty Acids Inhibit Retinal Vascular Inflammation. *Sci Rep*, **6**, 39211.

Chen, W., Jump, D.B., Grant, M.B., Esselman, W.J. & Busik, J.V. (2003) Dyslipidemia, but not hyperglycemia, induces inflammatory adhesion molecules in human retinal vascular endothelial cells. *Invest Ophthalmol Vis Sci*, **44**, 5016-5022.

Coughlin, B.A., Feenstra, D.J. & Mohr, S. (2017) Muller cells and diabetic retinopathy. *Vision Res*, **139**, 93-100.

Dalkara, D., Goureau, O., Marazova, K. & Sahel, J.A. (2016) Let There Be Light: Gene and Cell Therapy for Blindness. *Hum Gene Ther*, **27**, 134-147.

Funatsu, H., Noma, H., Mimura, T., Eguchi, S. & Hori, S. (2009) Association of Vitreous Inflammatory Factors with Diabetic Macular Edema *OPHTHA*. American Academy of Ophthalmology, pp. 73-79.

Gerhardinger, C., Costa, M.B., Coulombe, M.C., Toth, I., Hoehn, T. & Grosu, P. (2005) Expression of acute-phase response proteins in retinal Muller cells in diabetes. *Invest Ophthalmol Vis Sci*, **46**, 349-357.

Ghasemi, H., Ghazanfari, T., Yaraee, R., Faghihzadeh, S. & Hassan, Z.M. (2011) Roles of IL-8 in ocular inflammations: a review. *Ocul Immunol Inflamm*, **19**, 401-412.

Jee, K., Rodrigues, M., Kashiwabuchi, F., Applewhite, B.P., Han, I., Lutty, G., Goldberg, M.F., Semenza, G.L., Montaner, S. & Sodhi, A. (2017) Expression of the angiogenic mediator, angiopoietin-like 4, in the eyes of patients with proliferative sickle retinopathy. *PloS one*, **12**, e0183320.

Jeon (2014) EFFECT OF INTRAVITREAL TRIAMCINOLONE IN DIABETIC MACULAR EDEMA UNRESPONSIVE TO INTRAVITREAL BEVACIZUMAB *Retina*, pp. 1-6.

Joussen, A.M., Poulaki, V., Le, M.L., Koizumi, K., Esser, C., Janicki, H., Schraermeyer, U., Kociok, N., Fauser, S., Kirchhof, B., Kern, T.S. & Adamis, A.P. (2004) A central role for inflammation in the pathogenesis of diabetic retinopathy. *FASEB J*, **18**, 1450-1452.

Keech, A.C., Mitchell, P., Summanen, P.A., O'Day, J., Davis, T.M., Moffitt, M.S., Taskinen, M.R., Simes, R.J., Tse, D., Williamson, E., Merrifield, A., Laatikainen, L.T., d'Emden, M.C., Crimet, D.C., O'Connell, R.L., Colman, P.G. & investigators, F.s. (2007) Effect of fenofibrate on the need for laser treatment for diabetic retinopathy (FIELD study): a randomised controlled trial. *Lancet*, **370**, 1687-1697.

Korani, M., Firoozrai, M., Maleki, J., Ghahramanpour, F., Heidari, I., Fallah, S. & Seifi, M. (2012) Fatty acid composition of serum lipids in patients with type 2 diabetes. *Clin Lab*, **58**, 1283-1291.

Kusner, L.L., Sarthy, V.P. & Mohr, S. (2004) Nuclear translocation of glyceraldehyde-3-phosphate dehydrogenase: a role in high glucose-induced apoptosis in retinal Muller cells. *Invest Ophthalmol Vis Sci*, **45**, 1553-1561.

Lee, T.H., Avraham, H., Lee, S.H. & Avraham, S. (2002) Vascular endothelial growth factor modulates neutrophil transendothelial migration via up-regulation of interleukin-8 in human brain microvascular endothelial cells. *J Biol Chem*, **277**, 10445-10451.

McAuley, A.K., Sanfilippo, P.G., Hewitt, A.W., Liang, H., Lamoureux, E., Wang, J.J. & Connell, P.P. (2014) Vitreous biomarkers in diabetic retinopathy: a systematic review and meta-analysis. *Journal of diabetes and its complications*, **28**, 419-425.

Mizutani, M., Gerhardinger, C. & Lorenzi, M. (1998) Muller cell changes in human diabetic retinopathy. *Diabetes*, **47**, 445-449.

Mohamed, I.N., Hafez, S.S., Fairaq, A., Ergul, A., Imig, J.D. & El-Remessy, A.B. (2014) Thioredoxin-interacting protein is required for endothelial NLRP3 inflammasome activation and cell death in a rat model of high-fat diet. *Diabetologia*, **57**, 413-423.

Patel, J.I., Tombran-Tink, J., Hykin, P.G., Gregor, Z.J. & Cree, I.A. (2006) Vitreous and aqueous concentrations of proangiogenic, antiangiogenic factors and other cytokines in diabetic retinopathy patients with macular edema: Implications for structural differences in macular profiles *Experimental eye research*, pp. 798-806.

Petrovic, M.G., Korosec, P., Kosnik, M. & Hawlina, M. (2007) Vitreous levels of interleukin-8 in patients with proliferative diabetic retinopathy. *Am J Ophthalmol*, **143**, 175-176.

Reichman, S., Slembrouck, A., Gagliardi, G., Chaffiol, A., Terray, A., Nanteau, C., Potey, A., Belle, M., Rabesandratana, O., Duebel, J., Orieux, G., Nandrot, E.F., Sahel, J.A. & Goureau, O. (2017) Generation of Storable Retinal Organoids and Retinal Pigmented Epithelium from Adherent Human iPS Cells in Xeno-Free and Feeder-Free Conditions. *Stem Cells*, **35**, 1176-1188.

Rubsam, A., Parikh, S. & Fort, P.E. (2018) Role of Inflammation in Diabetic Retinopathy. *Int J Mol Sci*, **19**.

Rungger-Brandle, E., Dosso, A.A. & Leuenberger, P.M. (2000) Glial reactivity, an early feature of diabetic retinopathy. *Invest Ophth Vis Sci*, **41**, 1971-1980.

Schroder, K. & Tschopp, J. (2010) The inflammasomes. *Cell*, **140**, 821-832.

Schweighofer, B., Testori, J., Sturtzel, C., Sattler, S., Mayer, H., Wagner, O., Bilban, M. & Hofer, E. (2009) The VEGF-induced transcriptional response comprises gene clusters at the crossroad of angiogenesis and inflammation. *Thromb Haemost*, **102**, 544-554.

Semple, B.D., Kossmann, T. & Morganti-Kossmann, M.C. (2010) Role of chemokines in CNS health and pathology: a focus on the CCL2/CCR2 and CXCL8/CXCR2 networks. *J Cereb Blood Flow Metab*, **30**, 459-473.

Sodhi, A. & Montaner, S. (2015) Angiopoietin-like 4 as an Emerging Therapeutic Target for Diabetic Eye Disease. *JAMA ophthalmology*, **133**, 1375-1376.

Wright, A.D. & Dodson, P.M. (2011) Medical management of diabetic retinopathy: fenofibrate and ACCORD Eye studies. *Eye (Lond)*, **25**, 843-849.

Yang, X., Cheng, Y. & Su, G. (2018) A review of the multifunctionality of angiopoietin-like 4 in eye disease. *Biosci Rep*, **38**.

Yego, E.C., Vincent, J.A., Sarthy, V., Busik, J.V. & Mohr, S. (2009) Differential regulation of high glucose-induced glyceraldehyde-3-phosphate dehydrogenase nuclear accumulation in Muller cells by IL-1beta and IL-6. *Invest Ophthalmol Vis Sci*, **50**, 1920-1928.

Yoshida, A., Yoshida, S., Khalil, A.K., Ishibashi, T. & Inomata, H. (1998) Role of NF-kappaB-mediated interleukin-8 expression in intraocular neovascularization. *Invest Ophthalmol Vis Sci*, **39**, 1097-1106.

Yoshimura, T., Sonoda, K.-H., Sugahara, M., Mochizuki, Y., Enaida, H., Oshima, Y., Ueno, A., Hata, Y., Yoshida, H. & Ishibashi, T. (2009) Comprehensive Analysis of Inflammatory Immune Mediators in Vitreoretinal Diseases *PLoS ONE*, pp. e8158-8159.

Zeng, H.Y., Green, W.R. & Tso, M.O. (2008) Microglial activation in human diabetic retinopathy. *Arch Ophthalmol*, **126**, 227-232.

Zhao, C., Wang, Q. & Temple, S. (2017) Stem cell therapies for retinal diseases: recapitulating development to replace degenerated cells. *Development*, **144**, 1368-1381.

Zhou, T., Che, D., Lan, Y., Fang, Z., Xie, J., Gong, H., Li, C., Feng, J., Hong, H., Qi, W., Ma, C., Yang, Z., Cai, W., Zhong, J., Ma, J., Yang, X. & Gao, G. (2017) Mesenchymal marker expression is elevated in Muller cells exposed to high glucose and in animal models of diabetic retinopathy. *Oncotarget*, **8**, 4582-4594.

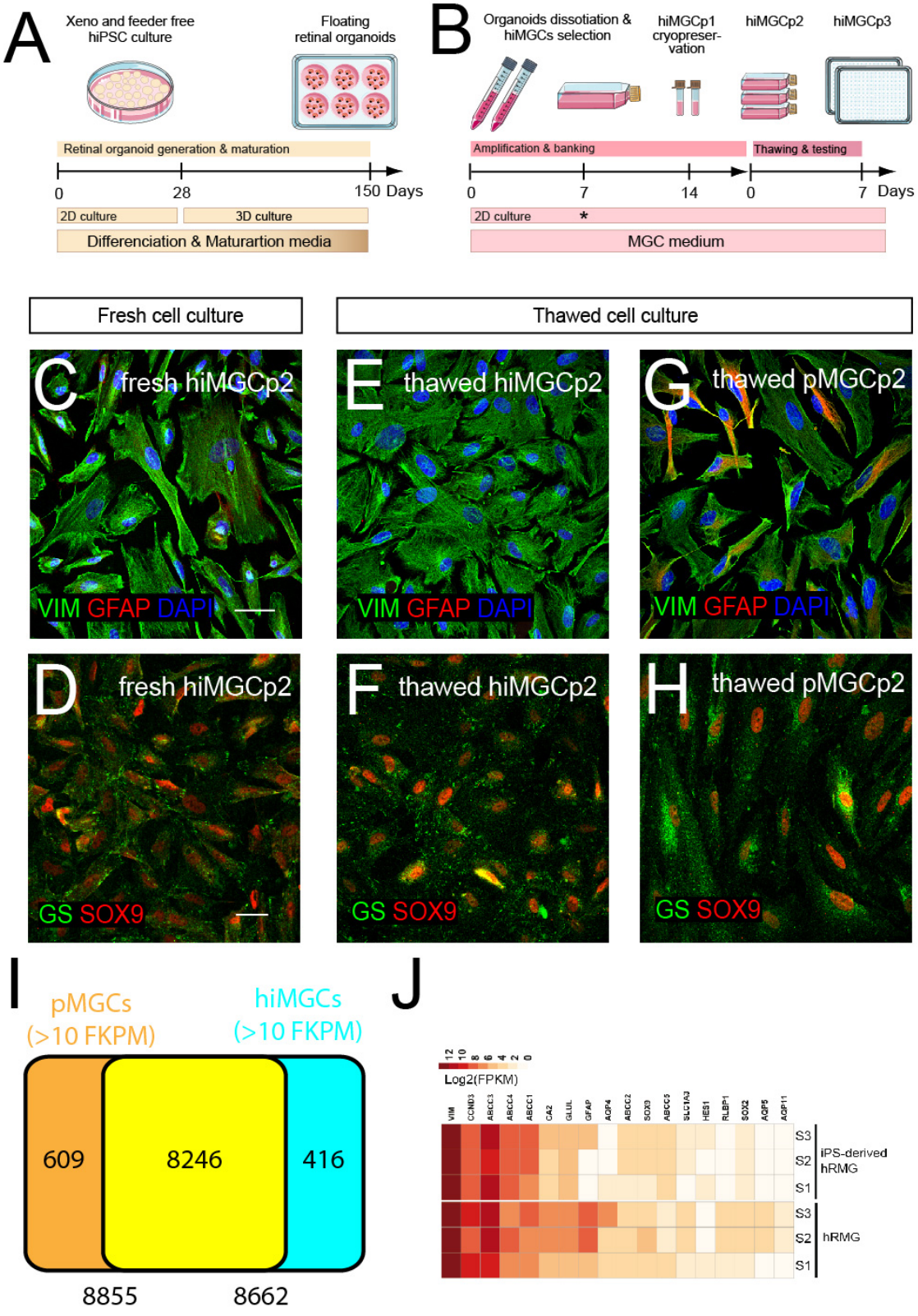
A
Xeno and feeder free hiPSC culture
Floating retinal organoids
Retinal organoid generation & maturation
0
28
150 Days
2D culture
3D culture
Differenciation & Maturartion media
B
Organoids dissotiation & hiMGCs selection
hiMGCp1 cryopreser-vation
hiMGCp2
hiMGCp3
Amplification & banking
Thawing & testing
0
7
14
0
7 Days
2D culture
*
MGC medium
Fresh cell culture
Thawed cell culture
C fresh hiMGCp2
VIM GFAP DAPI
E thawed hiMGCp2
VIM GFAP DAPI
G thawed pMGCp2
VIM GFAP DAPI
D fresh hiMGCp2
GS SOX9
F thawed hiMGCp2
GS SOX9
H thawed pMGCp2
GS SOX9
I
pMGCs (>10 FKPM)
hiMGCs (>10 FKPM)
609
8246
416
8855
8662
J
Log2(FPKM)
VIM
CCND3
ABCC3
ABCC4
ABCC1
CA2
GLUL
GFAP
AQP4
ABCC2
SOX9
ABCC5
SLC1A3
HES1
RLBP1
SOX2
AQP5
AQP11
S3
S2
S1
iPS-derived hRMG
S3
S2
S1
hRMG

Figure 1

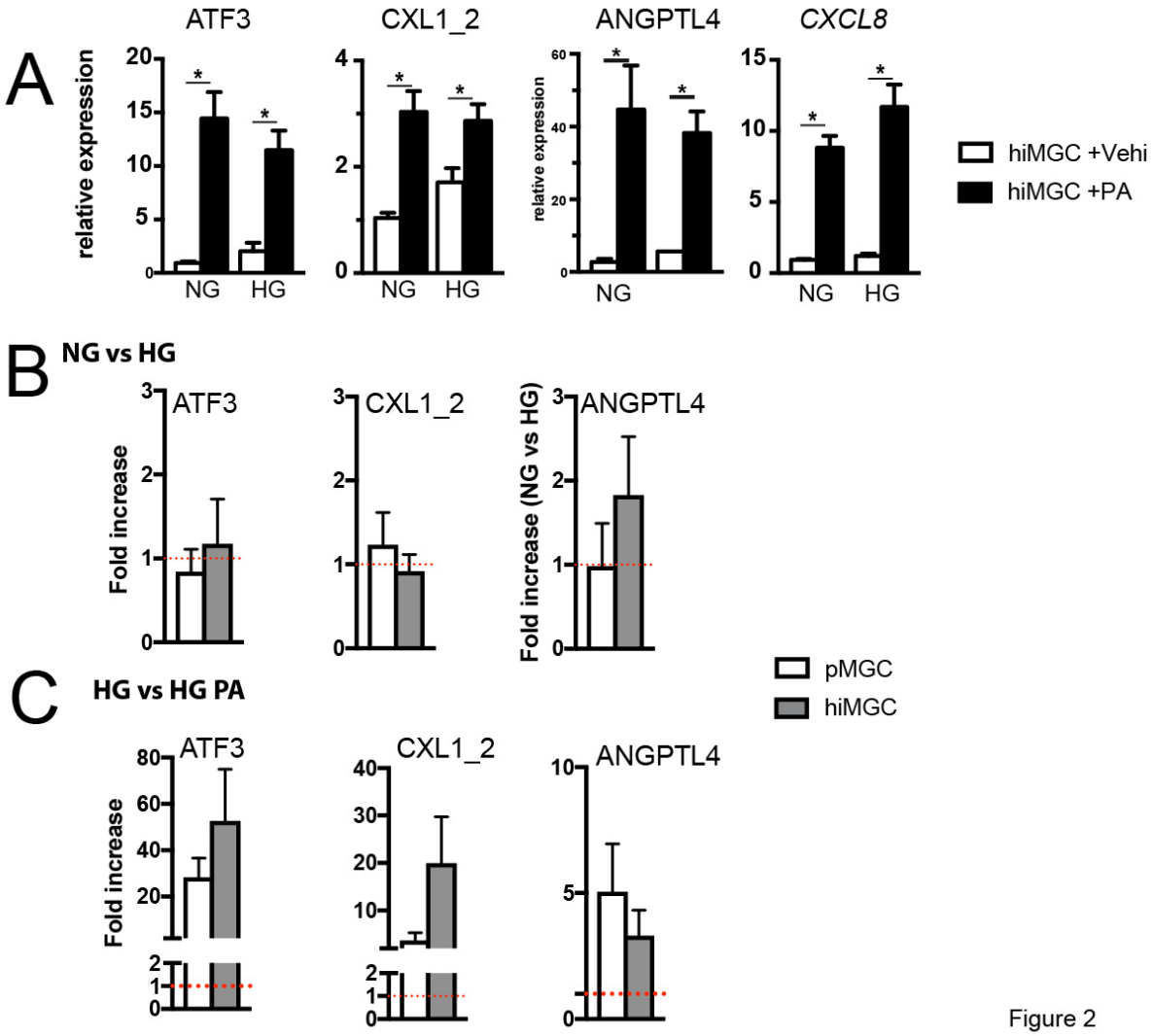
A
ATF3
CXL1_2
ANGPTL4
CXCL8
relative expression
NG
HG
hiMGC +Vehi
hiMGC +PA
B
NG vs HG
Fold increase
Fold increase (NG vs HG)
C
HG vs HG PA
pMGC
hiMGC

Figure 2

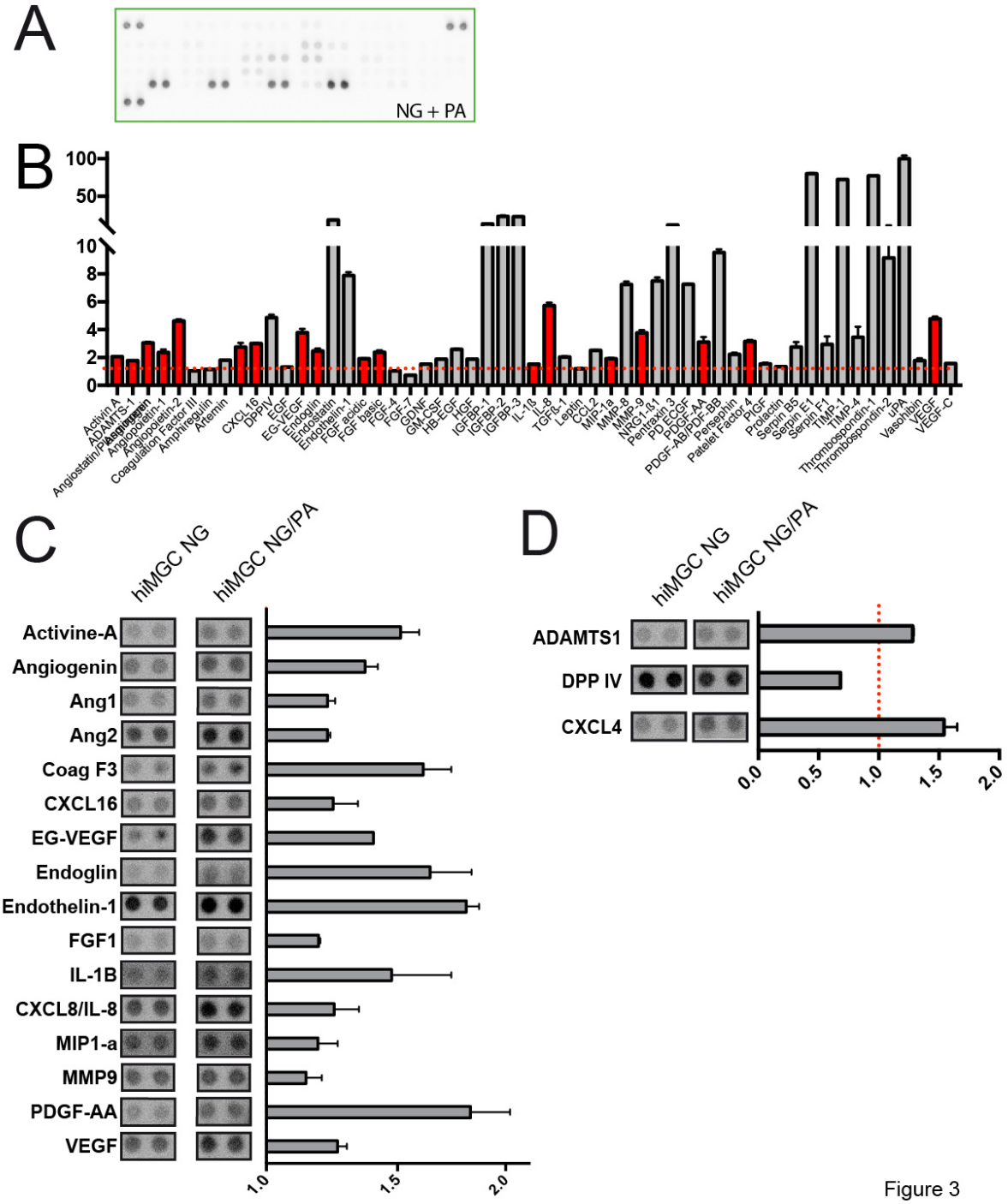
A
NG + PA
B
100
50
10
8
6
4
2
0
Activin A
ADAMTS-1
Angiogenin
Angiopoietin-1
Angiopoietin-2
Coagulation Factor III
Amphiregulin
Aremin
CXCL16
DPPIV
EGF
EG-VEGF
Endoglin
Endostatin
Endothelin-1
FGF acidic
FGF basic
FGF-4
FGF-7
GDNF
GM-CSF
HB-EGF
HGF
IGFBP-1
IGFBP-2
IGFBP-3
IL-1ß
IL-8
TGFß-1
Leptin
CCL2
MIP-1a
MMP-8
MMP-9
NRG1-ß1
Pentraxin 3
PD ECGF
PDGF-AA
PDGF-AB/PDF-BB
Persephin
Platelet Factor 4
PlGF
Prolactin
Serpin B5
Serpin E1
Serpin F1
TIMP-1
TIMP-4
Thrombospondin-1
Thrombospondin-2
uPA
Vasohibin
VEGF
VEGF-C
C
hiMGC NG
hiMGC NG/PA
Activine-A
Angiogenin
Ang1
Ang2
Coag F3
CXCL16
EG-VEGF
Endoglin
Endothelin-1
FGF1
IL-1B
CXCL8/IL-8
MIP1-a
MMP9
PDGF-AA
VEGF
1.0
1.5
2.0
D
hiMGC NG
hiMGC NG/PA
ADAMTS1
DPP IV
CXCL4
0.0
0.5
1.0
1.5
2.0

Figure 3

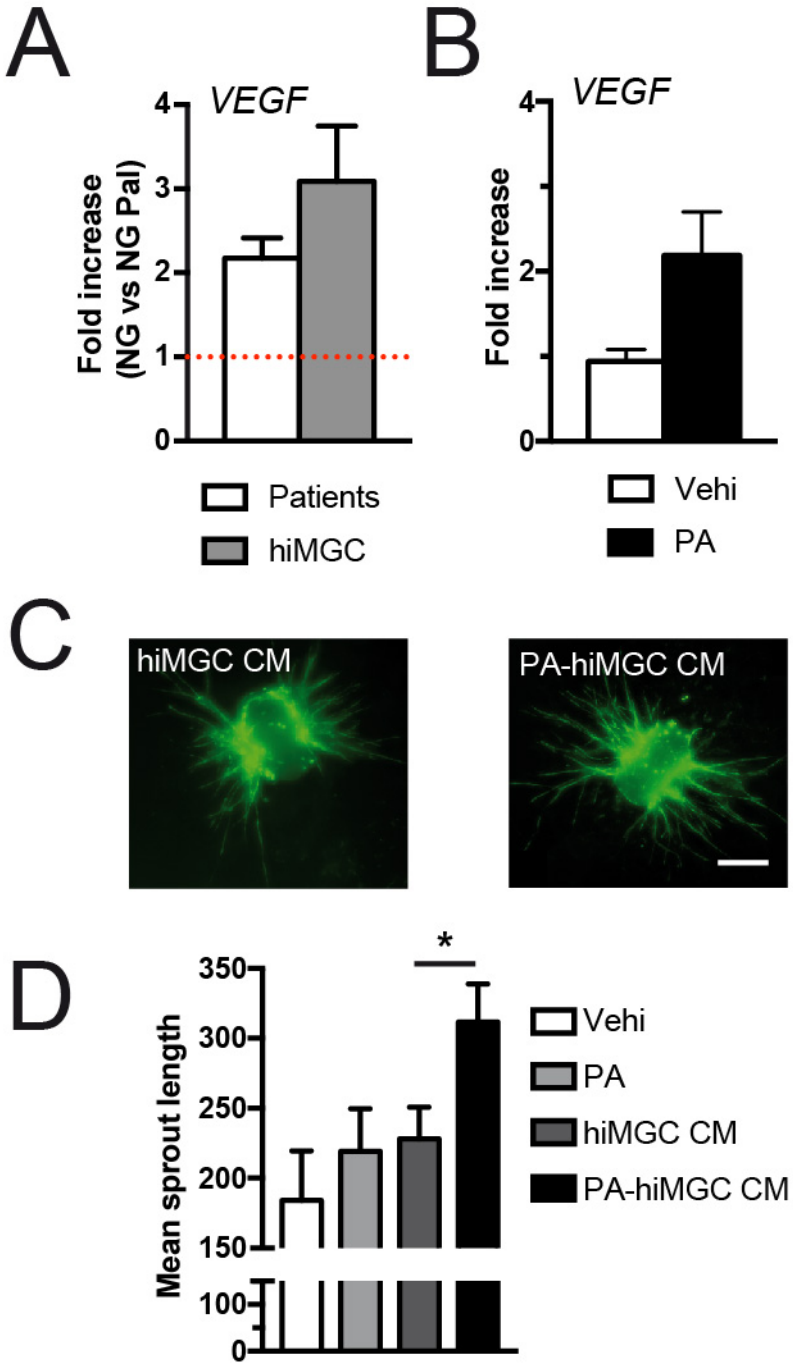
A
VEGF
Fold increase (NG vs NG Pal)
4
3
2
1
0
Patients
hiMGC
B
VEGF
Fold increase
4
2
0
Vehi
PA
C
hiMGC CM
PA-hiMGC CM
D
*
Mean sprout length
350
300
250
200
150
100
0
Vehi
PA
hiMGC CM
PA-hiMGC CM

Figure 4

III. Hyperreflective fluid in diabetic macular edema

1. Rational and aim of the project

The emergence of new *in vivo* imaging techniques such as Optical Coherence Tomography Angiography (OCTA) and Adaptive Optics (AO) has recently opened up new possibilities for imaging more precisely and non-invasively macular microvasculature. OCTA has allowed for the first time studying the relationship between the capillary dropout and intraretinal cystic spaces induced by capillary leakage. Our previous work using OCTA showed that cystoid spaces were co-localized within non-perfusion areas especially in the deep capillary plexus (DCP) in patients with chronic DME, suggesting a possible relationship between the capillary dropout and the occurrence of edema (Couturier A et al., 2015; Mané V et al., 2016). We also showed that decreased vision is mainly related to a loss of capillary perfusion in the DCP in type 1 diabetic patients (Dupas B et al., 2018). Whether it is due to hemodynamic conditions or to a more complex dysfunction of the neuroglial vascular coupling remains unknown. Indeed, early changes in retinal function have been reported in diabetes patients before detecting retinal vascular lesions, suggesting that some neurodegenerative events could precede vascular changes.

Diabetic hyperreflective foci in the outer retinal layers and hyperreflective content of cystoid spaces in DME are clinically relevant finding on SD-OCT images, although their origin and role in the disease remains to be elucidated.

Recently, hyperreflective content of cystoid spaces in DME have been studied using OCT-angiography. Presence of suspended particles in motion (SSPiM) in these cysts was reported to explain the hyperreflectivity and false decorrelation signal observed in these cases and may origin from a lipid extravasation from blood retinal barrier rupture in DME cases (Kashani et al., 2018). Indeed, few of these cases with SSPiM were shown to develop hard exudates in the same region during the follow-up. However, the exact nature and origin the hyperreflective content of some cystoid spaces was not fully elucidated.

In this study, we aim to investigate the origin and the evolution of hyperreflective content of cystoid spaces in DME cases.

2. Article 2

Hyperreflective fluid with extravascular signal on optical coherence tomography angiography is a sign of acute capillary occlusion in diabetic macular edema

Aude Couturier[1,2], MD, Valérie Mané[1], MD, Carlo Lavia[1], MD, Alain Gaudric[1], MD, Ramin Tadayoni[1], MD, PhD

[1] Department of Ophthalmology, Hôpital Lariboisière, AP-HP, Université Paris 7 – Sorbonne Paris Cité, Paris, France
[2] Institut de la Vision, Sorbonne Université, INSERM, CNRS, Paris, France

Short Title: Hyperreflective fluid with extravascular signal in diabetic macular edema

Corresponding author: Aude Couturier
Address for correspondence:
Service d'Ophtalmologie - Hôpital Lariboisière
2 rue Ambroise Paré
75010 Paris, France
Tel: +(33)1 49 95 24 74
Fax: +(33)1 49 95 64 83
Email: aude.couturier@aphp.fr

Conflicts of interest / Disclosures
The following authors have the proprietary interest to disclose:
Aude Couturier is a board membership for Allergan (Ireland), Bayer HealthCare (Germany), Novartis Pharma (Switzerland) and has received travel grants from Allergan (Ireland), Bayer HealthCare (Germany) and Novartis Pharma (Switzerland).
Alain Gaudric has received travel grants from Novartis Pharma (Switzerland) and Bayer HealthCare (Germany), and honoraria for an educational project from Novartis Pharma (Switzerland).
Ramin Tadayoni: Board membership (Alcon, Switzerland; Novartis, Switzerland; Roche, Switzerland; Allergan,USA; Bausch and Lomb, USA; Genentech, USA; Pfizer, USA; Alimera, USA; Bayer, Germany; FCI-Zeiss, France; Thrombogenics, Belgium), consultant (Allergan, USA; DORC, Netherlands; Alcon, Switzerland; Novartis, Switzerland; Bausch and Lomb, USA; FCI-Zeiss, France; Thrombogenics, Belgium), lecture fees (Alcon, USA; Bausch and Lomb, USA; Novartis, Switzerland; Allergan, USA; Bayer, Germany; Alimera, USA), educational presentation fee (Bausch and Lomb, USA; Novartis, Switzerland; Zeiss, Germany; Sony, Japan; Alcon, Switzerland; Allergan, USA), meeting expenses (Novartis, Switzerland; Alcon, Switzerland; Allergan, USA; Bausch and Lomb, USA; Pfizer, USA; Bayer, Germany; DORC, Netherlands; Alimera, USA.

The following authors have no financial disclosures: Valérie Mané, Carlo Lavia

Source of funding:
The Department of Ophthalmology received an independent research grant from Novartis Pharma SAS to study macular edema. The funding organization had no role in the design or conduct of this particular research.

Key Words: optical coherence tomography angiography; diabetic macular edema; cysts; hyperreflective fluid, hyperreflective foci, hypersignal; false decorrelation signal, hard exudates; retinal capillary density; deep capillary plexus; superficial capillary plexus, blood-retinal barrier.

Abstract

Purpose: To analyze the origin and evolution of hyperreflective fluid with extravascular signal (EVAS) detected by Optical Coherence Tomography Angiography (OCTA) in diabetic macular edema (DME).

Methods: A retrospective study of all consecutive eyes with DME imaged using OCTA 3x3mm (AngioVue, Optovue, Inc., Freemont, CA) was conducted in a tertiary care referral center. Demographics data, visual acuity, SD-OCT, fluorescein angiography and OCTA images were reviewed. All DME eyes with EVAS at baseline and at least three months of follow-up and 2 OCTA examinations in a one-year period were included in the longitudinal analysis.

Results : Over 165 eyes with DME imaged using OCTA, 61 eyes (37%) showed hyperreflective fluid with EVAS. In almost of all the eyes (97%, n= 59/61), hyperreflective fluid with EVAS were observed within the foveal avascular zone (FAZ) area, and in 49% (30/61), it was located in the OPL-ONL junction. Presence of hyperreflective foci within the EVAS was observed in 85% (52/61) of eyes. In all eyes, EVAS was not corrected by the PAR algorithm and lead to an overestimation of the automatically assessed capillary density.

The longitudinal study included 33 eyes from 24 patients, with a mean follow up time of 14.2 ± 9.2 months. Ten eyes were only observed while 23 eyes received anti-VEGF injections during the follow-up. The hyperreflective fluid with EVAS was transient in 85% (28/33) of eyes, with a complete (6/33) or partial (20/33) resolution. The resolution of EVAS resulted in the disappearance of retinal capillaries in the area of former hyperreflective fluid in 46% (13/28) of eyes. Hard exudates appeared in the same area in 39% (11/28) of eyes.

No significant differences were observed regarding the evolution of hyperreflective fluid with EVAS in treated eyes compared with observed eyes

Conclusion : Hyperreflective fluid with EVAS was detected by OCTA in more than one-third of DME eyes. These hyperreflective content may origin from an acute blood retinal barrier rupture with extravasation of lipids that may deposit as hard exudates but mostly resolved either spontaneously or under anti-VEGF therapy. As hyperreflective fluid resolution often preceded the disappearance of capillaries, it may represent an early sign of capillary closure in DME.

Introduction

Diabetes is a multifactorial pathology and dyslipidemia was shown to be one of the risk factors in the development of type 2 diabetes. Indeed, an imbalance in lipid metabolism is correlated with chronic inflammation in most tissues including the retina. In diabetic patients, three main morphologic patterns of diabetic macular edema (DME) have been described on B-scan Optical Coherence Tomography (OCT), including cystoid macular edema with various reflective content, serous retinal detachment, and sponge-like retinal swelling (Barthelmes D et al., 2008; Otani et al., 1999; Horii et al., 2012). The higher resolution spectral domain OCT (SD-OCT) has also allowed visualizing the presence of hyperreflective foci and hyperreflective fluid (Boltz et al., 2009; Horii et al., 2010, Liang MC et al., 2013). More recently, OCT-angiography (OCTA) imaging has correlated the presence of this hyperreflective content within cystoid spaces with extravascular OCTA signals (Kashani AH et al, 2018). This hyperreflective fluid with extravascular signal (EVAS) detected using OCTA seem to be consistently associated with DME; however its nature, origin and evolution remain largely unknown.

The aim of this study was to analyze the prevalence, characteristics and evolution of hyperreflective fluid EVAS in patients with DME.

Patients and Methods

We conducted an observational retrospective study in an institutional reference ophthalmologic center (Lariboisière Hospital, Paris Diderot University, Paris, France).

The study was conducted in compliance with the tenets of the Declaration of Helsinki. All data acquisitions were approved by our Institutional Review Board (SFO N°#...., Paris, France). All subjects signed written informed consent forms for using their fundus images.

Patients

The records of all consecutive diabetic patients with DME and imaged using the spectral domain OCTA RTVue XR Avanti (Optovue, Fremont, CA, USA) during a one-year period (from 1st February 2015 to 1st February 2016) were reviewed.

Inclusion criteria were: patients 18 years age or older with diabetes type 1 or 2; DME defined as a retinal thickness of > 298 µm in the central subfield corresponding to the normal value plus 2 SDs: 260 + (2 × 19) µm (Lavia C et al., accepted in Retina 2018), with intra- or subretinal fluid seen on B-scan OCT; and the presence of EVAS on OCTA flow images.

Exclusion criteria were: the presence of any other retinal disorder (i.e. retinal vein occlusion, uveitis or other maculopathy) or of media opacities such as vitreous hemorrhage or cataract;

poor-quality OCTA images defined by a signal strength index (SSI) below 50/100 and quality index (QI) below 5/10; and evidence of motion artifacts on OCTA images.

Baseline data collection included demographics and diabetes characteristics (gender, type of diabetes, diabetes duration, glycosylated hemoglobin, DME duration, diabetic retinopathy severity), previous ophthalmological history (intravitreal or laser treatment for DME, surgery for diabetes-related complications), and ophthalmological findings at the time of inclusion (best-corrected visual acuity, BCVA; slit-lamp biomicroscopy, fundus examination, spectral domain OCT, En-Face OCT and OCTA).

A longitudinal observational study was also performed and included patients with hyperreflective fluid with EVAS on the baseline OCTA images, for whom follow-up OCTA examinations were available. Patients were included in the longitudinal analysis when they had at least three months of follow-up and at least 2 OCTA examinations in a one-year period, from baseline to 1st October 2018. Image quality assessment was performed using the same criteria applied at the baseline. Follow-up duration, number of OCTA examination in the study period, BCVA and treatments for DME during the study period were recorded.

OCTA images acquisition

All eyes were imaged using the spectral domain OCTA RTVue XR Avanti (Optovue, Fremont, CA, USA) with phase 7 AngioVue software and the 3D projection artifact removal (PAR) algorithm. This PAR algorithm removes projection artifacts from the OCTA volume on a per voxel basis (Zhang M. et al., 2016; Wang J et al., 2017) using information from the OCT.
The device operates 70,000 A-scans per second with an 850-nm center wavelength. To correct motion artifacts, OCTA combines orthogonal fast-scan directions (horizontal and vertical) and is equipped with the DualTrac™ Motion Correction technology.
The machine extracts flow signals basing on the Split-spectrum amplitude-decorrelation angiography (SSADA) algorithm, as previously described (Jia Y et al., 2012). In brief, consecutive B-scans are acquired to calculate the contrast between the decorrelation of blood flow and static tissue, detecting the motion of highly reflective materials.

Images analysis

The scanning area analyzed in this study was 3 x 3 mm, centered on the fovea and composed by volumes of 304-mm x 304-mm A-scans.

All OCTA images were carefully reviewed by two blind expert examiners, looking for the presence of hyperreflective fluid with EVAS on en face OCTA images.
OCTA images were analyzed using the preset superficial vascular plexus slab (SVP, comprised between the internal limiting membrane and 9µm over the inner plexiform layer-inner nuclear layer junction), the deep vascular complex slab (DVC, comprised between the lower boundary of the SVP and 9µm below the outer plexiform layer-outer nuclear layer junction), the outer retina slab (comprised between the lower boundary of the DVC and 9µm over the Bruch's membrane), and by scrolling a thin customized slab (10 µm) through the en face OCTA image. The corresponding structural en face OCT images were also reviewed using the same slabs. The corresponding structural and "angio overlay" B-scans OCT were contemporarily reviewed to evaluate the exact location of EVAS and to detect the presence and axial distribution of hyperreflective material.
Follow-up OCTA images were analyzed with the same method.

When available, good quality fluorescein angiograms performed on the same day as the OCTA examinations were reviewed as well.

Results

The records of 165 eyes from 108 consecutive patients with DME imaged using OCTA (RTVue XR Avanti) were reviewed.

Prevalence

Over these 165 eyes with DME, hyperreflective fluid with EVAS was detected at baseline in 61 eyes of 46 patients, resulting in a prevalence of 37% (61/165) among DME eyes.
The presence of hyperreflective fluid with EVAS was mainly unilateral, in 31 of the 46 (67%) patients. Among them, 5 patients had no DME in fellow eye and 7 had low OCTA image quality.
Among the 61 eyes presenting with hyperreflective fluid with EVAS, 43% (26/61) were treatment-naïve. Previous treatment for DME included intravitreal anti-VEGF injections only in 21% (13/61) of eyes, focal laser only in 16% (10/61) of eyes and both treatments in 20% (12/61) of eyes. Patients previously treated by intravitreal anti-VEGF had received a mean of 4.6 ± 5.3 injections (range 1-20, median 2).
Patient baseline characteristics are summarized in **Table 1**.

Baseline OCTA images analysis

In 97% (59/61) of eyes, hyperreflective fluid with EVAS were observed within the foveal avascular zone (FAZ) area (**Figure 1**), in areas of vessel anomalies (i.e. presence of microaneurysms and pruned vessels) or of reduced vessel density. In 34% eyes (21/61), hyperreflective fluid with EVAS were found in areas of interruption of the FAZ ring. Of note, in 4 eyes (7%) the FAZ was hardly detectable due to severe capillary dropout.

Presence of hyperreflective foci within the EVAS was observed in 85% (52/61) of eyes with different patterns of distribution. Hyperreflective fluid with EVAS had an homogeneous content in 69% (42/61) of eyes. In these cases, hyperreflective foci were detected mainly at the borders of the cysts (**Figure 2**). The remaining 19 eyes had an heterogeneous content and a lower EVAS intensity.

On B-scans OCT images with the "angio overlay", hyperreflective fluid with EVAS was mainly located in the OPL-ONL junction, in 49% (30/61) of eyes, corresponding to the deeper part of the DVC slab. Hyperreflective fluid with EVAS was also detected in both ONL and INL in 44% (27/61) of eyes. Less frequently, hyperreflective fluid was detected in the SVP slab, in 7% (4/61) of eyes.

Two others types of EVAS were detected outside the cysts with hyperreflective fluid:

- In 15% (9/61) of eyes, EVAS were detected inside the cysts wall, presenting with low intensity and with a ring-like pattern;
- In 5 cases (8%), EVAS with an elongated shape and a radial distribution were detected at the OPL-ONL junction and corresponded to hyperreflective material or exudates on the B-scan OCT.

No EVAS was detected in the fluid of central neuro-retinal detachment, when the latter was present (in 7 eyes from 7 patients, 11%).

The presence of EVAS consequently led to false positives in the vessel density automatic measurement. In all eyes, EVAS was not corrected by the PAR algorithm, as its intensity was similar to that from surrounding retinal vessels. Using AngioVue software, it was not possible to precisely quantify the % VD derived from EVAS.

FA was performed on the day of OCTA in 33 eyes and high quality FA allowed FAZ analysis in 12 eyes. In all of these cases, a morphological match was observed between the hyperreflective fluid with EVAS and the fluorescein pooling (**Figure 1**). The intensity of the

dye pooling was generally low or moderate when compared to that coming from cysts with hyporeflective fluid and without EVAS on OCTA.

Follow-up

Longitudinal study included 33 eyes from 24 patients, with a mean follow up time of 14.2 ± 9.2 months (range 3-31, median 15) and a mean of 4.5 ± 2.6 OCTA examinations (range 2-11, median 4).

During the study period, 30% (10/33) of eyes were only observed and didn't receive any treatment for DME. Intravitreal injections for DME treatment was indicated in 70% (23/33) of eyes: all of these eyes received anti-VEGF therapy, with a mean of 4.6 ± 4.6 intravitreal anti-VEGF injections (range 1-20, median 3). Three eyes also received one intravitreal dexamethasone implant during the follow-up time.

Functional and anatomical changes within the study period are reported in **Table 2**.

Regarding anatomic changes in EVAS during the follow-up, 18% (6/33) of eyes showed a complete resolution of the edema with complete disappearance of the hyperreflective fluid with EVAS. In 67% (22/33) of eyes, the edema only partially regressed, and the hyperreflective fluid with EVAS partially resolved in hyporeflective cysts. In the 5 remaining eyes (15%), the hyperreflective fluid with EVAS remained unchanged.

The resolution of EVAS resulted in the formation of hard exudates detected on en face structural OCTA images as well as on fundus photographs in the areas of former hyperreflective in 39% (11/28) of eyes with complete or partial EVAS disappearance on OCTA (**Figure 3**).

The resolution of EVAS also resulted in the disappearance of retinal capillaries in the area of former hyperreflective fluid in 46% (13/28) of eyes (**Figure 4**).

In 45% (15/33) of eyes, new hyperreflective fluid with EVAS occurred either in the same or in a different area of the FAZ.

No case of occurrence of hyperreflective fluid within former hyporeflective cysts was observed.

No significant differences were observed regarding the evolution of hyperreflective fluid with EVAS in treated eyes compared with observed eyes (**Table 3**).

Discussion

In this first OCTA longitudinal analysis of hyperreflective fluid, we reviewed a large number of consecutive eyes with DME and reported a prevalence of hyperreflective fluid with EVAS

of 37% among DME eyes. Interestingly, we noted that the resolution of hyperreflective fluid with EVAS was not only associated with hard exudates but also with capillary closure in the foveal avascular zone (FAZ) area.

The prevalence of EVAS reported in this series is consistent with the data from Kasahani et al., who termed this extravascular signal as "suspended scattering particles in motion" (SSPiM) (Kashani AH et al., 2017) and reported a prevalence of 28% among eyes with DME (Kashani AH et al., 2018).

Baseline anatomic characteristics of hyperreflective fluid with EVAS in this OCTA study were consistent with published data (Kashani AH et al., 2018; Liang MC et al., 2013). Hyperreflective fluid with EVAS was detected within the FAZ area in almost all DME eyes (97%), mainly located in the OPL-ONL junction (49%) and was associated with hyperreflective foci in the vast majority of cases (85%).

In this longitudinal analysis of both observed and treated DME eyes with a mean follow-up of 14 months, we found that hyperreflective fluid with EVAS was mainly a transient phenomenon in DME, as its complete or partial resolution was observed in 85% (28/33) of the eyes. The resolution hyperreflective fluid with EVAS was associated with new occurrence of hard exudates in some cases (39%) but interestingly, it was also often associated with new capillary closure (46%) in the area of former hyperreflective fluid (**Figure**). Indeed, the disappearance of capillaries in the area of former EVAS was easily identified on OCTA images and was contemporary with the resolution of hyperreflective fluid. This finding may help to understand the origin of hyperreflective fluid with EVAS in vascular diseases.

Although many studies reported the features and OCT characteristics of hyperreflective fluid, its exact etiology and nature remained unknown. Based on its baseline characteristics and on its evolution on follow-up OCTA images, we hypothesized that hyperreflective fluid with EVAS corresponds to an acute extravasation of lipids or lipoproteins in case of severe blood-retinal barrier (BRB) rupture that precede capillary occlusion.

First, in this series, all eyes were imaged with the same OCTA device (RTVue XR Avanti, Optovue, Fremont, CA, USA) with phase 7 AngioVue software, which has a follow-up mode allowing precise follow-up of capillary changes in the FAZ area. Thus, in 46% of our cases, capillary loss in the area of resolved hyperreflective fluid was easily detected.

Second, this finding is consistent with the detection of hyperreflective fluid with EVAS in eyes with more advanced stages of diabetic retinopathy (i.e. severe non-proliferative or proliferative diabetic retinopathy) in this series as well as in previous reports (Kashani AH et al., 2018), as

these cases are more susceptible to progress and to show capillary closure in a one-year follow-up than more early stages of diabetic retinopathy.
This is also consistent with the location of hyperreflective fluid within the FAZ area, as FAZ interruption frequently worsened with the progression of diabetic retinopathy.
On fluorescein angiography, we found a modest pooling of hyperreflective cysts in this series, as it was previously reported by Horii et al., who described it as a sign of more severe BRB rupture and endothelial cell death (Horii T et al.,2012).
This more severe BRB rupture in eyes with hyperreflective fluid is confirmed by its frequent association with hyperreflective foci (85% in this series), which are reported to be a subclinical extravasation of lipoproteins and/or proteins, secondary to breakdown of the BRB (Bolz et al., 2009). Furthermore, hyperreflective foci have been shown to be associated with visual impairment in DME (Uji A et al., 2012; Murakami T et al., 2018).
Thus, all these data suggest that hyperreflective fluid with EVAS may not be only a sign of vascular permeability as previously described, but also a direct sign of capillary closure in DME.
No difference in the hyperreflective fluid evolution was detected between observed and treated eyes. Anti-VEGF therapy is known to improve blood-retinal barrier rupture and is effective in treating DME, however limited clinical evidence exist regarding its ability to reperfuse retinal capillaries or to reduce capillary occlusion as many studies are only based on color fundus photographs analysis (Bonnin et al. Accepted Retina 2018).
Future studies with longer follow-up and control arm may confirmed these data and determine if hyperreflective fluid with EVAS is a bad prognosis factor for diabetic retinopathy progression or functional outcomes in DME eyes.

Future OCTA studies need to account for these EVAS, as it systematically overestimate the vessel density measurement in the area of hyperreflective fluid and is not corrected by the PAR algorithm; thus vessel density may seem to be stable or to increase over time, even in the presence of visible vessel loss.

The EVAS detected by OCTA algorithm from hyperreflective fluid was attributed to particles in motion by Kashani et al. (Kashani AH et al., 2018). We believed that the nature or the concentration of fluid in case of acute capillary occlusion probably differs from that of chronic hyporeflective cysts and may contain different types of lipoproteins and/or cells. The EVAS detected by OCTA in hyperreflective fluid seems to us more likely to be due to eye micro-saccades leading to motion of these more dense molecules in hyperreflective fluid, than to the

motion of the particles themselves. This is consistent with the fact that EVAS were also detected in the wall of cysts (15% in this series) or in hyperreflective foci (8%), as described by Murakami et al (Murakami T et al., 2018).

There are some limitations to our study. First, it included only a small number of eyes with a short follow-up and needed to be confirmed on a more extensive series with a longer follow-up. Due to the retrospective nature of the study, OCTA examinations were not regularly spaced, and it is therefore difficult to offer a precise insight on the evolution of EVAS. Last, the OCTA technology only detects vessels with flow above a certain velocity range, and it is thus possible that OCTA did not visualize some portions of vessels with low flow.

To conclude, in this longitudinal retrospective analysis of 33 eyes with hyperreflective fluid with EVAS, we found that EVAS was transient in 85% of cases and often precede the occlusion of capillaries in the same area (46%). If these findings are confirmed in future prospective studies, hyperreflective fluid with EVAS may thus be a useful parameter to monitor new onset of capillary closure in clinical trials in DME eyes.

References

Barthelmes D, Sutter FK, Gillies MC. Differential optical densities of intraretinal spaces. Invest Ophthalmol Vis Sci. 2008 Aug;49(8):3529-34. doi: 10.1167/iovs.07-1320. Epub 2008 Apr 25.

Bolz, M, Schmidt-Erfurth U, Deak G, Mylonas G, Kriechbaum K, Scholda C; Diabetic RetinopathyResearch Group Vienna. Optical coherence tomographic hyperreflective foci: a morphologic sign of lipid extravasation in diabetic macular edema. Ophthalmology 2009,116: 914–920, doi:10.1016/j.ophtha.2008.12.039.

Bonnin S, Dupas B, Lavia C, Erginay A, Dhundass, Couturier A, Gaudric A, Tadayoni R. Anti-VEGF therapy can improve diabetic retinopathy score without change in retinal perfusion. Accepted Retina 2018.

Horii T, Murakami T, Nishijima K, Akagi T, Uji A, Arakawa N, Muraoka Y, Yoshimura N. Relationship between fluorescein pooling and optical coherence tomographic reflectivity of cystoid spaces in diabetic macular edema. Ophthalmology. 2012 May;119(5):1047-55. doi: 10.1016/j.ophtha.2011.10.030. Epub 2012 Feb 11.

Jia Y., Tan O., Tokayer J., Potsaid B., Wang Y., Liu J. J., Kraus M. F., Subhash H., Fujimoto J. G., Hornegger J., Huang D., "Split-spectrum amplitude-decorrelation angiography with optical coherence tomography," Opt. Express 2012, 20(4), 4710–4725.

Kashani A, Chen C-L, Gahm J, et al. Optical coherence tomography angiography: a comprehensive review of current methods and clinical applications. Prog Retin Eye Res. 2017;60:66e100.

Kashani AH, Green KM, Kwon J, Chu Z, Zhang Q, Wang RK, Garrity S, Sarraf D, Rebhun CB, Waheed NK, Schaal KB, Munk MR, Gattoussi S, Freund KB, Zheng F, Liu G, Rosenfeld PJ. Suspended Scattering Particles in Motion: A Novel Feature of OCT Angiography in Exudative Maculopathies. Ophthalmol Retina. 2018 Jul;2(7):694-702. doi:10.1016/j.oret.2017.11.004. Epub 2017 Dec 15.

Lavia C, Bonnin S, Maule M, Erginay A, Tadayoni R, Gaudric A. Vessel density of superficial, intermediate and deep capillary plexuses in healthy eyes using Optical Coherence Tomography Angiography. Accepted Retina 2018

Liang MC, Vora RA, Duker JS, Reichel E. Solid-appearing retinal cysts in diabetic macular edema: a novel optical coherence tomography finding. Retin Cases Brief Rep. 2013 Summer;7(3):255-8. doi:10.1097/ICB.0b013e31828eef49.

Murakami T, Suzuma K, Dodo Y, Yoshitake T, Yasukura S, Nakanishi H, Fujimoto M, Oishi M, Tsujikawa A. Decorrelation Signal of Diabetic Hyperreflective Foci on Optical Coherence Tomography Angiography. Sci Rep. 2018 Jun 11;8(1):8798. doi: 10.1038/s41598-018-27192-9.

Uji A, Murakami T, Nishijima K, Akagi T, Horii T, Arakawa N, Muraoka Y, Ellabban AA, Yoshimura N. Association between hyperreflective foci in the outer retina, status of photoreceptor layer, and visual acuity in diabetic macular edema. Am J Ophthalmol. 2012 Apr;153(4):710-7, 717.e1. doi: 10.1016/j.ajo.2011.08.041. Epub 2011 Dec 3.

Wang, J. et al. Reflectance-based projection-resolved optical coherence tomography angiography [Invited]. Biomed. Opt. Express 8, 1536–1548 (2017)

Zhang, M. et al. Projection-resolved optical coherence tomographic angiography. Biomed. Opt. Express 7, 816–828 (2016).

Legends to Figures

Figure 1: Hyperreflective fluid with extravascular signal (EVAS) in a 60-year-old patient with diabetes type 2. At baseline (A-C and E-G), hyperreflective fluid is easily detected in the foveal avascular zone area on OCTA image (C), as well as on B-scan OCT (E and G). Fluorescein angiography (A) shows a moderate pooling of this cyst (white arrow). Vessel density map (B) as well as B-scan OCT with angio overlay (F) show the EVAS in hyperreflective fluid (arrowheads). On follow-up OCTA examination (D and H) performed 8 months later, the hyperreflective fluid spontaneously resolved without any treatment.

Figure 2: Hyperreflective fluid with extravascular signal (EVAS) in a 53-year-old patient with diabetic macular edema treated with intravitreal anti-VEGF injections. On OCTA, several cysts with hyperreflective are detected in the FAZ area in both superficial (A1) and deep (B1 and C1) capillary plexus (arrows). On B-scan OCT, hyperreflective fluid is located in the Henle fiber layer and associated with hyperreflective foci (arrowheads).

Figure 3: Resolution of Hyperreflective fluid with extravascular signal (EVAS) in a 64-year-old diabetic patient with spontaneous resorption of edema after 6 months.
At baseline, hyperreflective fluid is detected on the DCP slab on OCTA (A1), and on B-scan OCT (A4 and A5). It is also visisble on the en-Face structural OCT (A2). Hard exudates are visible on the fundus photograph (A3) but are not in the same are as hyperreflective fluid (circle).
At 6 months, spontaneous resolution of edema and hyperreflective fluid in on OCTA image (B1) and B-scan OCT (B4 and B5). Hard exudates are detected in the same area (circle) of former hyperreflective fluid on en-face structural OCT (B2) as well as on the fundus photograph (B3), and corresponds to multiple coalescent hyperreflective foci (arrow) on B-Scan OCT (B4 and B5)

Figure 4: Partial resolution of hyperreflective fluid in a monthly anti-VEGF treated diabetic patient imaged at baseline (A), one month (B), two months (C) and three months (D).
Partial resolution of hyperreflective fluid is detected at 1 month and is contemporary of a capillary closure in the same area (arrow).

Table 1: Demographics and ocular characteristics of eyes with hyperreflective fluid and extravascular signal on OCTA at baseline.

Number of patients	46
Number of eyes	61
Age, mean ± SD (range), years	55.5 ± 10.6 (36-74)
Male gender, n (%)	29 (63%)
Diabete type 2, n (%)	40 (87%)
Diabetes duration, mean ± SD (range), years	19.5 ± 12.2 (2-59)
Glycated hemoglobin level, mean ± SD (range), %	8.2 ± 2.0 (5.6-15)
Central DME duration, mean ± SD (range), months	12.7 ± 3.8 (8-26)
Lens status : phakic, n (%)	53 (87%)
Diabetic retinopathy severity, n (%)	
Moderate non proliferative DR	4 (7%)
Severe non proliferative DR	42 (69%)
Proliferative DR inactivated by PRP	15 (25%)
BCVA, mean ± SD (range), LogMar	0.3 ± 0.3 (0-1)
History of anti-VEGF treatment, n (%)	26 (43%)
History of macular laser treatment, n (%)	22 (36%)

Abbreviations: SD = Standard deviation; DME = diabetic macular edema; DR = diabetic retinopathy; PRP = panretinal photocoagulation; BCVA = Best corrected visual acuity; LogMar = logarithm of the minimal angle of resolution.

Table 2: Demographics characteristics and ocular outcomes of eyes with hyperreflective fluid and extravascular signal on OCTA, included in the longitudinal study.

Number of eyes/patients (M/F)	33/24 (14/10)
Age, Mean ± SD (range), years	53.5 ± 11.6 (36-71)
Diabetes type (type 1/ type 2)	2/22
Duration of diabetes, Mean ± SD (range), years	19 ± 14 (2-59)
Duration of DME, Mean ± SD (range), months	18 ± 18 (3-75)
Lens status : phakic, n (%)	33 (100)
Non proliferative DR, n (%)	24 (73)
Proliferative DR Inactivated by PRP, n (%)	9 (27)
Treatment-naïve DME, n (%)	10 (30)
Treated DME eyes, n (%)	23 (70)
Follow-up time, Mean ± SD (range), months	14.2 ± 9.2 (3-31)
Change in BCVA, Mean ± SD (range), logMAR	-0.02 ± 0.2 (-0.60-+0.40)
Baseline BCVA, Mean ± SD (range), logMAR	0.27 ± 0.30 (0-1)
Final BCVA, Mean ± SD (range), logMAR	0.25 ± 0.21 (0-0,7)
Change in CMT, Mean ± SD (range), µm	-49.06 ± 110.3 (-451-+125)
Baseline CMT, Mean ± SD (range), µm	377.0 ± 100.7 (229-748)
Final CMT, Mean ± SD (range), µm	327.9 ± 85.3 (212-535)

BCVA: Best Visual Corrected Acuity; SD: Standard deviation; DME : diabetic macular edema ; DR: Diabetic Retinopathy; CFT: Central Macular Thickness

Table 3: Evolution of hyperreflective fluid with extravascular signal (EVAS) on OCTA in treated eyes compared with observed eyes

	Treated eyes	Observed eyes	p
Number of eyes	16	17	
Baseline BCVA, Mean ± SD (range), LogMar	0.30 ± 0.4 (0.0-1.0)	0.25 ± 0.3 (0.0-0.8)	0.6438
Follow-up BCVA, Mean ± SD (range), LogMar	0.29 ± 0.3	0.22 ± 0.2 (0.0-0.6)	0.3600
Mean change in BCVA, Mean ± SD (range), LogMar	-0.01 ± 0.28 (-0.6- +0.4)	-0.03 ± 0.20 (-0.6-+0.2)	0.8242
Baseline CMT, Mean ± SD (range), µm	386.3 ± 79.7 (233-548)	368,24 ± 119.1 (229-748)	0.6143
Follow-up CMT, Mean ± SD (range), µm	334.6 ± 105.9 (212-535)	321,65 ± 62.9 (219-461)	0.6694
Mean change in CMT, Mean ± SD (range), µm	-51.7 ± 98.6 (-223-+125)	-46.59 ± 123.3 (-451-+88)	0.8969
EVAS complete resolution	4	2	0.3399
EVAS partial resolution	8	14	0.4024
No change in EVAS	4	1	0.1339
New hyperreflective fluid with EVAS	8	6	0.6241
Occurrence of hard exudates	4	7	0.3399

BCVA: Best Visual Corrected Acuity; SD: Standard deviation; DME : diabetic macular edema ; DR: Diabetic Retinopathy; CMT: Central Macular Thickness, EVAS: extravascular signal

Figure 1

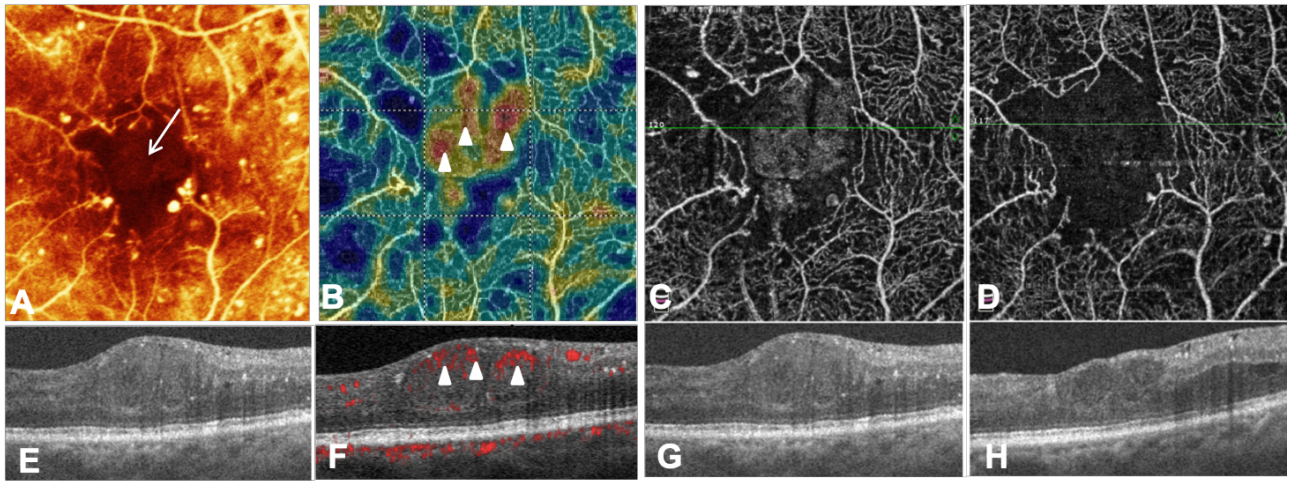

Figure 2

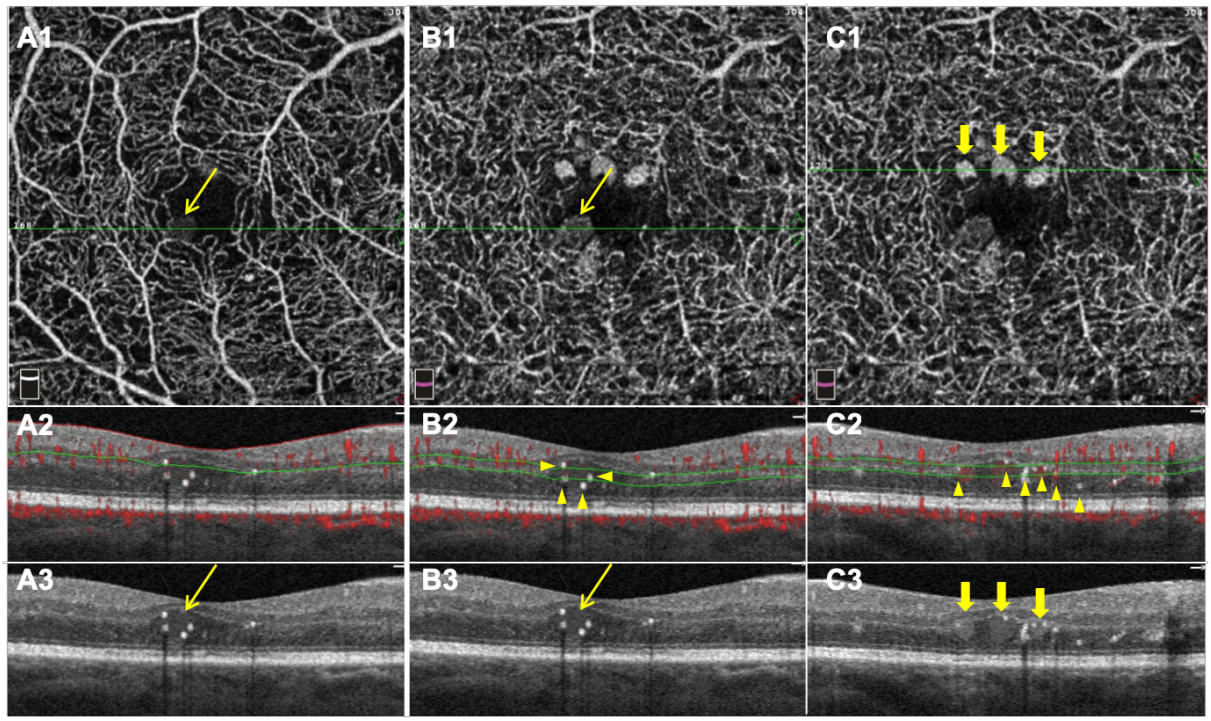

Figure 3:

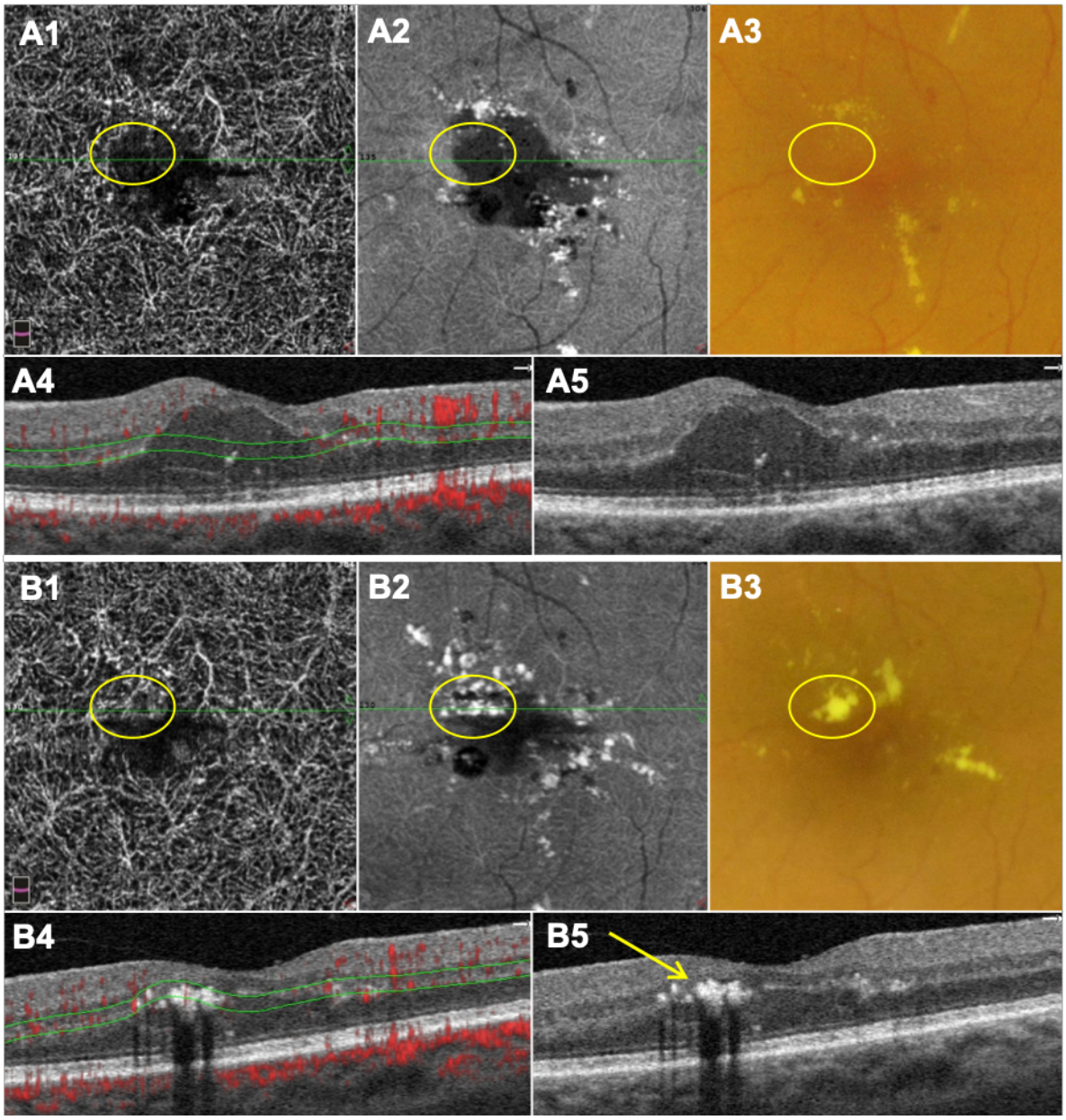

Figure 4:

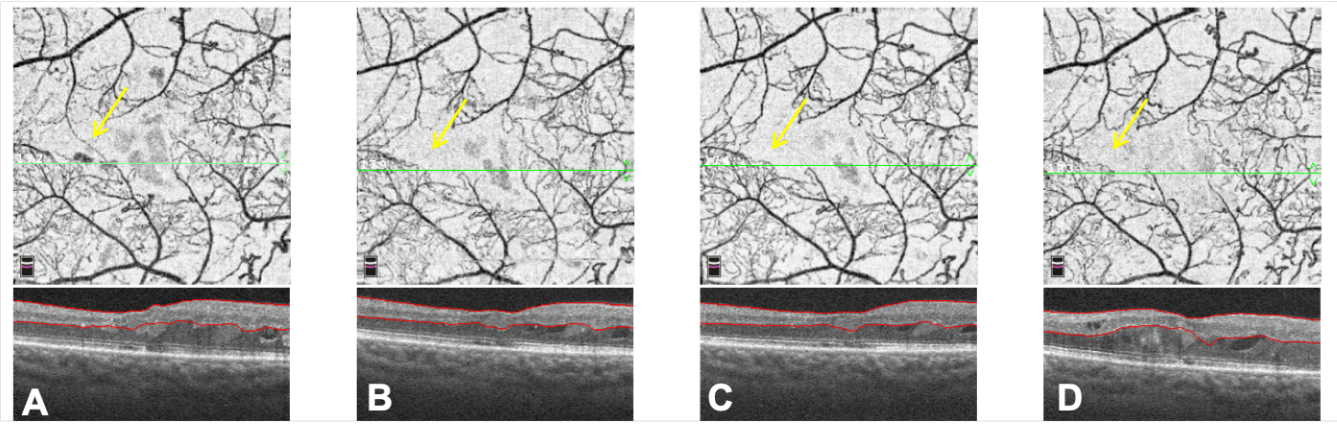

IV. DISCUSSION & PERSPECTIVES

I. Circulating monocytes exposed to high lipid differentiate in inflammatory macrophages and activate Müller glial cells

1. Rational and aim of the study

Diabetic retinopathy is now admitted being the result of several factors, including glial and neuronal cell dysfunction, inflammatory reaction, blood retinal barrier breakdown and capillary dropout. However, the factors that might predict edema occurrence or recurrence remain poorly identified. Further understanding of DME occurrence is crucially needed to allow an early detection, to improve the functional outcomes and also to identify new therapeutic targets in diabetic patients.

Growing evidences indicate that inflammation is involved in DME formation. Diabetic patients and animal models of type 2 diabetes (T2DM) demonstrate early retinal mononuclear phagocyte (MP) activation and intraocular elevated levels of inflammatory cytokines such as VEGF, IL-8, CCL2 and IL-6 (Abcouwer SF, 2013). Monocytes produce, under high-glucose conditions, tumor necrosis factor (TNF)-α and IL-6 (Morohoshi M et al., 1996).

Previous research of our team and others have shown in animal models that retinal MP responsible for diabetic retinopathy (DR) phenotype mainly derived from blood monocytes and account for most of the production of cytokine (Kermorvant-Duchemin E et al., 2013; Rangasamy S et al., 2014).

Our team reported differences in the transcription profile between MP derived from circulating monocytes from controls, diabetic patients with no sign of retinopathy, patients with non-proliferative DR (NPDR) without DME, and proliferative DR (PDR) patients. We showed that CCL2 expression is particularly high in MP derived from non-proliferative DR patients and VEGF transcription is elevated in MP from both NPDR and PDR patients while these differences are not seen in circulating monocytes.

Our preliminary data support a model in which circulating monocytes in patient with NPDR and PDR, in contrast to diabetic patient with no sign of retinopathy, are already engaged in pro-inflammatory functions such as macrophage recruitment or vascular remodeling that are hallmark of DR. We hypothesize that similar to the non-DME situation, a specific inflammatory status of circulating monocytes may predispose type 2 diabetic patients to develop DME.

Furthermore, MP derived cytokines may also be responsible for VEGF-independent DME formation and/or VEGF resistance. In line with that, intraocular IL-6 levels has been shown to be a better predictor of VEGF resistance than VEGF level itself (La O et al. 2013).

We aimed to evaluate the effect of palmitic acid (PA) exposure on circulating monocytes and to study the potential interactions between PA-induced inflammatory macrophages and retinal Müller cells.

2. Preliminary results

a) Palmitic acid induce circulating monocytes differentiation into inflammatory macrophages

Inflammatory macrophages (iMφs) present in the retina of diabetic eyes mostly derived from circulating monocytes (Mos) and account for most of the cytokine production. We hypothesized that Mos exposure to hyperglycemia and/or hyperlipidemia may induce their differentiation into iMφs.

To test that hypothesis, Mos were isolated from venous blood of healthy volunteer individuals and allowed to differentiate in Mφs for 18h. Mφs were then exposed to either: normoglycemic medium (NG: DMEM with 5 mM glucose plus Ethanol), or hyperglycemic medium (HG: DMEM with 25 mM glucose plus Ethanol) or palmitic acid (PA: DMEM with 5 mM glucose plus BSA-bounded palmitic acid) during 24h. Cytokines expression were quantified by RT-PCR and multiplex analysis. The expression of VEGF in Mφs was not alter under PA exposure.

Our team (Guillaume Blot) found that HG condition only slightly increased the expression and production of VEGF, CCL2 and IL-1ß compared with NG condition. In contrast, PA-treated Mφs exhibited elevated of pro-inflammatory cytokines, such as CCL2 and IL-1ß.

In this study, we found that only Mφs treated with PA differentiate into inflammatory Mφs. This data suggests that dyslipidemia, rather than hyperglycemia, may participate to the chronic inflammation in DR.

b) Macrophages induce Müller cell activation after palmitic acid exposure

To investigate the role of inflammatory Mφs in retinal inflammation, we aim to study the interaction between iMφs and Müller glial cells in culture. We exposed hiPSCs-derived Müller cells to PA-treated iMφs supernatants (treated as cited above) for 18 hours.

Peripheral blood mononuclear cells (PBMCs) were isolated from heparinized venous blood from healthy volunteer individuals. PBMCs were incubated in DMEM with 5 mM glucose for 18 hours at 37℃ to allow their adherence and differentiation in Mφs.
Mφs were then treated for 24 hours in either normoglycemic medium (NG/EtOH: DMEM with 5 mM glucose plus Ethanol) or hyperglycemic medium with palmitic acid (HG/PA :DMEM with 25 mM glucose plus PA).

hiPSCs-derived Müller cells were then exposed to supernatants obtained from Mφs culture in both conditions.
The expression of genes involved in angiogenesis and inflammatory DR-relevant pathways were then quantified by RT-PCR. Both angiogenesis factors, VEGF and ANGPTL4, and inflammatory factors, IL-1ß, CCL2, TNF-α and IL6, were significantly increased in hiPSCs-derived Müller cells after exposure to PA-treated iMφs supernatants (**Figure 29**).

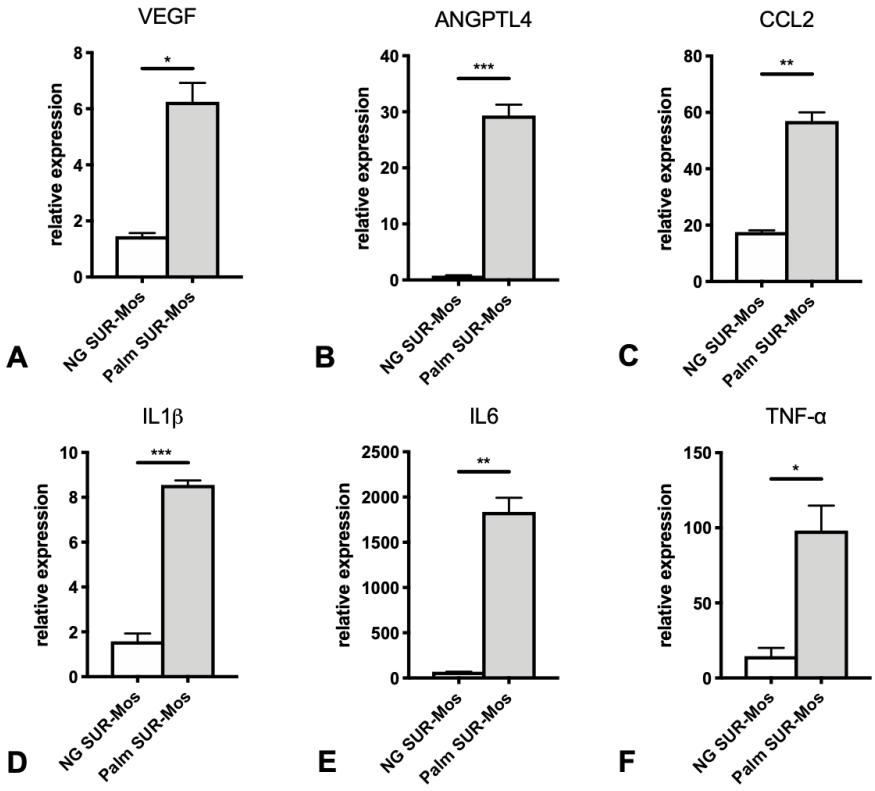

Figure 29: Expression of angiogenesis factors, VEGF and ANGPTL4, and inflammatory factors, CCL2, IL-1ß, IL6, and TNF-α in hiPSCs-derived Müller cells exposed for 24 hours to supernatants obtained from macrophages previously cultured for 24 hours in either normoglycemic medium (NG SUR-Mos: macrophages cultured DMEM with 5 mM glucose plus Ethanol) or hyperglycemic medium with palmitic acid (Palm SUR-Mos :DMEM with 25 mM glucose plus PA).

A) The mean value of VEGF was 1.458 in NG SUR-Mos versus 6.251 in Palm SUR-Mos (p = 0.0170) **B)** The mean value of ANGPTL4 was 0.7676 in NG SUR-Mos versus 29.34 in Palm SUR-Mos (p = 0.0001) **C)** The mean value of CCL2 was 17.54 in NG SUR-Mos versus 56.96 in Palm SUR-Mos (p = 0.0047) **D)** The mean value of IL-1ß was 1.581 in NG SUR-Mos versus 8.558 in Palm SUR-Mos (p = 0.0003) **E)** The mean value of IL6 was 69.00 in NG SUR-Mos versus 1836.00 in Palm SUR-Mos (p = 0.0077) **F)** The mean value of TNF-α 14.59 in NG SUR-Mos versus 98.18 in Palm SUR-Mos (p = 0.0274)

All results were normalized with expression of S26 and expressed as mean ± SEM (n = 6 in each group)

c) Role of IL-1ß and TNF-α in Müller cell activation

To further investigate the interaction of inflammatory macrophages and Müller glial cells in high lipid condition, we aim to determine which cytokines in iMφs supernatants caused Müller cell activation. We study the role of IL-1ß and TNF-α, two main inflammatory cytokines produced by iMφs, on hiPSCs-derived Müller cells.

For this experiment, A2 hiPSCs-derived Müller cells were treated for 18 hours in either:

- Normoglycemic condition (NG: DMEM with 5 mM glucose plus ethanol)
- Normoglycemic condition with Palmitate (NG plus BSA-bounded PA)
- Hyperglycemic condition (HG: DMEM with 25 mM glucose plus ethanol)
- Hyperglycemic condition with Palmitate (HG plus BSA-bouded PA)
- Normoglycemic condition with IL-1ß 10 ng/mL
- Normoglycemic condition with TNF-α 10 ng/mL

We evaluated the expression of angiogenesis genes, VEGF and ANGPTL4, as well as inflammatory factors, IL6 and IL-1ß, in hiPSCs-derived Müller cells par quantitative RT-PCR. The expression of VEGF, ANGPTL4 and IL6 was significantly increased in hiPSCs-derived Müller cells after PA treatment compared with NG or HG alone treatment. The treatment with IL-1ß did not alter the expression of VEGF and ANGPTL4 but had a positive feedback effect on his own expression in Müller cells. Similarly, the treatment with TNF-α did not alter the expression of VEGF and ANGPTL4 but significantly increase IL6 expression in hiPSCs-derived Müller cells compared with NG or HG treatment (**Figure 30**).

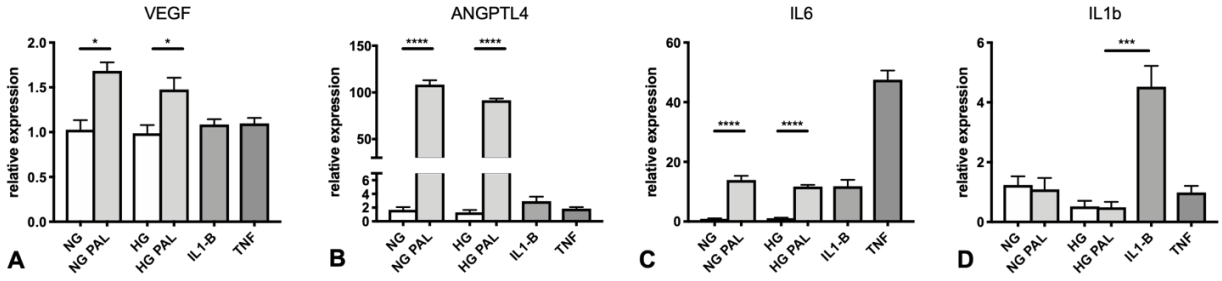

Figure 30: Expression of angiogenesis factors, VEGF and ANGPTL4, and inflammatory factors, IL6 and IL-1ß in hiPSCs-derived Müller cells exposed for 24 hours either to normoglycemic medium (NG: DMEM with 5 mM glucose plus Ethanol) or normoglycemic medium with palmitic acid (NG-Palm :DMEM with 25 mM glucose plus PA), or to

hyperglycemic medium (HG: DMEM with 25 mM glucose plus Ethanol) or hyperglycemic medium with palmitic acid (HG-Palm :DMEM with 25 mM glucose plus PA), or to IL1- ß, or TNF-α.

A) The mean value of VEGF was 1.028 in NG condition vs 1.685 in NG-Palm condition (p = 0.0009); and was 0.9871 in HG condition vs 1.476 in HG-Palm condition (p = 0.0121); and was 1.08516 in IL1- ß condition; and 1.09685 in TNF-α condition.

B) The mean value of ANGPTL4 was 1.689 in NG condition vs 108.4 in NG-Palm condition (p <0.0001); and was 1.325 in HG condition vs 91.65 in HG-Palm condition (p = <0.0001); and was 2.942 in IL1- ß condition; and 1.861 in TNF-α condition.

C) The mean value of IL6 was 0.9219 in NG condition vs 13.94 in NG-Palm condition (p <0.0001); and was 1.130 in HG condition vs 11.75 in HG-Palm condition (p = <0.0001); and was 11.84 in IL1- ß condition (p = 0.0004 versus NG condition; p = 0.0005 versus HG condition); and 47.52 in TNF-α condition (p <0.0001 versus NG condition and versus HG condition).

D) The mean value of IL-1ß was 1.236 in NG condition vs 1.091 in NG-Palm condition (p = 0.7682); and was 0.5200 in HG condition vs 0.4921 in HG-Palm condition (p = 0.9173); and was 4.523 in IL1- ß condition (p = 0.0015) versus NG condition; p = 0.0005 versus HG condition); and 0,9833 in TNF-α condition (p = 0.5017 versus NG condition and p = 0.1415 versus HG condition).

All results were normalized with expression of S26 and expressed as mean ± SEM (n = 6 in each group)

3. Conclusions

In DR patients, inflammatory mononuclear phagocytes found in the retina originate from local proliferation/activation of retinal microglia (the resident macrophage of the retina) but also from blood-born inflammatory monocytes. As in animal models the monocyte-derived inflammatory Mφs account for most of the production of cytokines and are responsible for most of the DR phenotype (Kermorvant-Duchemin E et al., 2013; Rangasamy et al., 2014), we further investigated interaction between Mφs and Müller glial cells.

Our preliminary results confirmed that Palmitic Acid is a DR-relevant stimulus. PA is able to induce Mos differentiation into inflammatory Mφs, exhibiting elevated of pro-inflammatory cytokines, such as CCL2 and IL-1ß.

The PA-treated Mφs were able to induce Müller glial cell activation, as demonstrated by an increase of both angiogenesis factors (VEGF and ANGPTL4) and inflammatory factors (IL-1ß, CCL2, TNF-α and IL6) expression in hiPSCs-derived Müller cells.
The main factors produced by inflammatory Mφs and inducing Müller cell reaction remain to be determined in future studies.

4. Methods

a) Monocytes preparation and culture

Peripheral blood mononuclear cells (PBMCs) were isolated from heparinized venous blood from healthy volunteer individuals. In accordance with the Declaration of Helsinki, volunteers provided written and informed consent for the human monocyte expression studies, which were approved by the Centre national d'Ophthalmologie des Quinze-Vingt hospital (Paris, France) ethics committees (no. 913572). PBMCs were isolated from blood by 1-step centrifugation on a Ficoll Paque layer (GE Healthcare) and sorted with EasySep Human Monocyte Enrichment Cocktail (StemCells Technology, Grenoble, France). Human Mos were incubated in DMEM for 18 hours at 37℃ to allow their adherence and differentiation in macrophages.

b) hiPSCs-derived Müller cells culture and treatment

For this study, hiPSCs-derived Müller cells were unfreezed and placed in a DMEM medium with 25 mM glucose with fetal bovine serum (FBS) at 37° for 10 days. At day 10, the medium was changed and hiPSCs-derived Müller cells were cultured under low-glucose and serum-free condition (DMEM with 5mM glucose without FBS) for 24 hours before treatment. Cells were then plated in coated 6-well dishes (150 000 cells/well).
hiPSCs-derived Müller cells were treated for 24 hours in serum-free medium containing

- Either low glucose fatty acid-free medium (DMEM with 5 mM glucose plus BSA 0,83 %, plus ethanol 0,5 % and 1.8g mannitol for osmotic control);
- Or elevated glucose fatty acid-free medium (DMEM with 25 mM glucose plus BSA 0,83 % plus ethanol 0,5 %);
- Or low glucose medium with PA (DMEM with 5 mM glucose plus BSA-bound PA 0.5 mM and 1.8g mannitol for osmotic control);

- Or elevated glucose medium with PA (DMEM with 25 mM glucose plus BSA-bound PA 0.5 mM).

c) RNA isolation, reverse transcription and real-time quantitative polymerase chain reaction

Treated hiPSCs-derived Müller cells were lysed and RNA purified using the RNA XS kit (740902, Macherey-Nagel, Düren, Germany) according to the manufacturer's protocol. Total RNA was isolated and converted to cDNA using oligo (dT) as primer and Superscript II (Life Technologies). Each reverse transcrition assay was performed in a 20mL reaction. Subsequent real-time PCR was performed using cDNA, Sybr Green PCR Master Mix (Life Technologies). Real-time PCR was performed using StepOne Plus real-time PCR system (Applied Biosystems) with the following profile: 10 min at 95°C, followed by a total of 4° two-temperature cycles (15 sec at 95°C and 1 min at 60°C). To verify the purity of the products, a melting curve was produced after each run according to the manufacturer's instructions. Results were expressed as fold induction after normalization by RPS26 or Actine. Primers for real-time PCR were purchased from IDT technology (primer sequences at request).

II. In vivo model of retinal glial cell response to high lipid exposure

1. Aim and background

We previously showed that hiPSCs-derived Müller cells behaved as primary human Müller cells to high glucose and high lipid exposure. Palmitic Acid (PA), the most elevated circulating free fatty acid in humans, was demonstrated to induce a strong Müller glial cell activation , resulting in a significantly increased expression of pro-inflammatory factors, such as ATF3 and IL8, as well as of pro-angiogenic factors such as VEGF and ANGPTL4.

Several *in vitro* studies have demonstrated the stimulating effect of free fatty acids on either Müller glial cells (Capozzi ME et al., 2018) or on endothelial cells (Othman A et al., 2013; Capozzi ME et al., 2016). However, only few evidence exits regarding their effect on the retina in vivo (Naveh-Floman N et al., 1984). We thus aimed to investigated the effect of PA *in vivo*.

2. Preliminary results

a) Intravitreal injection of palmitic acid

To confirm the reaction of activation of Müller glial cells to high lipid exposure, we studied the effect of intravitreal injection of palmitic acid (PA) in C57Bl6/J male mice. The first experiment aimed to analyze Müller glial cell reaction after one intravitreal injection of PA compared with one intravitreal injection of PBS. Mice were sacrificed 24 hours and 96 hours after the intravitreal injection. The relative expression of GFAP and VEGF in the entire retina was determined by quantitative RT-PCR.

No significant increase in GFAP expression indicative of a glial reaction in Müller glial cells, as well as no increase in VEGF expression were detected (**Figure 31**).

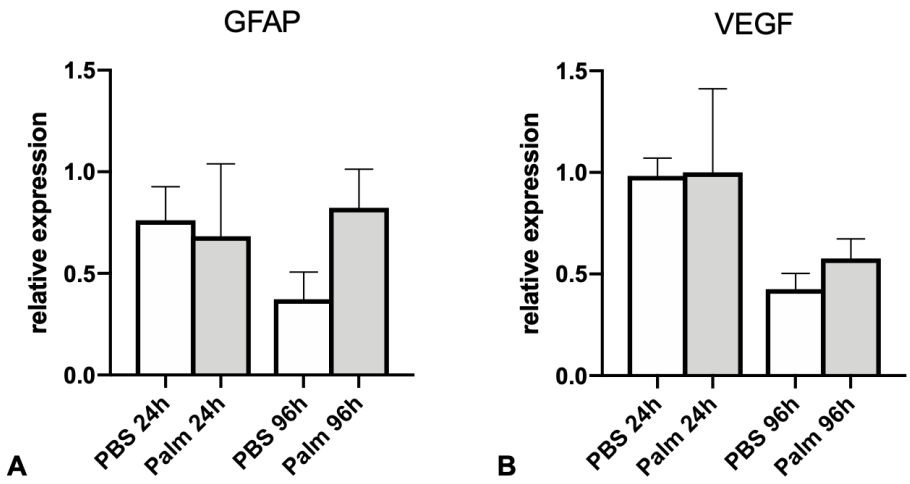

Figure 31 : Relative expression of GFAP and VEGF in the entire retina of C57Bl6/J mice after one intravitreal injection of either palmitic acid or PBS.

A) The mean value of GFAP expression in the retina was of 0.7616 and 0.3735 at 24h and 96h respectively after PBS intravitreal injection; and was of 0.6836 and 0.8235 at 24h and 96h respectively after PA intravitreal injection ($p = 0.8519$ at 24h and 0.1240 at 96h).

B) The mean value of VEGF expression in the retina was of 0.9837 and 0.4258 at 24h and 96h respectively after PBS intravitreal injection; and was of 1.001 and 0.5775 at 24h and 96h respectively after PA intravitreal injection ($p = 0.9695$ at 24h and 0.2862 at 96h).

All results were normalized with expression of S26 and expressed as mean ± SEM ($n = 3$ in each group)

In a second experiment, we performed three intravitreal injections of PA in C57Bl6/J male mice, at baseline, 48 hours and 7 days to increase PA intravitreal level. Mice were sacrificed 24 hours after the third intravitreal injection. The relative expression of GFAP and VEGF in the entire retina was determined by quantitative RT-PCR.

Similarly to the first experiment, ,no significant increase in GFAP expression or VEGF expression in Müller glial cells were detected.

b) Sub-retinal injection of palmitic acid

Given the property of the internal limiting membrane, we hypothesized that intravitreal injection of PA failed to activate Müller glial cells because it was not able to enter the retina and reach the glial cells. In human, fatty acids may enter the retina via the blood circulation, in case of blood-retinal barrier rupture. We then conducted an experiment to analyze glial cell

reaction after sub-retinal injection of PA. The relative expression of VEGF, ANGPTL4 and IL6 in the entire retina was determined by quantitative RT-PCR.

A non-significant increase in VEGF, ANGPTL4 and IL6 relative expression was detected 24 hours after one sub-retinal injection of PA (**Figure 32**).

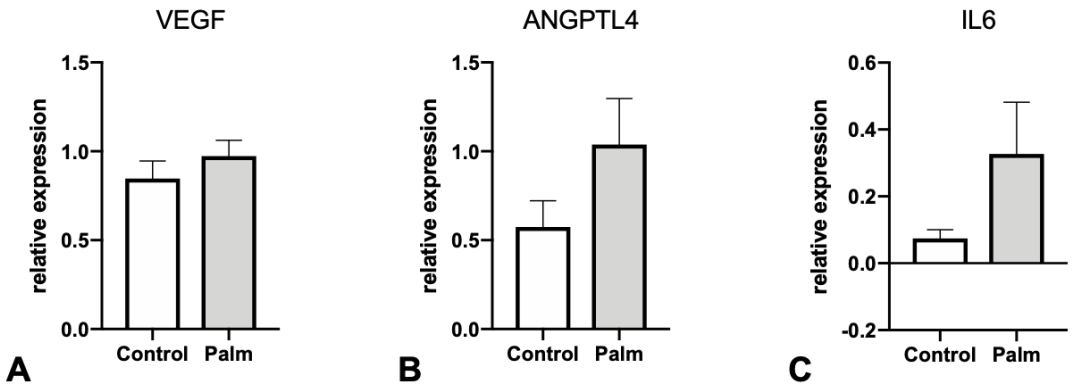

Figure 32 : Relative expression of VEGF, ANGPTL4 and IL6 in the entire retina of C57Bl6/J mice 24 hours after one sub-retinal injection of either palmitic acid or PBS (control).

A) The mean value of VEGF expression in the retina was of 0.8463 and 0.9733 after PBS and PA subretinal injection respectively ($p = 0.3614$).

B) The mean value of ANGPTL4 expression in the retina was of 0.5738 and 1.038 after PBS and PA subretinal injection respectively ($p = 0.1661$).

C) The mean value of IL6 expression in the retina was of 0.07444 and 0.3271 after PBS and PA subretinal injection respectively ($p = 0.2330$).

All results were normalized with expression of S26 and expressed as mean ± SEM ($n = 6$ in the control group and $n = 8$ in the PA-treated group)

c) Total retinal explants exposed to palmitic acid

We also analyzed the reaction of total retinal explants cultured in PA medium. As previously described, total retinal explants were obtained by entire retina dissection from C57/Bl6 mice and were incubated in either low glucose fatty acid-free medium (DMEM with 5 mM glucose plus BSA 0,83 %, plus ethanol 0,5 % and 1.8g mannitol for osmotic control); or in low glucose medium with PA (DMEM with 5 mM glucose plus BSA-bound PA 0.5 mM and 1.8g mannitol for osmotic control) for 48 hours.

A significant increase of ANGPTL4 and IL6 relative expression was detected in the entire retinal after a 48-hours-PA exposure (**Figure 33**).

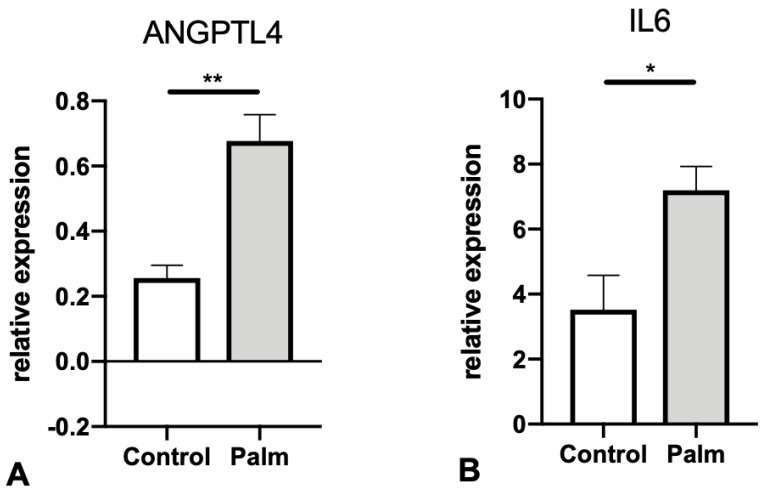

Figure 33 : Relative expression of ANGPTL4 and IL6 in total retinal explants obtained from C57Bl6/J mice and cultured for 24 hours in either low glucose fatty acid-free medium palmitic acid (control) or in low glucose medium with palmitic acid (Palm).

A) The mean value of ANGPTL4 expression in the retina was of 3.522 in control explants versus 7.198 in PA-treated explants ($p = 0.0301$).

B) The mean value of IL6 expression in the retina was of 0.2562 in control explants versus 0.6770 in PA-treated explants ($p = 0.0041$). All results were normalized with expression of S26 and expressed as mean ± SEM ($n = 6$ in each group)

3. Perspectives

In these preliminary results, we showed that palmitic acid did not exert any significant pro-inflammatory or pro-angiogenic effect on retinal Müller glial cells, when injected intravitreally or sub-retinally. These results might be explained by the only slight contact between PA and the Müller glial cells using these injection routes in non-diabetic wild-type mice, having preserved inner limiting membrane and preserved blood-retinal barrier.

It may be of interest to study the effect of sub-retinal injections of PA in an animal model of blood-barrier rupture or in newborns animals. The potential pro-angiogenic effect of PA on Müller glial cells could also be studied in vitro in oxygen-induced retinopathy model.

III. Histopathologic study of hyperreflective fluid in post-mortem human diabetic retina

The composition of intra-retinal hard exudates has been reported to be hyaline deposits and lipid-laden macrophages in histological studies (Toussaint D, 1962; Wolter JR, 1957; Cusik M et al., 2003).

To our knowledge, no data exits regarding the molecular content of hyperreflective fluid in human retina with DME. It is unclear which type of particles present in hyperreflective fluid are detected by OCT in vivo, although it is likely a combination of lipid and proteinaceous macromolecules.
Elevated serum lipid levels were associated with increased retinal hard exudates in diabetic retinopathy. Histologic evidence of concentrations of the two primary components of high-density lipoprotein (LDL) have suggested possible extravasation of LDL core components (Cusik M et al , 2003).

Futures histopathological studies of post-mortem retinas of diabetic patients with hyperreflective fluid identified on OCT, may be of high interest. To identify which lipid or molecule are present in these hyperreflective cysts would allow studying their effect of Müller glial cell activation and give opportunities to identify new therapeutic targets in DME.

References

Abcouwer SF. Direct effects of PPARα agonists on retinal inflammation and angiogenesis may explain how fenofibrate lowers risk of severe proliferative diabetic retinopathy. Diabetes. 2013 Jan;62(1):36-8. doi: 10.2337/db12-1223. No abstract available.

Abcouwer SF, Antonetti DA. A role for systemic inflammation in diabetic retinopathy. Invest Ophthalmol Vis Sci. 2013 Mar 28;54(3):2384. doi: 10.1167/iovs.13-11977.

Abcouwer SF. Angiogenic Factors and Cytokines in Diabetic Retinopathy.
J Clin Cell Immunol. 2013;Suppl 1(11). doi: 10.4172/2155-9899

Abu-El-Asrar AM, Dralands L, Missotten L, Al-Jadaan IA, Geboes K. Expression of apoptosis markers in the retinas of human subjects with diabetes. Invest Ophthalmol Vis Sci. 2004 Aug;45(8):2760-6.

ACCORD Study Group; ACCORD Eye Study Group, Chew EY, Ambrosius WT, Davis MD, Danis RP, Gangaputra S, Greven CM, Hubbard L, Esser BA, Lovato JF, Perdue LH, Goff DC Jr, Cushman WC, Ginsberg HN, Elam MB, Genuth S, Gerstein HC, Schubart U, Fine LJ. Effects of medical therapies on retinopathy progression in type 2 diabetes. N Engl J Med. 2010 Jul 15;363(3):233-44. doi: 10.1056/NEJMoa1001288. Epub 2010 Jun 29. Erratum in: N Engl J Med. 2011 Jan 13;364(2):190. N Engl J Med. 2012 Dec 20;367(25):2458.

Agte, S., Junek, S., Matthias, S., Ulbricht, E., Erdmann, I., Wurm, A., Schild, D., Kas, J.A. & Reichenbach, A. Muller glial cell-provided cellular light guidance through the vital guinea-pig retina. Biophysical journal, 2011; 101, 2611-2619.

Aiello LP. The potential role of PKC beta in diabetic retinopathy and macular edema. Surv Ophthalmol. 2002 Dec;47 Suppl 2:S263-9. Review.

Ali TK, Al-Gayyar MM, Matragoon S, Pillai BA, Abdelsaid MA, Nussbaum JJ, El-Remessy AB. Diabetes-induced peroxynitrite impairs the balance of pro-nerve growth factor and nerve growth factor, and causes neurovascular injury. Diabetologia. 2011 Mar;54(3):657-68. doi: 10.1007/s00125-010-1935-1. Epub 2010 Oct 19.

Antonetti DA, Barber AJ, Hollinger LA, Wolpert EB, Gardner TW. Vascular endothelial growth factor induces rapid phosphorylation of tight junction proteins occludin and zonula occluden 1. A potential mechanism for vascular permeability in diabetic retinopathy and tumors. J Biol Chem. 1999 Aug 13;274(33):23463-7.

Antonetti DA, Barber AJ, Bronson SK, Freeman WM, Gardner TW, Jefferson LS, Kester M, Kimball SR, Krady JK, LaNoue KF, Norbury CC, Quinn PG, Sandirasegarane L, Simpson IA; JDRF Diabetic Retinopathy Center Group. Diabetic retinopathy: seeing beyond glucose-induced microvascular disease.Diabetes. 2006 Sep;55(9):2401-11. doi:10.2337/db05-1635

Antonetti DA, Klein R, Gardner TW. Diabetic Retinoapthy N Engl J Med. 2012 Mar 29;366(13):1227-39. doi: 10.1056/NEJMra1005073.

Araújo R.S., Santos D.F., Silva G.A. The role of the retinal pigment epithelium
and Müller cells secretome in neovascular retinal pathologies, Biochimie 2018, doi: 10.1016/j.biochi.2018.06.019.

Asnaghi V, Gerhardinger C, Hoehn T, Adeboje A, Lorenzi M. A role for the polyol pathway in the early neuroretinal apoptosis and glial changes induced by diabetes in the rat. Diabetes. 2003 Feb;52(2):506-11.

Babapoor-Farrokhran S, Jee K, Puchner B, Hassan SJ, Xin X, Rodrigues M, Kashiwabuchi F, Ma T, Hu K, Deshpande M, Daoud Y, Solomon S, Wenick A, Lutty GA, Semenza GL, Montaner S, Sodhi A. Angiopoietin-like 4 is a potent angiogenic factor and a novel therapeutic target for patients with proliferative diabetic retinopathy. Proc Natl Acad Sci U S A. 2015 Jun 9;112(23):E3030-9. doi: 10.1073/pnas.1423765112. Epub 2015 May 26.

Bai, Y., Ma, J.X., Guo, J., Wang, J., Zhu, M., Chen, Y. & Le, Y.Z. Muller cell-derived VEGF is a significant contributor to retinal neovascularization. The Journal of pathology, 2009 ; 219, 446-454.

Barber AJ, Lieth E, Khin SA, Antonetti DA, Buchanan AG, Gardner TW. Neural apoptosis in the retina during experimental and human diabetes. Early onset and effect of insulin. J Clin Invest. 1998 Aug 15;102(4):783-91.

Barcelona, P.F., Ortiz, S.G., Chiabrando, G.A. & Sanchez, M.C. alpha2-Macroglobulin induces glial fibrillary acidic protein expression mediated by low-density lipoprotein receptor-related protein 1 in Muller cells. Investigative ophthalmology & visual science, 2011 ; 52, 778-786.

Barcelona, P.F., Sitaras, N., Galan, A., Esquiva, G., Jmaeff, S., Jian, Y., Sarunic, M.V., Cuenca, N., Sapieha, P. & Saragovi, H.U. p75NTR and Its Ligand ProNGF Activate Paracrine Mechanisms Etiological to the Vascular, Inflammatory, and Neurodegenerative Pathologies of Diabetic Retinopathy. The Journal of neuroscience, 2016; 36, 8826-8841.

Barnes AJ, Kohner EM, Johnston DG, Alberti KG. Severe retinopathy and mild carbohydrate intolerance: possible role of insulin deficiency and elevated circulating growth hormone. Lancet. 1985 Jun 29;1(8444):1465-8.

Barnes TC, Anderson ME, Moots RJ. The many faces of interleukin-6: the role of IL-6 in inflammation, vasculopathy, and fibrosis in systemic sclerosis. Int J Rheumatol. 2011;2011:721608.

Beach, K.M., Wang, J. & Otteson, D.C. (2017) Regulation of Stem Cell Properties of Muller Glia by JAK/STAT and MAPK Signaling in the Mammalian Retina. Stem cells international, 2017, 1610691.

Bearse MA Jr, Han Y, Schneck ME, Barez S, Jacobsen C, Adams AJ. Local multifocal oscillatory potential abnormalities in diabetes and early diabetic retinopathy. Invest Ophthalmol Vis Sci. 2004 Sep;45(9):3259-65.

Bengtsson B, Heijl A, Agardh E.Visual fields correlate better than visual acuity to severity of diabetic retinopathy. Diabetologia. 2005 Dec;48(12):2494-500. Epub 2005 Nov 1.

Biesecker, K.R., Srienc, A.I., Shimoda, A.M., Agarwal, A., Bergles, D.E., Kofuji, P. & Newman, E.A. Glial Cell Calcium Signaling Mediates Capillary Regulation of Blood Flow in the Retina. The Journal of neuroscience, 2016 ; 36, 9435-9445.

Bloodworth JM Jr. Diabetic retinopathy. Diabetes. 1962 Jan-Feb;11:1-22.

Boden G. Fatty acid-induced inflammation and insulin resistance inskeletal muscle and liver. Current Diabetes Reports 2006, 6: 177-181

Bolz, M, Schmidt-Erfurth U, Deak G, Mylonas G, Kriechbaum K, Scholda C; Diabetic RetinopathyResearch Group Vienna. Optical coherence tomographic hyperreflective foci: a morphologic sign of lipid extravasation in diabetic macular edema. Ophthalmology 2009,116: 914–920, doi:10.1016/j.ophtha.2008.12.039.

Bresnick GH, Palta M. Oscillatory potential amplitudes. Relation to severity of diabetic retinopathy. Arch Ophthalmol. 1987 Jul;105(7):929-33.

Bringmann, A., Pannicke, T., Uhlmann, S., Kohen, L., Wiedemann, P. & Reichenbach, A. Membrane conductance of Muller glial cells in proliferative diabetic retinopathy. Canadian journal of ophthalmology, 2002 ; 37, 221-227.

Brownlee M, Hirsch IB Glycemic variability: a hemoglobin A1c-independent risk factor for diabetic complications. JAMA 2006;295(14):1707-8.

Buraczynska M, Baranowicz-Gaszczyk I, Tarach J, Ksiazek A. Toll-like receptor 4 gene polymorphism and early onset of diabetic retinopathy in patients with type 2 diabetes. Hum Immunol 2009; 70, 121-124.

Busik JV, Mohr S, Grant MB. Hyperglycemia-induced reactive oxygen species toxicity to endothelial cells is dependent on paracrine mediators. Diabetes. 2008 Jul;57(7):1952-65. doi: 10.2337/db07-1520. Epub 2008 Apr 16.

Cacicedo JM, Benjachareowong S, Chou E, Ruderman NB, Ido Y. Palmitate-induced apoptosis in cultured bovine retinal pericytes: roles of NAD(P)H oxidase, oxidant stress, and ceramide. Diabetes. 2005 Jun;54(6):1838-45.

Cacicedo JM, Benjachareonwong S, Chou E, Yagihashi N, Ruderman NB, Ido Y.
Activation of AMP-activated protein kinase prevents lipotoxicity in retinal pericytes. Invest Ophthalmol Vis Sci. 2011 Jun 1;52(6):3630-9. doi: 10.1167/iovs.10-5784.

Caldwell RB, Bartoli M, Behzadian MA, El-Remessy AE, Al-Shabrawey M, Platt DH, Liou GI, Caldwell RW. Vascular endothelial growth factor and diabetic retinopathy: role of oxidative stress. Curr Drug Targets. 2005 Jun;6(4):511-24. Review.

Capozzi ME, Hammer SS, McCollum GW, Penn JS. Epoxygenated Fatty Acids Inhibit Retinal Vascular Inflammation. Sci Rep. 2016 Dec 14;6:39211. doi: 10.1038/srep39211

Capozzi ME, McCollum GW, Cousins DB, Penn JS. Linoleic Acid is a Diabetes-relevant Stimulator of Retinal Inflammation in Human Retinal Muller Cells and Microvascular Endothelial Cells. J Diabetes Metab. 2016 Dec;7(12). pii: 718. doi: 10.4172/2155-6156.1000718. Epub 2016 Nov 30.

Capozzi ME, Giblin MJ, Penn JS. Palmitic Acid Induces Müller Cell Inflammation that is Potentiated by Co-treatment with Glucose. Sci Rep. 2018 Apr 3;8(1):5459. doi:10.1038/s41598-018-23601-1.

Cepko C. Intrinsically different retinal progenitor cells produce specific types of progeny.
Nat Rev Neurosci. 2014 Sep;15(9):615-27. doi: 10.1038/nrn3767. Epub 2014 Aug 6. Review.

Chan JY, Cole E, Hanna AK. Diabetic nephropathy and proliferative retinopathy with normal glucose tolerance. Diabetes Care. 1985 Jul-Aug;8(4):385-90.

Chehade JM, Gladysz M, Mooradian AD. Dyslipidemia in type 2 diabetes: prevalence, pathophysiology, and management. Drugs. 2013 Mar;73(4):327-39. doi: 10.1007/s40265-013-0023-5. Review.

Chen, C., Chen, H., Xu, C., Zhong, Y. & Shen, X. Role of interleukin-1beta in hypoxia-induced depression of glutamate uptake in retinal Muller cells. Graefe's archive for clinical and experimental ophthalmology, 2014; 252, 51-58.

Chen X, Zhou H, Gong Y, Wei S, Zhang M. Early spatiotemporal characterization of microglial activation in the retinas of rats with streptozotocin-induced diabetes. Graefes Arch Clin Exp Ophthalmol. 2015 Apr;253(4):519-25. doi: 10.1007/s00417-014-2727-y. Epub 2014 Jul 13.

Chen W, Jump DB, Grant MB, Esselman WJ, Busik JV. Dyslipidemia, but not hyperglycemia, induces inflammatory adhesion molecules in human retinal vascular endothelial cells. Invest Ophthalmol Vis Sci. 2003 Nov;44(11):5016-22.

Chen Q, Tang L, Xin G, Li S, Ma L, Xu Y, Zhuang M, Xiong Q, Wei Z, Xing Z, Niu H, Huang W. Oxidative stress mediated by lipid metabolism contributes to high glucose-induced senescence in retinal pigment epithelium. Free Radic Biol Med. 2018 Oct 16;130:48-58. doi: 10.1016/j.freeradbiomed.2018.10.419. [Epub ahead of print]

Chorváthová V, Ondreicka R. The fatty acid composition of the tissues of streptozotocin-diabetic rats. Physiol Bohemoslov. 1983;32(5):466-75.

Coorey, N.J., Shen, W., Chung, S.H., Zhu, L. & Gillies, M.C. The role of glia in retinal vascular disease. Clinical & experimental optometry, 2012; 95, 266-281.

Couturier A, Bousquet E, Zhao M, Naud MC, Klein C, Jonet L, Tadayoni R, de Kozak Y, Behar-Cohen F. Anti-vascular endothelial growth factor acts on retinal microglia/macrophage activation in a rat model of ocular inflammation. Mol Vis. 2014 Jun 23;20:908-20.

Couturier A, Mané V, Bonnin S, Erginay A, Massin P, Gaudric A, Tadayoni R. CAPILLARY PLEXUS ANOMALIES IN DIABETIC RETINOPATHY ON OPTICAL COHERENCE TOMOGRAPHY ANGIOGRAPHY. Retina. 2015 Nov;35(11):2384-91.

Cusick M, Chew EY, Chan CC, Kruth HS, Murphy RP, Ferris FL 3rd. Histopathology and regression of retinal hard exudates in diabetic retinopathy after reduction of elevated serum lipid levels. Ophthalmology. 2003 Nov;110(11):2126-33. DOI: 10.1016/j.ophtha.2003.01.001

Decsi T, Szabó E, Burus I, Marosvölgyi T, Kozári A, Erhardt E, Soltész G. Low contribution of n-3 polyunsaturated fatty acids to plasma and erythrocyte membrane lipids in diabetic young adults. Prostaglandins Leukot Essent Fatty Acids. 2007 Mar;76(3):159-64. Epub 2007 Feb 23

Deeds MC, Anderson JM, Armstrong AS, Gastineau DA, Hiddinga HJ, Jahangir A, et al. Single dose streptozotocin-induced diabetes: considerations for study design in islet transplantation models. Lab Anim. 2011 Jul;45(3):131–40

Ding X, Zhang M, Gu R, Xu G, Wu H. Activated microglia induce the production of reactive oxygen species and promote apoptosis of co-cultured retinal microvascular pericytes. Graefes Arch Clin Exp Ophthalmol 2017, 255, 777-788.

Donato L, Bramanti P, Scimone C, Rinaldi C, D'Angelo R, Sidoti A. miRNA expression profile of retinal pigment epithelial cells under oxidative stress conditions, FEBS open bio. 2018 (8) 219-233.

Dupas B, Minvielle W, Bonnin S, Couturier A, Erginay A, Massin P, Gaudric A, Tadayoni R. Relationship between vessel density and visual impairment in type 1 diabetes patients with poor glycemic control. JAMA 2018

Falck JR, Reddy LM, Reddy YK, Bondlela M, Krishna UM, Ji Y, Sun J, Liao JK. 11,12-epoxyeicosatrienoic acid (11,12-EET): structural determinants for inhibition of TNF-alpha-induced VCAM-1 expression. Bioorg Med Chem Lett. 2003 Nov 17;13(22):4011-4.

Freitas HR, Ferraz G, Ferreira GC, Ribeiro-Resende VT, Chiarini LB, do Nascimento JL, Matos Oliveira KR, Pereira Tde L, Ferreira LG, Kubrusly RC, Faria RX, Herculano AM & Reis RA Glutathione-Induced Calcium Shifts in Chick Retinal Glial Cells. PloS one, 2016; 11, e0153677.

Fu, D., Yu, J.Y., Connell, A.R., Yang, S., Hookham, M.B., McLeese, R. & Lyons, T.J. Beneficial Effects of Berberine on Oxidized LDL-Induced Cytotoxicity to Human Retinal Muller Cells. Investigative ophthalmology & visual science, 2016; 57, 3369-3379.

Fukuda M, Nakanishi Y, Fuse M, Yokoi N, Hamada Y, Fukagawa M, Negi A, Nakamura M.Altered expression of aquaporins 1 and 4 coincides with neurodegenerative events in retinas of spontaneously diabetic Torii rats. Exp Eye Res. 2010 Jan;90(1):17-25. doi: 10.1016/j.exer.2009.09.003. Epub 2009 Sep 11.

Gaucher D, Chiappore J-A, Pâques M, Simonutti M, Boitard C, Sahel JA, et al. Microglial changes occur without neural cell death in diabetic retinopathy. Vision Res. 2007 Mar;47(5):612–23.

Gelman SK, Freund KB, Shah VP, Sarraf D. The pearl necklace sign: a novel spectral domain optical coherence tomography finding in exudative macular disease. Retina. 2014;34:2088e2095.

Gerhardinger C, Costa MB, Coulombe MC, Toth I, Hoehn T, Grosu P. Expression of acute-phase response proteins in retinal Müller cells in diabetes. Invest Ophthalmol Vis Sci. 2005 Jan;46(1):349–57.

Greenstein VC, Shapiro A, Zaidi Q, Hood DC.Psychophysical evidence for post-receptoral sensitivity loss in diabetics. Invest Ophthalmol Vis Sci. 1992 Sep;33(10):2781-90.

Grosche A, Hauser A, Lepper MF, Mayo R, von Toerne C, Merl-Pham J, Hauck SM.
The Proteome of Native Adult Müller Glial Cells From Murine Retina. Mol Cell Proteomics. 2016 Feb;15(2):462-80. doi: 10.1074/mcp.M115.052183. Epub 2015 Aug 31.

Gross JG, Glassman AR, Liu D, Sun JK, Antoszyk AN, Baker CW, Bressler NM, Elman MJ, Ferris FL 3rd, Gardner TW, Jampol LM, Martin DF, Melia M, Stockdale CR, Beck RW; Diabetic Retinopathy Clinical Research Network. Five-Year Outcomes of Panretinal

Photocoagulation vs Intravitreous Ranibizumab for Proliferative Diabetic Retinopathy: A Randomized Clinical Trial. JAMA Ophthalmol. 2018 Oct 1;136(10):1138-1148. doi: 10.1001/jamaophthalmol.2018.3255.

Hamon A, Roger JE, Yang XJ, Perron M. Müller glial cell dependent regeneration of the neural retina: an overview across vertebrate model systems. Dev Dyn 2016, 245:727-738.

Han Y, Schneck ME, Bearse MA Jr, Barez S, Jacobsen CH, Jewell NP, Adams AJ. Formulation and evaluation of a predictive model to identify the sites of future diabetic retinopathy. Invest Ophthalmol Vis Sci. 2004 Nov;45(11):4106-12.

Hang, H., Yuan, S., Yang, Q., Yuan, D. & Liu, Q. Multiplex bead array assay of plasma cytokines in type 2 diabetes mellitus with diabetic retinopathy. Molecular vision, 2014 ; 20, 1137-1145.

Harada T, Harada C, Kohsaka S, Wada E, Yoshida K, Ohno S, Mamada H, Tanaka K, Parada LF & Wada K. Microglia-Muller glia cell interactions control neurotrophic factor production during light-induced retinal degeneration. The Journal of neuroscience, 2002 ; 22 : 9228-9236.

Harrower AD, Clarke BF. Diabetic retinopathy with normal glucose tolerance. Br J Ophthalmol. 1976 Jun;60(6):459-63.

Hirsch IB, Brownlee M. Beyond hemoglobin A1c--need for additional markers of risk for diabetic microvascular complications. JAMA. 2010 Jun 9;303(22):2291-2. doi: 10.1001/jama.2010.785

Hurley JB, Lindsay KJ & Du J. Glucose, lactate, and shuttling of metabolites in vertebrate retinas. Journal of neuroscience research, 2015 ; 93, 1079-1092.

Ibrahim AS, Tawfik AM, Hussein KA, Elshafey S, Markand S, Rizk N, Duh EJ, Smith SB, Al-Shabrawey M. Pigment epithelium-derived factor inhibits retinal microvascular dysfunction induced by 12/15-lipoxygenase-derived eicosanoids. Biochim Biophys Acta. 2015 Mar;1851(3):290-8. doi: 10.1016/j.bbalip.2014.12.017. Epub 2015 Jan 3.

Jacobo, SM. & Kazlauskas, A. Insulin-like growth factor 1 (IGF-1) stabilizes nascent blood vessels. The Journal of biological chemistry, 2015 ; 290, 6349-6360.

Joussen AM, Poulaki V, Le ML, Koizumi K, Esser C, Janicki H, et al. A central role for inflammation in the pathogenesis of diabetic retinopathy. FASEB J Off Publ Fed Am Soc Exp Biol. 2004 Sep;18(12):1450–2.

Kandpal RP, Rajasimha HK, Brooks MJ, Nellissery J, Wan J, Qian J, Kern TS, Swaroop A.Transcriptome analysis using next generation sequencing reveals molecular signatures of diabeticretinopathy and efficacy of candidate drugs. Mol Vis. 2012;18:1123-46. Epub 2012 May 2.

Karakurum M, Shreeniwas R, Chen J, Pinsky D, Yan SD, Anderson M, Sunochi K, Major J, Hamilton T, Kuwabara K, et al: Hypoxic induction of interleukin-8 gene expression in endothelial cells. J Clin Invest 1994; 93: 1564–1570.

Keech AC, Mitchell P, Summanen PA, O'Day J, Davis TM, Moffitt MS, Taskinen MR, Simes RJ, Tse D, Williamson E, Merrifield A, Laatikainen LT, d'Emden MC, Crimet DC, O'Connell

RL, Colman PG; FIELD study investigators. Effect of fenofibrate on the need for laser treatment for diabetic retinopathy (FIELD study): a randomised controlled trial. Lancet. 2007 Nov 17;370(9600):1687-97. Epub 2007 Nov 7.

Kermorvant-Duchemin E, Pinel AC, Lavalette S, Lenne D, Raoul W, Calippe B, Behar-Cohen F, Sahel JA, Guillonneau X, Sennlaub F. Neonatal hyperglycemia inhibits angiogenesis and induces inflammation and neuronal degeneration in the retina. PLoS One. 2013 Nov 21;8(11):e79545. doi: 10.1371/journal.pone.0079545. eCollection 2013.

Klein R, Knudtson MD, Lee KE, Gangnon R, Klein BE. The Wisconsin Epidemiologic Study of Diabetic Retinopathy: XXII the twenty-five-year progression of retinopathy in persons with type 1 diabetes. Ophthalmology. 2008 Nov;115(11):1859-68. doi: 10.1016/j.ophtha.2008.08.023.

Kilpatrick ES. Arguments for and against the role of glucose variability in the development of diabetes complications. J Diabetes Sci Technol. 2009 Jul 1;3(4):649-55. Review.

Korani M, Firoozrai M, Maleki J, Ghahramanpour F, Heidari I, Fallah S, Seifi M.Fatty acid composition of serum lipids in patients with type 2 diabetes. Clin Lab. 2012;58(11-12):1283-91.

Kur, J. & Newman, E.A. Purinergic control of vascular tone in the retina. The Journal of physiology, 2014; 592, 491-504.

Othman A, Ahmad S, Megyerdi S, Mussell R, Choksi K, Maddipati KR, Elmarakby A, Rizk N, Al-Shabrawey M. 12/15-Lipoxygenase-derived lipid metabolites induce retinal endothelial cell barrier dysfunction: contribution of NADPH oxidase. PLoS One. 2013;8(2):e57254. doi: 10.1371/journal.pone.0057254. Epub 2013 Feb 20.

Owen LA, Hartnett ME. Soluble mediators of diabetic macular edema: the diagnostic role of aqueous VEGF and cytokine levels in diabetic macular edema. Curr Diab Rep. 2013 Aug;13(4):476-80. doi: 10.1007/s11892-013-0382-z.

Lachin JM, Bebu I, Bergenstal RM, Pop-Busui R, Service FJ, Zinman B, Nathan DM; DCCT/EDIC Research Group. Association of Glycemic Variability in Type 1 Diabetes With Progression of Microvascular Outcomes in the Diabetes Control and Complications Trial. Diabetes Care. 2017 Jun;40(6):777-783. doi: 10.2337/dc16-2426. Epub 2017 Apr 12.

Layton, C.J., Becker, S. & Osborne, N.N. The effect of insulin and glucose levels on retinal glial cell activation and pigment epithelium-derived fibroblast growth factor-2. Molecular vision, 2006; 12, 43-54.

Lardenoye CW, Probst K, DeLint PJ, Rothova A. Photoreceptor function in eyes with macular edema. Invest Ophthalmol Vis Sci. 2000 Nov;41(12):4048-53.

Lebrun-Julien, F., Bertrand, M.J., De Backer, O., Stellwagen, D., Morales, C.R., Di Polo, A. & Barker, P.A. ProNGF induces TNFalpha-dependent death of retinal ganglion cells through a p75NTR non-cell-autonomous signaling pathway. Proceedings of the National Academy of Sciences of the United States of America, 2010 ; 107, 3817-3822.

Lecleire-Collet, A., Tessier, L.H., Massin, P., Forster, V., Brasseur, G., Sahel, J.A. & Picaud, S. Advanced glycation end products can induce glial reaction and neuronal degeneration in retinal explants. The British journal of ophthalmology, 2005; 89, 1631-1633.

Lecomte M, Paget C, Ruggiero D, Wiernsperger N, Lagarde M. Docosahexaenoic acid is a major n-3 polyinsaturated fatty acid in bovine retinal microvessels. J Neurochem 1996; 66: 2160-2167

Li Q, Puro DG. Diabetes-induced dysfunction of the glutamate transporter in retinal Müller cells. Invest Ophthalmol Vis Sci. 2002 Sep;43(9):3109–16.

Lieth E, Barber AJ, Xu B, Dice C, Ratz MJ, Tanase D, et al. Glial reactivity and impaired glutamate metabolism in short-term experimental diabetic retinopathy. Penn State Retina Research Group. Diabetes. 1998 May;47(5):815–20.

Lieth, E.; Gardner, T.W.; Barber, A.J.; Antonetti, D.A.; Penn State Retina Research, G. Retinal neurodegeneration: Early pathology in diabetes. Clin. Exp. Ophthalmol. 2000, 28, 3–8.

Lindsay KJ, Du J, Sloat SR, Contreras L, Linton JD, Turner SJ, Sadilek M, Satrustegui J & Hurley JB. Pyruvate kinase and aspartate-glutamate carrier distributions reveal key metabolic links between neurons and glia in retina. Proceedings of the National Academy of Sciences of the United States of America, 2014; 111, 15579-15584.

Liu, X., Ye, F., Xiong, H., Hu, D., Limb, G.A., Xie, T., Peng, L., Yang, W., Sun, Y., Zhou, M., Song, E. & Zhang, D.Y. IL-1beta Upregulates IL-8 Production in Human Muller Cells Through Activation of the p38 MAPK and ERK1/2 Signaling Pathways. Inflammation, 2014; 37, 1486-1495.

Liu, Y., Biarnes Costa, M. & Gerhardinger, C. IL-1beta is upregulated in the diabetic retina and retinal vessels: cell-specific effect of high glucose and IL-1beta autostimulation. PloS one, 2012a ; 7, e36949.

Lorenc, V.E., Jaldin-Fincati, J.R., Luna, J.D., Chiabrando, G.A. & Sanchez, M.C. IGF-1 Regulates the Extracellular Level of Active MMP-2 and Promotes Muller Glial Cell Motility. Investigative ophthalmology & visual science, 2015; 56, 6948-6960.

Lu M, Kuroki M, Amano S, Tolentino M, Keough K, Kim I, Bucala R, Adamis AP. Advanced glycation end products increase retinal vascular endothelial growth factor expression. J Clin Invest. 1998 Mar 15;101(6):1219-24.

Lu Z, Li Y, Ru JH, Lopes-Virella MF, Lyons TJ, Huang Y. Interaction of palmitate and LPS regulates cytokine expression and apoptosis through sphingolipids in human retinal microvascular endothelial cells. Exp Eye Res. 2018 Sep 28;178:61-71. doi: 10.1016/j.exer.2018.09.016. [Epub ahead of print]

MacDonald RB, Charlton-Perkins M, Harris WA. Mechanisms of Müller glial cell morphogenesis. Curr Opin Neurobiol. 2017 Dec;47:31-37. doi: 10.1016/j.conb.2017.08.005. Epub 2017 Aug 29. Review.

Mané V, Dupas B, Gaudric A, Bonnin S, Pedinielli A, Bousquet E, Erginay A, Tadayoni R, Couturier A. Correlation between Cystoid Spaces in Chronic Diabetic Macular Edema and

Capillary Non-perfusion Detected by Optical Coherence Tomography Angiography. Retina. 2016 Dec;36 Suppl 1:S102-S110.

Martin PM, Roon P, Van Ells TK, Ganapathy V, Smith SB. Death of retinal neurons in streptozotocin-induced diabetic mice. Invest Ophthalmol Vis Sci. 2004 Sep;45(9):3330-6.

McAuley AK, Sanfilippo PG, Hewitt AW, Liang H, Lamoureux E, Wang JJ, et al. Vitreous biomarkers in diabetic retinopathy: a systematic review and meta-analysis. J Diabetes Complications. 2014 Jun;28(3):419–25.

Miyamoto K, Khosrof S, Bursell SE, Rohan R, Murata T, Clermont AC, Aiello LP, Ogura Y, Adamis AP. Prevention of leukostasis and vascular leakage in streptozotocin-induced diabetic retinopathy via intercellular adhesion molecule-1 inhibition. Proc Natl Acad Sci U S A. 1999 Sep 14;96(19):10836-41.

Monnier L, Colette C. Glycemic variability: should we and can we prevent it? Diabetes Care. 2008 Feb;31 Suppl 2:S150-4. doi: 10.2337/dc08-s241.

Morohoshi M, Fujisawa K, Uchimura I, Numano F. Glucose-dependent interleukin 6 and tumor necrosis factor production by human peripheral blood monocytes in vitro. Diabetes. 1996;45:954–959

Murakami T, Suzuma K, Dodo Y, Yoshitake T, Yasukura S, Nakanishi H, Fujimoto M, Oishi M, Tsujikawa A. Decorrelation Signal of Diabetic Hyperreflective Foci on Optical Coherence Tomography Angiography. Sci Rep. 2018 Jun 11;8(1):8798. doi: 10.1038/s41598-018-27192-9.

Murugeswari P, Shukla D, Rajendran A, Kim R, Namperumalsamy P, Muthukkaruppan V. Proinflammatory cytokines and angiogenic and anti-angiogenic factors in vitreous of patients with proliferative diabetic retinopathy and eales' disease. Retina. 2008;28:817–824.

Miyahara S, Kiryu J, Yamashiro K, Miyamoto K, Hirose F, Tamura H, Katsuta H, Nishijima K, Tsujikawa A, Honda Y. Simvastatin inhibits leukocyte accumulation and vascular permeability in the retinas of rats with streptozotocin-induced diabetes. Am J Pathol. 2004 May;164(5):1697-706.

Naveh-Floman N, Weissman C, Belkin M. Arachidonic acid metabolism by retinas of rats with streptozotocin-induced diabetes. Curr Eye Res. 1984 Sep;3(9):1135-9.

Newman EA, Frambach DA, Odette LL. Control of extracellular potassium levels by retinal glial cell K+ siphoning. Science. 1984 Sep 14;225(4667):1174-5.

Ning X, Baoyu Q, Yuzhen L, Shuli S, Reed E, Li QQ. Neuro-optic cell apoptosis and microangiopathy in KKAY mouse retina. Int J Mol Med. 2004 Jan;13(1):87-92.

Nunes S, Ribeiro L, Lobo C, Cunha-Vaz J. Three different phenotypes of mild nonproliferative diabetic retinopathy with different risks for development of clinically significant macular edema. Invest Ophthalmol Vis Sci. 2013 Jul 10;54(7):4595-604. doi: 10.1167/iovs.13-11895. DOI: 10.1167/iovs.13-11895

Ola, M.S. Effect of hyperglycemia on insulin receptor signaling in the cultured retinal Muller glial cells.

Biochemical and biophysical research communications, 2014; 444, 264-269.

Omri S, Behar-Cohen F, de Kozak Y, Sennlaub F, Verissimo LM, Jonet L, et al. Microglia/macrophages migrate through retinal epithelium barrier by a transcellular route in diabetic retinopathy: role of PKCζ in the Goto Kakizaki rat model. Am J Pathol. 2011, Aug;179(2):942–53.

Parisi V, Uccioli L. Visual electrophysiological responses in persons with type 1 diabetes. Diabetes Metab Res Rev. 2001 Jan-Feb;17(1):12-8. Review.

Park SH, Park JW, Park SJ, Kim KY, Chung JW, Chun MH, Oh SJ. Apoptotic death of photoreceptors in the streptozotocin-induced diabetic rat retina. Diabetologia. 2003 Sep;46(9):1260-8. Epub 2003 Jul 31.

Petrovic MG, Korosec P, Kosnik M, Hawlina M. Vitreous levels of interleukin-8 in patients with proliferative diabetic retinopathy. Am J Ophthalmol. 2007;143:175–176.

Pournaras CJ, Rungger-Brändle E, Riva CE, Hardarson SH, Stefansson E. Regulation of retinal blood flow in health and disease. Prog Retin Eye Res. 2008 May;27(3):284-330. doi: 10.1016/j.preteyeres.2008.02.002. Epub 2008 Feb 23. Review.

Qiu, A.W., Bian, Z., Mao, P.A. & Liu, Q.H. IL-17A exacerbates diabetic retinopathy by impairing Muller cell function via Act1 signaling. Experimental & molecular medicine, 2016 ; 48, e280.

Ralston JC, Metherel AH, Stark KD, Mutch DM. SCD1 mediates the influence of exogenous saturated and monounsaturated fatty acids in adipocytes: Effects on cellular stress, inflammatory markers and fatty acid elongation. J Nutr Biochem. 2016 Jan;27:241-8. doi: 10.1016/j.jnutbio.2015.09.011. Epub 2015 Sep 25.

Rangasamy S, McGuire PG, Franco Nitta C, Monickaraj F, Oruganti SR, Das A. Chemokine mediated monocyte trafficking into the retina: role of inflammation in alteration of the blood-retinal barrier in diabetic retinopathy. PLoS One. 2014 Oct 20;9(10):e108508. doi: 10.1371/journal.pone.0108508. eCollection 2014.

Reichenbach A, Frömter C, Engelmann R, Wolburg H, Kasper M, Schnitzer J. Müller glial cells of the tree shrew retina. J Comp Neurol. 1995 Sep 18;360(2):257-70.

Reichenbach,A. & Bringmann A. Role of Purines in Muller Glia. Journal of ocular pharmacology and therapeutics, 2016 ; 32, 518-533.

Reyes-Aguirre, L.I. & Lamas, M. Oct4 Methylation-Mediated Silencing As an Epigenetic Barrier Preventing Muller Glia Dedifferentiation in a Murine Model of Retinal Injury. Frontiers in neuroscience, 2016 ; 10, 523.

Ridano, ME, Subirada, P.V., Paz, M.C., Lorenc, V.E., Stupirski, J.C., Gramajo, A.L., Luna, J.D., Croci, D.O., Rabinovich, G.A. & Sanchez, M.C. Galectin-1 expression imprints a neurovascular phenotype in proliferative retinopathies and delineates responses to anti-VEGF. Oncotarget, 2017 ; 8, 32505-32522.

Ruberte, J., Ayuso, E., Navarro, M., Carretero, A., Nacher, V., Haurigot, V., George, M., Llombart, C., Casellas, A., Costa, C., Bosch, A. & Bosch, F. Increased ocular levels of IGF-1

in transgenic mice lead to diabetes-like eye disease. The Journal of clinical investigation, 2004. 113, 1149-1157.

Rübsam A, Parikh S, Fort PE. Role of Inflammation in Diabetic Retinopathy. Int J Mol Sci. 2018 Mar 22;19(4). pii: E942. doi: 10.3390/ijms19040942. Review.

Rungger-Brändle E, Dosso AA, Leuenberger PM. Glial reactivity, an early feature of diabetic retinopathy. Invest Ophthalmol Vis Sci. 2000 Jun;41(7):1971–80.

Sakai H, Tani Y, Shirasawa E, Shirao Y, Kawasaki K. Development of electroretinographic alterations in streptozotocin-induced diabetes in rats. Ophthalmic Res. 1995;27(1):57-63.

Sanchez, M.C., Luna, J.D., Barcelona, P.F., Gramajo, A.L., Juarez, P.C., Riera, C.M. & Chiabrando, G.A. Effect of retinal laser photocoagulation on the activity of metalloproteinases and the alpha(2)-macroglobulin proteolytic state in the vitreous of eyes with proliferative diabetic retinopathy. Experimental eye research, 2007 ; 85, 644-650.

Sasaki M, Kawasaki R, Rogers S, Man RE, Itakura K, Xie J, Flood V, Tsubota K, Lamoureux E, Wang JJ. The Associations of Dietary Intake of Polyunsaturated Fatty Acids With Diabetic Retinopathy in Well-Controlled Diabetes. Invest Ophthalmol Vis Sci. 2015 Nov;56(12):7473-9. doi: 10.1167/iovs.15-17485.

Schwartzman ML, Iserovich P, Gotlinger K, Bellner L, Dunn MW, Sartore M, Grazia Pertile M, Leonardi A, Sathe S, Beaton A, Trieu L, Sack R. Profile of lipid and protein autacoids in diabetic vitreous correlates with the progression of diabetic retinopathy. Diabetes. 2010 Jul;59(7):1780-8. doi: 10.2337/db10-0110. Epub 2010 Apr 27.

Shen W, Li S, Chung SH, Gillies MC. Retinal vascular changes after glial disruption in rats. J Neurosci Res. 2010 May 15;88(7):1485-99. doi: 10.1002/jnr.22317.

Simon, M.V., Prado Spalm, F.H., Politi, L.E. & Rotstein, N.P. Sphingosine-1-Phosphate Is a Crucial Signal for Migration of Retina Muller Glial Cells. Investigative ophthalmology & visual science, 2015 ; 56, 5808-5815.

Singh K, Kant S, Singh VK, Agrawal NK, Gupta SK, Singh K. Toll-like receptor 4 polymorphisms and their haplotypes modulate the risk of developing diabetic retinopathy in type 2 diabetes patients. Mol Vis 2014; 20, 704-713.

Stitt AW. The role of advanced glycation in the pathogenesis of diabetic retinopathy. Exp Mol Pathol. 2003 Aug;75(1):95-108. Review.

Subirada PV, Paz MC, Ridano ME, Lorenc VE, Vaglienti MV, Barcelona PF, Luna JD, Sánchez MC. A journey into the retina: Müller glia commanding survival and death. Eur J Neurosci. 2018 Jun;47(12):1429-1443. doi: 10.1111/ejn.13965. Epub 2018 Jun 8.

Takeuchi, M., Sato, T., Tanaka, A., Muraoka, T., Taguchi, M., Sakurai, Y., Karasawa, Y. & Ito, M. Elevated Levels of Cytokines Associated with Th2 and Th17 Cells in Vitreous Fluid of Proliferative Diabetic Retinopathy Patients. PloS one, 2015 ; 10, e0137358.

Thanos S, Mey J, Wild M. Treatment of the adult retina with microglia-suppressing factors retards axotomy-induced neuronal degradation and enhances axonal regeneration in vivo and in vitro.J Neurosci. 1993 Feb;13(2):455-66.

Tikhonenko M, Lydic TA, Wang Y, Chen W, Opreanu M, Sochacki A, McSorley KM, Renis RL, Kern T, Jump DB, Reid GE, Busik JV. Remodeling of retinal Fatty acids in an animal model of diabetes: a decrease in long-chain polyunsaturated fatty acids is associated with a decrease in fatty acid elongases Elovl2 and Elovl4. Diabetes. 2010 Jan;59(1):219-27. doi: 10.2337/db09-0728. Epub 2009 Oct 29.

Treins, C., Giorgetti-Peraldi, S., Murdaca, J., Monthouel-Kartmann, M.N. & Van Obberghen, E. Regulation of hypoxia-inducible factor (HIF)-1 activity and expression of HIF hydroxylases in response to insulin-like growth factor I. Molecular endocrinology, 2005; 19, 1304-1317.

Toft-Kehler AK, Skytt DM, Kolko M. A Perspective on the Müller Cell-Neuron Metabolic Partnership in the Inner Retina. Mol Neurobiol. 2018 Jun;55(6):5353-5361. doi: 10.1007/s12035-017-0760-7. Epub 2017 Sep 19.

Tolentino MJ, Miller JW, Gragoudas ES, Jakobiec FA, Flynn E, Chatzistefanou K, Ferrara N, Adamis AP. Intravitreous injections of vascular endothelial growth factor produce retinal ischemia and microangiopathy in an adult primate. Ophthalmology. 1996 Nov;103(11):1820-8.

Tolentino MJ, McLeod DS, Taomoto M, Otsuji T, Adamis AP, Lutty GA.Pathologic features of vascular endothelial growth factor-induced retinopathy in the nonhuman primate. Am J Ophthalmol. 2002 Mar;133(3):373-85.

Toussaint D, Cogan DG, Kuwabara T. Extravascular lesions of diabetic retinopathy. Arch Ophthalmol. 1962 Jan;67:42-7. doi:10.1001/archopht.1962.00960020044007

Tso MO. Pathology of cystoid macular edema. Ophthalmology. 1982 Aug;89(8):902-15.

Unterlauft JD, Claudepierre T, Schmidt M, Müller K, Yafai Y, Wiedemann P, Reichenbach A, Eichler W. Enhanced survival of retinal ganglion cells is mediated by Müller glial cell-derived PEDF. Exp Eye Res. 2014 Oct;127:206-14. doi:10.1016/j.exer.2014.08.004. Epub 2014 Aug 14.

Van den Oever IA, Raterman HG, Nurmohamed MT, Simsek S. Endothelial dysfunction, inflammation, and apoptosis in diabetes mellitus. Mediators Inflamm. 2010;2010:792393. doi: 10.1155/2010/792393. Epub 2010 Jun 15. Review.

Vecino E, Rodriguez FD, Ruzafa N, Pereiro X, Sharma SC. Glia-neuron interactions in the mammalian retina. Prog Retin Eye Res. 2016 Mar;51:1-40. doi: 10.1016/j.preteyeres.2015.06.003. Epub 2015 Jun 23.

Villacampa, P., Ribera, A., Motas, S., Ramirez, L., Garcia, M., de la Villa, P., Haurigot, V. & Bosch, F. Insulin-like growth factor I (IGF-I)-induced chronic gliosis and retinal stress lead to neurodegeneration in a mouse model of retinopathy. The Journal of biological chemistry, 2013 ; 288, 17631-17642.

Vincent JA, Mohr S. Inhibition of caspase-1/interleukin-1beta signaling prevents degeneration of retinal capillaries in diabetes and galactosemia. Diabetes. 2007 Jan;56(1):224–30.

Vogler, S., Pannicke, T., Hollborn, M., Kolibabka, M., Wiedemann, P., Reichenbach, A., Hammes, H.P. & Bringmann, A. Impaired Purinergic Regulation of the Glial (Muller) Cell

Volume in the Retina of Transgenic Rats Expressing Defective Polycystin-2. Neurochemical research, 2016 ; 41, 1784-1796.

Vujosevic S, Bini S, Torresin T, et al. Hyperreflective retinal spots in normal and diabetic eyes: B-scan and en face spectral domain optical coherence tomography evaluation. Retina. 2017;37:1092e1103.

Wan J, Goldman D: Retina regeneration in zebrafish. Curr Opin Genet Dev 2016, 40:41-47.

Wang, J., Xu, X., Elliott, M.H., Zhu, M. & Le, Y.Z. Muller cell-derived VEGF is essential for diabetes-induced retinal inflammation and vascular leakage. Diabetes, 2010; 59, 2297-2305.

Wolter JR, Goldsmith RI, Phillips RL. Histopathology of the star figure of the macular area in diabetic and angiospastic retinopathy. AMA Arch Ophthalmol. 1957 Mar;57(3):376-85.

Wolter JR. Diabetic Retinopathy. Am J Ophthalmol. 1961 May;51:1123-41.

Wolter JR. Cystoid macular edema in vitreo-retinal traction. Ophthalmic Surg. 1981 Dec;12(12):900-4.

Xu L, Xun G, Yao Z, Liu Y, Qiu Y, Liu K, Zhu D, Gu Q, Xu X, Ho PC. Effects of generated trans-arachidonic acids on retinal capillary during nitrative stress in diabetic rats. Ophthalmologica. 2008;222(1):37-41. Epub 2007 Dec 19.

Xu Y, Jiang Z, Huang J, Meng Q, Coh P, Tao L. The association between toll-like receptor 4 polymorphisms and diabetic retinopathy in Chinese patients with type 2 diabetes. Br J Ophthalmol 2015; 99, 1301-1305.

Xue Y, Shen SQ, Jui J, Rupp AC. Byrne LC, Hattar S, Flannery JG, Corbo JC & Kefalov VJ. CRALBP supports the mammalian retinal visual cycle and cone vision. The Journal of clinical investigation, 2015; 125, 727-738.

Yafai, Y., Eichler, W., Iandiev, I., Unterlauft, J.D., Jochmann, C., Wiedemann, P. & Bringmann, A. Thrombospondin-1 is produced by retinal glial cells and inhibits the growth of vascular endothelial cells. Ophthalmic research, 2014 ; 52, 81-88.

Yamagishi S, Okamoto T, Amano S, Inagaki Y, Koga K, Koga M, Choei H, Sasaki N, Kikuchi S, Takeuchi M, Makita Z. Palmitate-induced apoptosis of microvascular endothelial cells and pericytes. Mol Med. 2002 Apr;8(4):179-84.

Yamaguchi M, Nakao S, Kaizu Y, Kobayashi Y, Nakama T, Arima M, Yoshida S, Oshima Y, Takeda A, Ikeda Y, Mukai S, Ishibashi T, Sonoda KH. High-Resolution Imaging by Adaptive Optics Scanning Laser Ophthalmoscopy Reveals Two Morphologically Distinct Types of Retinal Hard Exudates. Sci Rep. 2016 Sep 19;6:33574. doi: 10.1038/srep33574. Erratum in: Sci Rep. 2016 Nov 03;6:35127.

Yego ECK, Vincent JA, Sarthy V, Busik JV, Mohr S. Differential regulation of high glucose-induced glyceraldehyde-3-phosphate dehydrogenase nuclear accumulation in Müller cells by IL-1beta and IL-6. Invest Ophthalmol Vis Sci. 2009 Apr;50(4):1920–8.

Yong PH, Zong H, Medina RJ, Limb GA, Uchida K, Stitt AW, Curtis TM. Evidence supporting a role for N-(3-formyl-3,4-dehydropiperidino)lysine accumulation in Müller glia dysfunction and death in diabetic retinopathy. Mol Vis. 2010 Dec 2;16:2524-38.

Yoshida A, Yoshida S, Khalil AK, Ishibashi T, Inomata H: Role of NF-kappaB-mediated interleukin-8 expression in intraocular neovascularisation. Invest Ophthalmol Vis Sci 1998; 39: 1097–1106.

Yoshida Y, Yamagishi S, Matsui T, Jinnouchi Y, Fukami K, Imaizumi T, Yamakawa R. Protective role of pigment epithelium-derived factor (PEDF) in early phase of experimental diabetic retinopathy. Diabetes Metab Res Rev. 2009 Oct;25(7):678-86. doi: 10.1002/dmrr.1007.

Yuuki T, Kanda T, Kimura Y, Kotajima N, Tamura J, Kobayashi I, Kishi S: Inflammatory cytokines in vitreous fluid and serum of patients with diabetic vitreoretinopathy. J Diabetes Complications 2001; 15: 257–259.

Zeng XX, Ng YK, Ling EA. Neuronal and microglial response in the retina of streptozotocin-induced diabetic rats. Vis Neurosci. 2000 Jun;17(3):463–71.

Zhang HY, Wang JY, Yao HP. Epigallocatechin-3-gallate attenuates lipopolysaccharide-induced inflammation in human retinal endothelial cells. Int J Ophthalmol 2014; 7, 408-412.

Zhou, T., Che, D., Lan, Y., Fang, Z., Xie, J., Gong, H., Li, C., Feng, J., Hong, H., Qi, W., Ma, C., Yang, Z., Cai, W., Zhong, J., Ma, J., Yang, X. & Gao, G. Mesenchymal marker expression is elevated in Muller cells exposed to high glucose and in animal models of diabetic retinopathy. Oncotarget 2017; 8, 4582-4594.

Zhu X, Sun Y, Wang Z, Cui W, Peng Y, Li R. Expression of glial cell line-derived neurotrophic factor and its receptors in cultured retinal Müller cells under high glucose circumstance. Anat Rec (Hoboken). 2012 Mar;295(3):532-9. doi: 10.1002/ar.22404. Epub 2012 Jan 20.

Zong H, Ward M, Madden A, Yong PH, Limb GA, Curtis TM, Stitt AW. Hyperglycaemia-induced pro-inflammatory responses by retinal Muller glia are regulated by the receptor for advanced glycation end-products (RAGE). Diabetologia. 2010 Dec;53(12):2656-66. doi: 10.1007/s00125-010-1900-z. Epub 2010 Sep 12.

Abstract

Diabetic retinopathy (DR) remains the first cause of visual loss in the age-working population in industrialized countries, and current treatments of the disease are not fully satisfying. Growing evidences indicate that Müller glia cells (MGCs) activation is involved in DR formation and may occur early, even before any vascular changes. Glucose may not be the only factor leading to inflammatory and vascular changes in DR, and recent studies demonstrated the role of dyslipidemia and fatty acids in this disease.
We aimed to investigate MGCs inflammatory and angiogenic response to high glucose and high lipid exposure.
In this work, we described for the first time the production of Müller cells from reprogrammed induced pluripotent stem iPS (hiMGCs) from different origins, and assayed their response to DR-relevant stress to evaluate their potential use in disease modeling approaches.
Using a transcriptomic approach, we showed that unstimulated hiMGCs express 18 key MGCs proteins at similar levels to post-mortem human retina. Similar to primary MGCs, hiMGCs poorly respond to glucose but respond to high lipid exposure by up-regulating their inflammatory and angiogenesis reactions. Finally, we showed that PA stimulated hiMGCs secrete angiogenic factors related to DR such as VEGF, IL-8, IL-1ß and ANGPTL4 and have a pro-angiogenic activity ex-vivo. Taken together, these hiMGCs represent an extremely valuable tool to better understand mechanisms of complex diseases and for the development of new therapeutics. In particular, hiMGCs can be generated from donors and easily expanded to be used in high-throughput drug screens.

Résumé

La rétinopathie diabétique (RD) reste la première cause de cécité dans la population active dans les pays industrialisés et les traitements actuels ne sont pas totalement satisfaisants. De nombreuses études ont démontré l'implication précoce de l'activation des cellules gliales de Müller (CGMs) dans la survenue de la RD, même avant l'apparition des lésions vasculaires. Par ailleurs, le glucose ne serait pas le seul facteur impliqué dans ces modifications vasculaires et inflammatoires, et des études récentes ont montré le rôle de la dyslipidémie et des acides gras dans la RD.
L'objectif de ce travail était d'évaluer la réaction inflammatoire et angiogénique des CGMs en réponse à l'hyperglycémie et l'hyperlipidémie.
Dans ce travail, nous avons tout d'abord décrit la première production de CGMs à partir de cellules souches pluripotentes de différentes origines (hiMGCs), puis évaluer leur réponse aux différents stimuli de la RD. L'étude de la transcriptomique a montré que les hiMGCs exprimaient 18 protéines clé des CGMs. Tout comme les CGMs primaires, les hiMGCs répondent peu à l'hyperglycémie mais sont très activées par l'exposition aux acides gras, notamment le palmitate. Enfin, nous avons montré que le palmitate stimulait la sécrétion par les hiMGCs de facteurs pro-angiogéniques, tels que le VEGF, l'IL-8, l'IL1 ß et ANGPTL4 et que les hiMGCs exposées au palmitate exerçaient une activité pro-angiogénique ex-vivo. Ainsi, ces hiMGCs, qui peuvent être générées à partir de donneurs sains et facilement multipliées représentent un outil fiable pour mieux comprendre les mécanismes complexes impliqués dans la RD et pour le développement de nouvelles thérapeutiques.